# SYSTEM IDENTIFICATION OF VENTILATION INHOMOGENEITY BY MULTIBREATH WASHOUT

by

JAFAR SANIIE

Submitted in partial fulfillment of the requirements for the degree of Master of Science

Thesis Advisors: Dr. Gerald M. Saidel

Dr. Edward H. Chester

Department of Biomedical Engineering

CASE WESTERN RESERVE UNIVERSITY

August 1977

. RECOMMENDATION FOR DEGREE
Graduate Studies - Case Western Reserve University

MASTER'S DEGREE

Date 5-20-77

Name Jafar Saniie Department Biomedical Engineering

Degree Sought MS in Biomedical Engineering under Plan A

Full Thesis Title (where applicable) SYSTEM IDENTIFICATION OF VENTILATION INHOMOGENEITY BY MULTIBREATH WASHOUT

We certify that the aforementioned student has completed the following requirements and is recommended for the degree:

Date of comprehensive or final oral examination: 31 May 1977

Date of thesis approval: 31 May 1977

Credit hours required for the degree: 30

Robert Plonsey
(Chairman, Department/Division/School)

Gerald M. Saidel
(Chairman, Examining Committee)

Edward C. McKannan

Cecil W. Thomas

RETURN TO GRADUATE STUDIES OFFICE, ROOM 103, PARDEE HALL

SYSTEM IDENTIFICATION OF VENTILATION INHOMOGENEITY BY MULTIBREATH WASHOUT

Abstract

by

JAFAR SANIIE

Ventilation inhomogeneity, which is due to uneven intrapulmonary gas distribution and imperfect mixing, can be studied by multibreath nitrogen washout of the lungs. The objective of this work is to determine what indices can be used to quantify the ventilation inhomogeneity in subjects with normal, mildly abnormal and severely abnormal lungs. For this purpose, multibreath washout tests were performed with spontaneous breathing by 39 subjects: 6 normal nonsmokers, 4 normal smokers, 13 with diffuse interstitial lung disease, 6 asthmatics, and 10 with chronic obstructive pulmonary disease. Nitrogen fraction and flow were measured continuously at the mouth. These signals were appropriately conditioned and analyzed in real time by a digital computer. Ventilation inhomogeneity was quantified by moment ratios, model parameters, and by other ventilatory indices described in the literature. From end-tidal and average-expired nitrogen fractions as functions of cumulative expired volume divided by functional

residual capacity, the zeroth, first, and second moments were computed. Parameters from a two-alveolar compartment model were estimated using the modified Gauss-Newton algorithm. All the ventilatory indices were examined with respect to their sensitivity to mild and severe abnormality and to their variability for all subjects and for subjects within a given diagnostic group. We have observed that among the ventilatory indices, the ratio of first moment to zeroth moment derived from end-tidal nitrogen fraction provides the best quantitative distinction from mild to severe ventilation inhomogeneity as well as the greatest reproducibility.

To my father, Ali, and my mother, Ashraf

## ACKNOWLEDGEMENTS

This work was supported by the Pulmonary Laboratory, Veteran Administration Hospital, Cleveland, Ohio 44106.

The author wishes to express his sincere gratitude and appreciation to Drs. Gerald M. Saidel and Edward H. Chester for their guidance and assistance throughout all stages of this work.

Thanks are also given to Dr. Gerald Fleming for assisting in performing the test and providing the clinical diagnoses, and Mrs. Lida Gamon for her valuable technical assistance.

Finally, the author wishes to thank Mrs.Beatrice McNaught, Miss Karen Kurtinaitis, and Mrs. Barbara Johnson who helped in preparation and typing of this thesis.

TABLE OF CONTENTS

LIST OF FIGURES

LIST OF TABLES

# CHAPTER I

## INTRODUCTION

Ventilation inhomogeneity, an important characteristic of abnormal lung function, can be quantified by a non-invasive, multibreath washout of the lung with a nitrogen free gas such as 100% oxygen. Since a washout procedure is used to determine the functional residual capacity (FRC), no additional patient time is necessary to obtain a measure of ventilation inhomogeneity from the expired nitrogen ($N_2$) dynamics. The envelope of the expired $N_2$ dynamics, i.e. the sequence of end-tidal $N_2$ fractions, forms the "washout curve". The expired $N_2$ dynamics depend on the breathing pattern as well as on the ventilation inhomogeneity of the lung. With spontaneous breathing, the operating point, amplitude, and period may change with each breath. As described by Saidel et al, (1975), the effects of breathing pattern variations can be significantly reduced by expressing the end-tidal $N_2$ fractions as a function of cumulative expired volume, CEV, (cumulative inspired volume, CIV) divided by FRC. In this form the washout curves of an individual become nearly superimposable for typical variation which may occur during spontaneous breathing.

To quantify the degree of ventilation inhomogeneity, many measures (indices or parameters) have been

proposed. Some of the measures require that a model fit the washout curve (Chiang and Yang, 1974; Fowler et al, 1952; Gomez et al, 1964; Nakamura et al, 1966; Paiva and Demeester, 1971;Saidel et al, 1971). Other measures which do not use curve fitting can be grouped as model independent (Becklake, 1952; Bouhuys, 1963) and model dependent (Bates and Christie, 1950; Cumming and Jones, 1966; Edelman et at, 1968; Lieheneckert and Lundgren, 1963; Roos et al, 1955).

Model independent indices. Cournand and coworkers (1941) proposed the 7-minute multibreath washout of nitrogen to evaluate FRC. The $N_2$ fraction in the lung at the end of the 7 minutes, which is usually greater in emphysematous than in normal lungs, served as an index of ventilation inhomogeneity. Other model-free indices related to the number of "volume turnover" (CEV/ FRC or CIV/FRC) rather than time are the Becklake Index (BI) and the lung clearance index (LCI). The BI, introduced by Becklake (1952), is ventilation volume (CEV or CIV) required to clear the lungs of 90% of its $N_2$ (or, equivalently, to reduce the $N_2$ to 10% of its initial fraction) divided by 90% FRC. The LCI, suggested by Bouhuys (1963), and also studied by Edelman (1968), is defined as the ventilation volume required to reduce end-tidal nitrogen to 2% divided by FRC.

By using the ventilation volume, the BI and LCI should reduce the effect of naturally occurring variations in amplitude (tidal volume) and frequency of breathing. Normalizing the ventialtion volume with FRC accounts for differences in the operating point.

Model Independent indices. As a reference by which to evaluate experimental washout data, many investigators use the single alveolar-space model (Fowler et al, 1952). For given values of FRC, tidal volume ($V_T$), and dead space volume ($V_D$), the $N_2$ fraction in the lungs is uniquely related to the number of breaths from the start of the washout. The ideal number of breaths computed from this model would be the minimum for the specified values of FRC, $V_T$, and $V_D$. Incorporating this model are the following indices: Bates and Christie Index (BCI), ventilatory efficiency ($E_{90\%}$), mixing ratio (MR), index of alveolar ventilation (IAV), and five breath index (5BI).

The BCI (Bates and Christie, 1950) is the ratio of theoretical to actual anumber of breaths needed to reduce the nitrogen fraction in the lung to 10%. MR (Edelman, 1968) is inversely related to BCI and is defined as the ratio of actual number of breaths to the ideal number at which the $N_2$ fraction of the lung is 2%. The $E_{90\%}$ (Prowse and Cumming, 1973) is defined in

terms of the number of volume turnovers as the ideal to experimental numbers of turnovers needed to reduce the $N_2$ fraction in the lung by 90%. This index is essentially the same as the BCI; the two indices are identical for a constant tidal volume. Licktneckert and Lundgren (1963) introduced the IAV defined in terms of a clearance coefficient, which is the ratio of cumulative inspired volume to cumulative expired nitrogen. Specifically, the IAV is the ratio of ideal to actual clearance coefficient at which the nitrogen fraction in the lung is 2%. Operationally, it is similar to $E_{90\%}$. Except for inclusion of the "ideal" model, the $E_{90\%}$ and IAV correspond to model-independent indices BI and LCI respectively. The 5BI introduced by Roos et al (1955) and re-examined by Weygandt (1976), is computed after five breaths as a ratio of the actual amount of $N_2$ exhaled to the ideal amount of $N_2$ exhaled.

Model indices with curve fitting. The single alveolar space model of Fowler et al (1952) predicts that the $N_2$ fraction of the lung should decrease exponentially with breath number. Experimentally, only washout curves from normal lung with little ventilation inhomogeneity can be represented by a single exponential. As the ventilation inhomogeneity in lungs

becomes greater, deviations from the single exponential model become more noticeable. Consequently, general models of washout involve more than one alveolar space. The models may be derived from compartmental mass balances or arbitrarily specified in an algebraic form such as a sum of exponentials. The independent variable of such models may be the discrete breath number, continuous time, or a volume evaluated at discrete breath numbers.

A model of two exponentials that are coninuous in time, such as that by Chiang and Yang (1975), contains four parameters. Nakamura et al (1965) deal with a sum of an arbitrarily large number of exponentials which is taken to the continuous limit. Consequently, that model requires the system identification of a continuous response function. From an arbitrarily large number of compartments in series, Gomez (1962) also takes the model solution to the continuous limit. Models developed from compartments in series and parallell have been presented by Saidel et al ( 1971) and Paivi and Demeester (1971). The former model consists of 5 perfectly mixed compartments in which the $N_2$ concentrations, derived from balance equations, are continuous function of time. The model by Paivi and Demeester has from 5 to 31 compartments

with 2 to 16 compartments having the dead space of conducting airway represented as a time-delay. Both of these last models have multiple parameters.

All of the above models can simulate washout curves of great variety and provide some insight into the factors governing the washout. For clinical purposes, however, models proposed to date are not practical. Furthermore, most of these models can not take into account the effects of breathing pattern variability, especially on a breath-by-breath basis. For clinical applicability, models must fit experimental washout curves uniquely and efficiently to yield some index of ventilation inhomogeneity. Consequently, techniques of system identification and optimal parameter estimation are required.

Alternative approaches. The goal of this thesis is to describe some alternative approaches to quantify ventilation inhomogeneity for regular clinical use. Since the modern pulmonary function laboratory has a mini-computer (or micro-processor), the data processing and analysis used clinically need not be trivial. Consequently, breathing pattern variations can be taken into account so that subjects can breathe spontaneously. Also, when computations, such as signal conditioning, filtering, and integration are done by

computer, the experimental system may be simplified.

In the following sections the identification techniques of moment analysis and parameter estimation will be developed. For evaluation of these indices of ventilation inhomogeneity, experimental studies are performed with patients with documented lung disease, as well as normal subjects.

# CHAPTER II

## IDENTIFICATION TECHNIQUES

### Volume Parameters

Several types of volume parameters are of value in characterizing lung function. When effective respiratory muscle pressure is a maximum, minimum, or zero, the corresponding absolute volumes are defined as the total lung capacity (TLC), residual volume (RV), and the functional residual capacity (FRC). All other volumes (of physiologic interest) can then be derived from TLC, RV, and FRC. In addition, conceptual volumes can be defined from models of the lung.

Anatomical dead space is the region of the lung in which conceptually only plug transport, or a pure-time delay, occurs. The volume of the dead space can be estimated from the nitrogen washout curve of each breath, assuming plug transport through the dead space and a perfectly mixed alveolar space. This model implies that after inhalation of an $N_2$-free gas, the $N_2$ exhaled subsequently comes from the alveolar space. On expiration, volume change of the alveolar space is

$$\Delta V_A = \int_E Q(t)dt - V_D$$

where $V_D$ is the volume of the dead space and the total volume exhaled is represented by the integral of flow, Q(t). If the total nitrogen exhaled is expressed as

$$\int_E C(t)Q(t)dt = C_{ET}\Delta V_A$$

where the end-tidal concentration, $C_{ET}$, is taken to be representative of the alveolar concentration, we obtain

$$V_D = \int_E Q(t)dt - \int_E [C(t)/C_{ET}]Q(t)dt$$

Functional residual capacity is the volume of gas in the lung at the end of an expiration during tidal breathing. An estimate of the FRC can be made by analyzing nitrogen washout from the lung with an $N_2$-free gas. From an $N_2$ mass balance, the difference in the amount of $N_2$ in the lung at the beginning of the first inspiration and the end of the expiration K equals the cumulative amount of $N_2$ expired over breaths J = 1,2,....,K:

$$C(0,E)V(0,E) - C(K,E)V(K,E) = \sum_{J=1}^{K} \int_{E(J)} C(t)Q(t)dt$$

At the end of breath K, the $N_2$ concentration in the lung is C(K,E) and the volume is V(K,E). From a total gas balance assuming constant gas density and no net transport into capillaries, we obtain the volume difference over K breaths:

$$V(0,E) - V(K,E) = \sum_{J=1}^{K} \left[\int_{I(J)} Q(t)dt - \int_{E(J)} Q(t)dt\right]$$

This accounts for volume differences on each inspiration, $I(J)$, and expiration, $E(J)$. Combining equations to eliminate $V(K,E)$, we find

$$V(0,E) = \sum_{J=1}^{K} \int_{E(J)} C(t)Q(t)dt / \left[C(0,E) - C(K,E)\right] +$$

$$\sum_{J=1}^{K} \left[\int_{I(J)} Q(t)dt - \int_{E(J)} Q(T)dt\right] / \left[\frac{C(0,E)}{C(K,E)} - 1\right]$$

As $K$ gets large, $C(0,E) >> C(K,E)$ so that the second term in this equation becomes negligible. In our experiments, we make the approximations that FRC $\simeq$ $V(0,E)$ and that at the end of expiration $K$, the nitrogen concentration leaving the lung, $C_{ET}(K)$, is approximately equal to $N_2$ concentration within the lung, $C(K,E)$.

Model Analysis

The dynamics of multibreath $N_2$ washout from subjects breathing spontaneously or with mechanical assistance can be better characterized from successive end-tidal concentrations than from intra-breath concentration changes. The latter is most appropriate for a large-volume breathing maneuver. Data from tidal-volume breathing can be most suitably incorpor-

ated into a multi-alveolar space model (Fig.2-1). Between the environment and the perfectly mixed alveolar spaces, plug transport occurs through a constant volume dead space. From the integrated mass balances equations of the alveolar spaces, we get a discrete-time, lumped-parameter model.

If the gas density is constant, the total mass balance over alveolar space i reduces to

$$\frac{dV_i}{dt} = Q_i \quad ; \quad i=2,3,.....,N+1 \tag{1}$$

where $V_i$ is the volume and $Q_i$ is the flow rate. Let us assume that a constant flow fraction, $f_i=Q_i/Q$, exists such that

$$\sum_{i=2}^{N+1} f_i = 1 \tag{2}$$

Upon integration of equation (1), the volume $V_i(K,I)$ at the end of inspiration K can be related to the volume $V_i(K-1,E)$ at the end of expiration K-1:

$$V_i(K,I)=V_i(K-1,E) + f_i\Delta V(K,I) \tag{3}$$

where $\Delta V(K,I)$ is the lung volume change over the inspiration K. Summing equation (3) over all alveolar spaces, i = 2,3,. . . ., N + 1, we find

$$V_A(K,I)=V_A(K-1,E) + \Delta V(K,I) \tag{4}$$

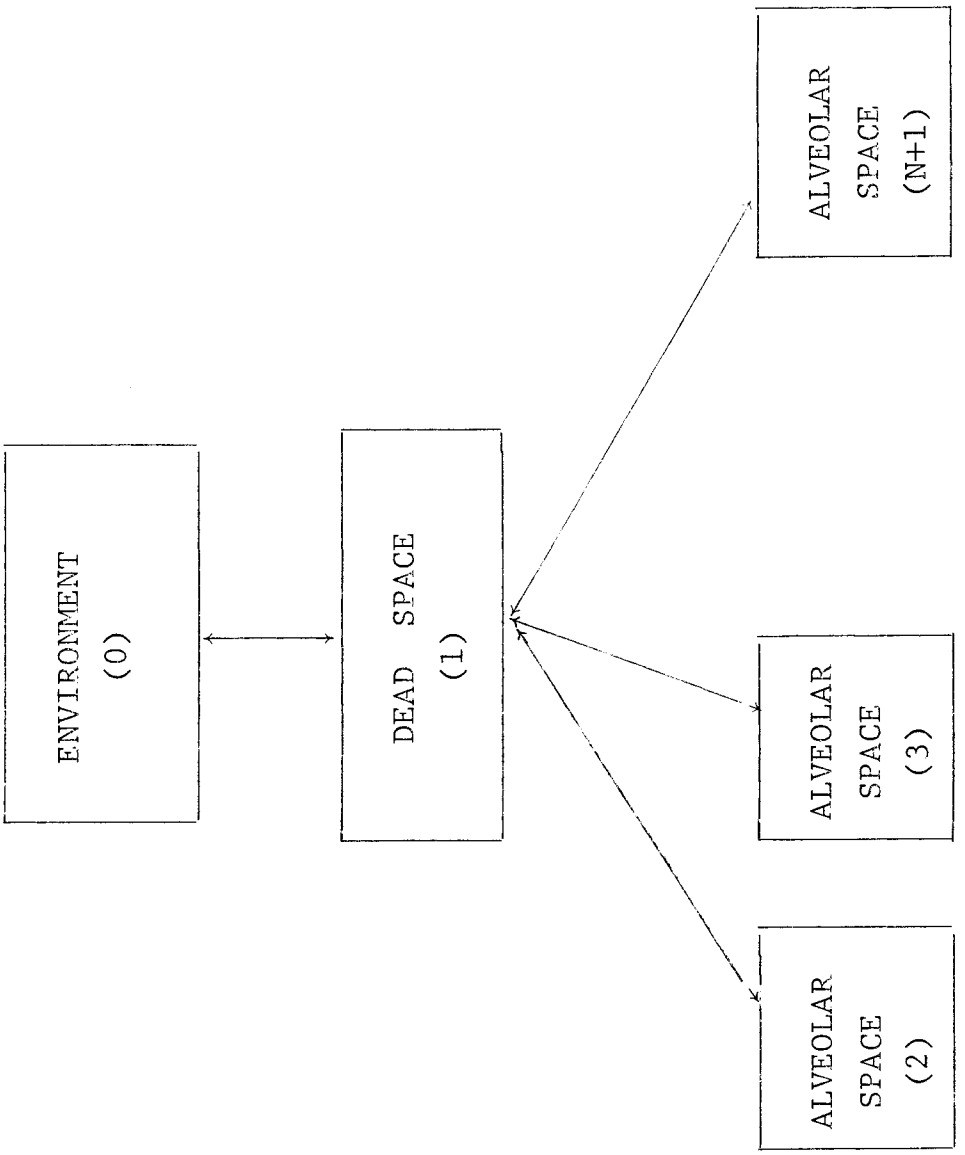


FIGURE 2-1. MULTI-ALVEOLAR SPACE (MAS) MODEL.

where $V_A$ is the total alveolar volume. Next, let us assume that the alveolar volume fractions at the end of inspiration and expiration are constants:

$$v_i(\tau) = V_i(K,\tau)/V_A(K,\tau) \tag{5}$$

where $V_A(K,\tau)$ is the alveolar volume at the end of the K-th inspiration ($\tau$=I) or expiration ($\tau$=I) and

$$\sum_{i=2}^{N+1} v_i(\tau) = 1 \tag{6}$$

The parameters $v_i(I)$, $v_i(E)$ and $f_i$ can be related by combining equations (3) and (5):

$$v_i(I)V_A(K,I) = v_i(E)V_A(K-1,E)+f_i\Delta V(K,I) \tag{7}$$

The species mass balance for an inert, insoluable gas (e.g., nitrogen) in alveolar space i can be written as

$$\frac{d[C_iV_i]}{dt} = \begin{cases} C_{1i}Q_1 \ , \ Q_i>0 & \text{(Inspiration)} \\ C_iQ_i \ , \ Q_i>0 & \text{(Expiration)} \end{cases} \tag{8}$$

where $C_i$ is the species concentration in alveolar space i and $C_{1i}$ is the species concentration that enters from the dead space. During expiration, the combination of equations (1) and (8) yields

$$V_i\frac{dC_i}{dt} = 0 \Rightarrow C_i(K,E) - C_i(K,I) = 0$$

That is, the concentration $C_i$ does not change between

the end of inspiration K and the end of expiration K. For $|\Delta V| > V_D$, the species mass flow rate leaving the lung is

$$C_{10}(K)Q = \sum_{i=2}^{N+1} Q_i C_i(K,E) \quad K = 1,2, \ldots.$$

Upon substitution of the flow fraction, we get the species concentration leaving the lung:

$$C_{10}(K) = \sum_{i=2}^{N+1} f_i C_i(K,E) \tag{10}$$

During inspiration K, the concentration $C_{1i}$ is piece-wise constant:

$$C_{1i} = \begin{cases} C_{10}(K-1,E), & \Delta V < V_D \\ C_{01}, & \Delta V > V_D \end{cases}$$

where $C_{01}$ is the constant input concentration from the environment into the dead space. From integration of the species balance (8) and introduction of the flow-fraction, we obtain the difference between the species mass in alveolar i at the end of inspiration K and end of expiration K-1, that is for $\Delta V > V_D$,

$$C_i(K,I)V_i(K,I) - C_i(K-1,E)V_i(K-1,E) = f_i(\Delta V(K,I) - V_D)C_{01} + f_i V_D C_{10}(K-1,E) \tag{11}$$

The terms on the right are the species mass that enters alveolar space i on inspiration K from the environment and dead space, respectively. Combining

equations (7), (9), and (11), we get

$$C_i(K,E) - C_{01} = \alpha_i(K)[C_i(K-1,E) - C_{01}] + \beta_i(K)[C_{10}(K-1) - C_{01}]$$

where

$$\alpha_i(K) = [1+f_i \Delta V(K,I)/v_i(E)V_A(K-1,E)]^{-1} \qquad (12)$$

$$\beta_i(K) = f_i\alpha_i(K)V_D/v_i(E)V_A(K-1,E)$$

In this model formulation, the alveolar volume fractions are taken at the end of expiration $v_i = v_i(E)$, but another expression for $\alpha_i(K)$ and $\beta_i(K)$ can be given in terms of volume fraction at the end of inspiration. The parameters $f_i$ and $v_i(E)$ or $v_i(I)$ characterize the distribution of ventilation. Taking these parameters as constants implies that mechanical properties of the lung are invariant.

If we define the dimensionless consentrations,

$$Y_i(K) = \frac{C_i(K,E)-C_{01}}{C_{10}(0)-C_{01}}, \quad X(K) = \frac{C_{10}(K)-C_{01}}{C_{10}(0)-C_{01}} \qquad (13)$$

then the multi-alveolar space (MAS) model (i = 2,3, ... N+1) becomes

$$Y_i(K+1) = \alpha_i(K)Y_i(K) + \beta_i(K)X(K) \qquad (14)$$

$$X(K) = \sum_{i=2}^{N+1} f_iY_i(K) \qquad (15)$$

with the initial conditions $X(0) = Y_i(0) = 1$.

The ratios of flow fraction to alveolar volume

fraction $f_i/v_i$, where $v_i \equiv v_i(E)$, are the key independent parameters of our MAS lung model. By setting this ratio equal for any two alveolar spaces p and q ($p \neq q$), the N-alveolar space model can be reduced to a N-1 alveolar space model. For

$$f_p/v_p = f_q/v_q$$

we find

$$\alpha_p(K) = \alpha_q(K) \ , \ \beta_p(K) = \beta_q(K)$$

Equation (14) shows that the normalized nitrogen fractions in alveolar compartments p and q are the same:

$$Y_p(K) = Y_q(K) \equiv Y(K), \ K = 1 \tag{16}$$

Substituting of this equality into equation (15) we find:

$$X(K) = \sum_{\substack{i=2 \\ i \neq p, \ q}}^{N+1} f_i Y_i(K) + fY(K) \ , \quad K = 1 \tag{17}$$

where $f \equiv f_p + f_q$. Further substitution of equation (17) into equation (14) and then into equation (15) shows that equations (16) and (17) hold for any breath K. If we set $v \equiv v_p + v_q$, then

$$f_p/v_p = f_q/v_q \equiv f/v \tag{18}$$

Consequently, equations (16), (17), and (18) imply that

the number of alveolar spaces and independent parameters has been reduced to N-1.

By extension, one can show that

$$\frac{f_2}{v_2} = \frac{f_3}{v_3} = \ldots\ldots\ldots\ldots = \frac{f_{N+1}}{v_{N+1}}$$

implies

$$\frac{f_i}{v_i} = 1 \quad i = 2,3, \ldots\ldots, N+1$$

In this case, the coefficients $\alpha_i(K)$ and $\beta_i(K)$ become the same for all alveolar spaces:

$$\alpha_i(K) \equiv \alpha(K) = [1+\Delta V(K,I)/V_A(K-1,E)]^{-1}$$

$$\beta_i(K) \equiv \beta(K) = \alpha(K)V_D/V_A(K-1,E)$$

Therefore, equations (14) and (15) reduce to a single alveolar space model:

$$X(K+1) = X(K)\left[\frac{V_A(K-1,E) + V_D}{V_A(K-1,E) + \Delta V(K,I)}\right] \tag{19}$$

If only two of the ratios are independent, then for $i = 2,3, \ldots\ldots, M < N+1$ we find

$$\frac{f_i}{v_i} = \frac{f_p}{v_p} \Rightarrow \alpha_i(K) = \alpha_p(K) \;,\quad \beta_i(K) = \beta_p(K)$$

and for $i = M+1, M+2, \ldots\ldots\ldots, N+1$

$$\frac{f_i}{v_i} = \frac{f_q}{v_q} \Rightarrow \alpha_i(K)=\alpha_q(K) \;,\quad \beta_i(K)=\beta_q(K)$$

Consequently, the model acts as if it has only two alveolar spaces:

$$Y_i(K+1)=\alpha_i(K)Y_i(K)+ \beta_i(K)X(k);\ Y_i(0)=1;\ i=p,q$$

$$X(K)= f_p Y_p(K) + f_q Y_q(K);\quad X(0)=1 \qquad (20)$$

where

$$f_p = \sum_{i=2}^{M} f_i \quad \text{and} \quad f_q = \sum_{i=M+1}^{N+1} f_i$$

Since the multibreath washout from subjects can not in general be described by one exponential function, the model of choice must have at least two alveolar spaces. If one chooses a model with three instead of two alveolar spaces, then the number of independent parameters needed to be estimated from the multibreath washout increases from two to four. The additional parameters not only make the estimation procedure much more costly, but also lead to problems of non-unique parameter values. Consequently, with a view toward clinical application, we shall analyze the data using the two alveolar space model.

Time-Invariant Model

To examine the characteristics of the model directly by analytical techniques, we shall deal with the special case of a periodic breathing pattern such

that

$$\Delta V(K,I)=\Delta V(K,E)=V_T \ , \ V_A(K,E)=V_A \ , \ V_A(K,I)=V_A+V_T$$

and for which the coefficients $\alpha_i(K)$ and $\beta_i(K)$ become constant:

$$\alpha_i(K)\equiv\alpha_i=(1+f_iV_T/v_iV_A)^{-1} \ , \beta_i(K)\equiv\beta_i=f_iV_D\alpha_i/v_iV_A$$

Consequently, the model reduces to a set of time invariant, linear difference equations for i= 2,3,... , N + 1:

$$Y_i(K+1) = \alpha_iY_i(K) + \beta_iX(K)$$

$$X(K) = \sum_{i=2}^{N+1} f_iY_i(K)$$

Introducing the generating functions

$$H_i = \sum_{K=0}^{\infty} Y_i(K)Z^K \ , \ G = \sum_{K=0}^{\infty} X(K)Z^K$$

we can transform the problem as follows:

$$Z^{-1}[H_i-1] = \alpha_iH_i+\beta_iG \ , \ i=2,3 \ .. \ .. \ , \ N+1$$

$$G = \sum_{i=2}^{N+1} f_iH_i$$

The solution for G is given by

$$G = \sum_{i=2}^{N+1} f_i(1-\alpha_iZ)^{-1} \ / \ [1-Z \sum_{i=2}^{N+1} f_j\beta_i(1-\alpha_iZ)^{-1}]$$

Upon rearrangement, this becomes

$$G = \sum_{i=2}^{N+1} [f_i \prod_{\substack{j=2,N+1 \\ j\neq i}} (1-\alpha_j Z)] / [\prod_{i=2,N+1} (1-\alpha_i Z) - Z \sum_{i=2}^{N+1} (f_i \beta_i \prod_{\substack{j=2,N+1 \\ j\neq 1}} (1-\alpha_j Z))]$$

The numerator of the generating functions is a polynominal of order N-1 and the denominator is a polynominal of order N. Generally, G can be presented in the form

$$G = \sum_{i=2}^{N+1} q_i/(1-Zp_i)$$

where $p_i$ and $q_i$ are nonlinear function of our MAS model parameters. Consequently, the solution for normalized end-tidal nitrogen fraction becomes the summation of N different exponential decay function.

$$X(K) = \sum_{i=2}^{N+1} q_i \exp (K \ell n p_i)$$

For a single alveolar space, the generating function simplifies to

$$G = \frac{1}{1-Z(\alpha_i+\beta_i)} \equiv \sum_{K=0}^{\infty} (\alpha_i+\beta_i)^K Z^K$$

where

$$\alpha_i = \frac{V_A}{V_A+V_T} \quad \text{and} \quad \beta_i = \frac{V_D}{V_A+V_T}$$

Comparing the above equation to the definition of the transform, we see that

$$X_K = (\alpha_i + \beta_i)^K = \left(\frac{V_A + V_D}{V_A + V_T}\right)^K$$

which is the expression for washout of an inert gas from a uniformly ventilated lung presented by Fowler et al (1952).

With the two independent alveolar spaces, the generating function becomes

$$G = (1 - cZ)/(aZ^2 - bZ + 1)$$

where

$$a = \alpha_2\alpha_3 + f_2\beta_2\alpha_3 + f_3\beta_3\alpha_2$$

$$b = \alpha_2 + \alpha_3 + f_2\beta_2 + f_3\beta_3$$

$$c = f_2\alpha_3 + f_3\alpha_2$$

The generating function can be expressed in partial fractions as

$$G = \sum_{i=1}^{2} q_i/(1 - Zp_i)$$

where

$$P_{1,2} = 2a/(b \pm \sqrt{b^2 - 4a}) \quad , \quad q_1 = (p_1 - c)/(p_1 - p_2),$$

and $$q_2 = (p_2 - c)/(p_2 - p_1)$$

Since

$$b^2 - 4a = (\alpha_2 - \alpha_3 + f_2\beta_2 + f_3\beta_3)^2 + 4f_2f_3\beta_2\beta_3 > 0$$

and

$$b \pm \sqrt{b^2-4a} > 0$$

we see that $p_1$ and $p_2$ are real and positive. Furthermore, one can show that $p_i<1$ for $i= 1,2$. Hence, the nitrogen washout curve is simply summation of two different exponential decay curves.

$$X(K)= \sum_{i=1}^{2} q_i \exp (K \ell n p_i)$$

Moment Analysis

Partial system identification of multibreath washout can be obtained from the first few moments of the response function, which is the sequence of normalized end-tidal concentrations (Saidel et al, 1975). The r-th moment of dimensionless nitrogen end-tidal concentration as a function of breath number X(K) is given by

$$\lambda_r = \sum_K K^r X(K) \quad ; \; r=0,1,2$$

Of particular interest is the mean defined as $\lambda_1/\lambda_0$. From the transform function defined as

$$G(Z) = \sum_K^{\infty} Z^K X(K)$$

the moments can be determined from successive derivatives, e.g.,

$$\lambda_0=G(1) \quad , \quad \lambda_1 = \left. \frac{dG}{dZ} \right|_{Z=1}$$

For the simplest time-invariant model with one alveolar space,

$$G(Z)=[1-Z(V_A+V_D)/(V_A+V_T)]^{-1}$$

the mean is

$$\lambda_1/\lambda_0=(V_A+V_D)/(V_T-V_D)=FRC/(V_T-V_D)$$

To eliminate FRC and reduce the effect of $V_T$ on the moment ratio, one can express the dimensionless end-tidal concentration as a function of a dilution number (Saidel et al, 1975). The dilution number, defined as the ratio of cumulative expired volume divided by FRC, is for the time-invariant model simply

$$\eta_K = K\ V_T/FRC$$

The moments using this independent variable are given by

$$\mu_r = \sum_K \eta_K^r\ X\ (\eta_K)[\eta_K-\eta_{K-1}] = (V_T/FRC)^{r+1}\lambda_r$$

Consequently, for the one alveolar space model

$$\frac{\mu_1}{\mu_o} = (V_T/FRC)\frac{\lambda_1}{\lambda_o} = \frac{V_T}{V_T-V_D}$$

Now, let us define a modified dilution number as the ratio of cumulative alveolar ventilation divided by FRC, which for the time-invariant model is

$$\hat{\eta}_K = K(V_T-V_D)/FRC$$

The moments for this independent variable are

$$\hat{\mu}_r = \sum_K \hat{\eta}_K^r \; X(\hat{\eta}_K)[\hat{\eta}_K - \hat{\eta}_{K-1}] = [(V_T - V_D)/FRC]^{r+1} \lambda_r$$

and

$$\frac{\hat{\mu}_1}{\hat{\mu}_o} = [(V_T - V_D)/FRC] \frac{\lambda_1}{\lambda_o} = 1$$

Since this moment ratio is independent of other parameters, it can serve as a convenient reference. That is, the degree of ventilation inhomogeneity is indicated by deviation of this ratio from unity.

Moments of the two alveolar space model are not simply related to model parameters.

Parameter Estimation

To estimate the model parameters which yield the best fit of the model to experimental data, we apply an optimization procedure. Each multibreath washout, comprised of a set of end-tidal $N_2$ concentrations, is analyzed by the dimensionless model for two alveolar spaces (i = 2,3):

$$Y_i(K) = \alpha_i(K-1) Y_i(K-1) + \beta_i(K-1) X(K-1)$$

$$X(K) = f_2 Y_2(K) + f_3 Y_3(K)$$

where $Y_i(0) = 1$ , $X(0) = 1$ , and

$$\alpha_i(K) = [1 + f_i \Delta V(K,I)/v_i V_A(K-1,E)]^{-1}$$

$$\beta_i(K) = \alpha_i(K) f_i V_D / v_i V_A(K-1,E)$$

The parameters $\Delta V(K,I)$ and $V_A(K-1,E)$ are obtained directly from the flow signal and the parameter $V_D$ is computed from the intra-breath flow and nitrogen signals. From the dimensionless end-tidal concentrations, we can estimate the remaining two independent parameters, which can be chosen from among $f_2, v_2$ , $f_3, v_3$, $f_2/v_2$ and $f_3/v_3$. Arbitrarily, we decided to evaluate the parameter vector $\underline{\theta} = [f_2, v_2]$ for each multibreath washout.

The parameter values are chosen such that the sum of the squared differences between the experimental data and model values of the set of end-tidal nitrogen fractions were minimized in a least-squares sense. Let $\underline{X} = [X_1 , X_2, \ldots\ldots , X_m]^T$ be the vector of the experimental values, $\underline{\hat{X}} = [\hat{X}_1, \hat{X}_2, \ldots\ldots\ldots, \hat{X}_m]^T$ be the vector of model values, and $\underline{\omega} = [\omega_1, \omega_2, \ldots., \omega_m]^T$ be a weighting vector with non-negative elements. The parameters of $\underline{\theta}$ are chosen such that $\sum_{i=1}^{M} \omega_i (X_i - \hat{X}_i)^2$ is a minimum subject to the inequality constraints:

$$f_2 \geq 0 \ , \ 1 - f_2 \geq 0 \ , \quad v_2 \geq 0 \ , \ 1 - v_2 \geq 0$$

If we define the constraint vector $\underline{\psi} = [f_2, 1-f_2, v_2, 1-v_2]$ and an arbitrary vector $\underline{\lambda} = [\lambda_1, \lambda_2, \lambda_3, \lambda_4]^T$ with non-negative elements, the problem can be expressed as the minimization of the following objective function:

$$\Phi\ (\underline{\theta}) = \sum_{j=1}^{M} \omega_j [X_j - \hat{X}_j(\theta)]^2 + \sum_{i=1}^{4} \lambda_i\ /\psi_i(\underline{\theta})$$

The weighting vector $\underline{\omega}$ is chosen to compensate for variation in the reliability and scaling of measured data. Since our data are scaled into a dimensionless form and the measurement accuracy does not produce significant estimate errors, the elements of weighting vector are chosen to be unity. The second term of the objective function is a penalty function which allows the constraints to be incorporated directly into the minimization. The penalty function has negligible effect when the constraints are not close to zero, but its effect increases sharply as any constraint equality is approached.

Since this estimation problem requires the solution of non-linear equations, an iterative procedure is used. Given initial values of the parameter vector, $\underline{\theta}^0$ we seek a new value of $\underline{\theta}^1$ which is nearer the minimum in the sense that $\Phi\ (\underline{\theta}^1) < \Phi\ (\underline{\theta}^0)$. We proceed to find $\underline{\theta}^2, \underline{\theta}^3$, etc. such that

$$\Phi\ (\underline{\theta}^{i+1}) < \Phi\ (\underline{\theta}^i)$$

At some i = N, when the objective function is sufficiently small according to pre-set criteria, we take the values of $\underline{\theta}^N = \underline{\theta}^*$ as the optimal estimates

of the parameters. With our model, the objective function has two equivalent global optima:

$$\underline{\theta}^* = [f_2^*, v_2^*]^T \quad \text{or} \quad \underline{\theta}^* = [1-f_2^*, 1-v_2^*]^T$$

Both solutions have exactly the same physical meaning, and estimating one of the other dependents on the initial parameter vector, $\underline{\theta}^o$ relative to global minimum.

Let us arbitrarily set the initial guess of parameters well in the interior of feasible region, $\underline{\theta}^o = [0.3, 0.8]^T$. Since the magnitudes and ranges of $f_2$ and $v_2$ are of the same order, we chose $\lambda_i = \lambda$ for $i = 1,2,3,4$. Arbitrarily, $\lambda$ is set to $10^{-3}$ so that the contribution of the penalty functions are negligible in the feasible domain away from the border of the constraints. The value of $\lambda$ is decreased by $1/i^2$ on each interation i. Close to the optimal solution, the value of $\lambda$ is set to zero.

With a modified Gauss-Newton technique (Bard, 1974), the algorithm for choosing a new parameter vector requires only first derivatives with respect to the parameters. In particular

$$\underline{\theta}^{i+1} = \underline{\theta}^{i} - H_i^{-1} q_i$$

where $q_i = [\frac{\partial \Phi}{\partial \theta_1}, \frac{\partial \Phi}{\partial \theta_2}]^T$ is the gradient vector at

$\underline{\theta} = \underline{\theta}^i$ and $H_i$ is the approximated Hessian matrix with the elements

$$H_{rs}(\underline{\theta}^i) \simeq 2\left[\sum_{j=1}^{M} \frac{\partial \hat{X}_j(\underline{\theta})}{\partial \epsilon_r} \frac{\partial \hat{X}_j(\underline{\theta})}{\partial \theta_s} + \sum_{i=1}^{4} \lambda_i \psi_i^{-3} \frac{\partial \psi_i}{\partial \theta_r} \frac{\partial \psi_i}{\partial \theta_s}\right]$$

at $\underline{\theta} = \underline{\theta}^i$ and r,s = 1,2. To allow inversion of $H_i$ even with relatively poor initial guesses for the unknown parameters, we modify the approximate Hessian matrix using a Marquardt-type correction (Bard, 1974). In this method $H_i$ is replaced by $\hat{H}_i$ which is equivalent to $H_i + \gamma I$, where I is the identity matrix and $\gamma$ is a positive constant. Initially, we set $\gamma = 0.01$ and decrease it by $1/i^2$ on each iteration i. However, in the neighborhood of the minimum, when the objective function becomes approximately quadratic, $\gamma$ is set to zero.

Termination criteria must be carefully specified so that after some finite number of iterations, the estimated parameter is sufficiently close to the optimal solution, $\underline{\theta}^*$. A major difficulty with an iterative procedure is that convergence may occur at a local minimum rather than at a global minimum. We can increase the likelihood that the convergence point is the global minimum by repeating the process with different initial guesses of parameter values.

Practically, the search for the optimal point is terminated when

$$\Phi\ (\underline{\theta}^{i}) - \Phi\ (\underline{\theta}^{i+1}) < 10^{-5}$$

and for $j=1,2$

$$|\theta_j^{i+1} - \theta_j^{i}| \ / \ (|\theta_j^{i}| + 10^{-4}) < 10^{-3}$$

To optimize the least square objective function by a modified Gauss-Newton method, we need to calculate the elements of gradient vector q:

$$\frac{\partial \Phi(\underline{\theta})}{\partial \theta_r} = -2 \sum_{j=1}^{M} \frac{\partial \hat{X}_j}{\partial \theta_r}(X_j - \hat{X}_j) - \sum_{j=1}^{4} \frac{\lambda_j}{\psi_j^2} \frac{\partial \psi_j}{\partial \theta_r}$$

where $\theta_r = f_2$ or $v_2$. Consequently, we must evaluate the derivatives of the state variables $\hat{X}_j \equiv X(J)$ and $Y_i(J)$ and of the constraints $\psi_j$ with respect to these parameters. Taking the derivatives of the model equations, we get

$$\frac{\partial Y_i(K+1)}{\partial \theta_r} = \frac{\partial \alpha_i(K)}{\partial \theta_r} Y_i(K) + \alpha_i(K) \frac{\partial Y_i(K)}{\partial \theta_r} + \frac{\partial \beta_i(K)}{\partial \theta_r} X(K) +$$

$$\beta_i(K) \frac{\partial X(k)}{\partial \theta_r}$$

$$\frac{\partial X(K)}{\partial \theta_r} = \sum_{i=2}^{3} \frac{\partial f_i}{\partial \theta_r} Y_i(K) + \frac{\partial Y_i(K)}{\partial \theta_r} f_i$$

These equations can be solved sequentially with initial conditions

$$\frac{\partial Y_i(K)}{\partial \Theta_r} = \frac{\partial X(K)}{\partial \Theta_r} = 0 \quad , \quad K=0$$

where i = 2,3. The derivatives of the coefficients of the model equations and of the penalty function are given in Table 2-1.

Table 2-1. The partial derivatives of the coefficient of the model equations and of the penalty functions

| $\partial(\ )$ / $\partial(\ )$ | $f_2$ | $f_3$ | $\alpha_2$ | $\alpha_3$ | $\beta_2$ | $\beta_3$ | $\psi_1$ | $\psi_2$ | $\psi_3$ | $\psi_4$ |
|---|---|---|---|---|---|---|---|---|---|---|
| $f_2$ | 1 | -1 | $-v_2\sigma_2$ | $v_3\sigma_3$ | $v_2\rho_3$ | $-v_3\rho_3$ | 1 | -1 | 0 | 0 |
| $v_2$ | 0 | 0 | $f_2\sigma_2$ | $-f_3\sigma_2$ | $-f_2\rho_2$ | $f_3\rho_3$ | 0 | 0 | 1 | -1 |

Where

$$\sigma_i = \Delta V(K,I)V_A(K-1,E) \,/[v_i V_A(K-1,E) + f_i \Delta V(K,E)]^2 \quad ; \; i=2,3$$

$$\rho_i = V_D V_A(K-1,E) \,/\, [v_i V_A(K-1) + f_i \Delta V(K,E)]$$

# CHAPTER III

## EXPERIMENTAL STUDIES

### Clinical Subjects

In our study of ventilation inhomogeneity, we used clinical subjects with various pulmonary abnormalities and a control group of normal subjects. The following clinical classification was used in these patients.

1. Normal non-smoker. No history of chronic or recurrent lung disease, no respiratory symptoms, and no history of smoking.

2. Normal smoker. No history of chronic or recurrent lung disease, no respiratory symptoms, and a positive chronic and current cigarette smoking history.

3. Diffuse Interstitial Lung Disease (DILD). Diffuse chronic inflammatory disease of lung parenchyma:

4. Obstructive Asthma. Episodic wheezing and dyspnea with intervening symptom-free intervals.

5. Chronic Obstructive Pulmonary Disease (COPD). Persistent, chronic, obstructive airway disease including emphysema and bronchitis.

We studied 39 subjects who represented five

separate categories of respiratory dysfunction. The physiologic features of each group are illustrated in Table 3-1. Lung mechanics were assessed in all subjects by spirometry, open circuit nitrogen lung volumes, and body plethysmography. Gas transport was assessed by steady-state carbon monoxide diffusing capacities (Dss).

There were 6 normal non-smoking subjects who were normal by all pulmonary functions tested. The 4 normal smokers averaged 15 years of cigarette smoking and also were normal by all parameters measured.

The 6 asthmatic patients were all asymptomatic, but 5 of 6 had reduced forced expiratory flow rates from 25 to 75% of the total capacity. Four also had increased specific resistance (SRaw) in the body plethysmograph and 3 were hyperinflated. All had normal diffusing capacities. Only 1 was normal by all parameters tested and therefore in a true remission.

Thirteen subjects had a histologically verified diffuse interstitial lung disease: 8 with sarcoidosis and 5 with diffuse interstitial fibrosis. Ten of these 13 subjects had classical restrictive patterns manifested by reductions in total lung capacity and 8 to 13 had abnormal diffusing capacities. In addition, 8 of 13 had reduced $FEF_{25-75\%}$ and 5 had increased

Table 3-1. MULTIBREATH $N_2$ WASHOUT STUDY

GROUP CHARACTERISTICS

| | FORCED EXPIRATION | STATIC VOLUMES | AIRWAY RESISTANCE | DIFFUSING CAPACITIES |
|---|---|---|---|---|
| NORMAL NON-SMOKERS (N = 6) | N | N | N | N |
| "NORMAL" SMOKERS (N = 4) | N | N | N | N |
| ASTHMATICS (N = 6) | ↓FEF (5/6) | ↑FRC (3/6) | ↑SRaw (4/6) | N |
| DILD SUBJECTS (N = 13) | ↓FEF (8/13) | ↓TLC (10/13) | ↑SRaw (5/13) | ↓Dss (8/13) |
| COPD SUBJECTS (N = 10) | ↓↓FEF (10/10) | ↑FRC (9/10) | ↑↑SRaw (10/10) | ↓Dss (8/10) |

specific resistance.

The classical extreme patterns of ventilation inhomogeneity were provided by 10 patients with chronic obstructive pulmonary disease, all of whom had moderate-to-severe obstructive ventilatory patterns and 8 of whom had abnormal carbon monoxide diffusing capacities.

Testing Procedure and Apparatus

In a relaxed, spontaneous fashion, the subject inhales and exhales through a flowmeter open to ambient air (Fig. 3-1). After he becomes adjusted to the situation, the subject inhales fully to the total lung capacity (TLC), exhales slowly as much gas as possible to the residual volume (RV) of the lung, and returns to spontaneous breathing about the functional residual capacity (FRC). Then, at the end of a quiet expiration, a valve is turned so that the inhaled gas is switched from ambient air to humidified oxygen. This begins the nitrogen washout procedure which continues over a number of breaths until the end-tidal $N_2$ fraction is less than 2% or 100 breaths are completed.

The expired gas is sampled continuously through a needle valve inserted at the mouthpiece which regulates the sampling flow rate (3ml/sec.). The sampled gas goes to a nitrogen analyzer (Med-Science 505),consist-

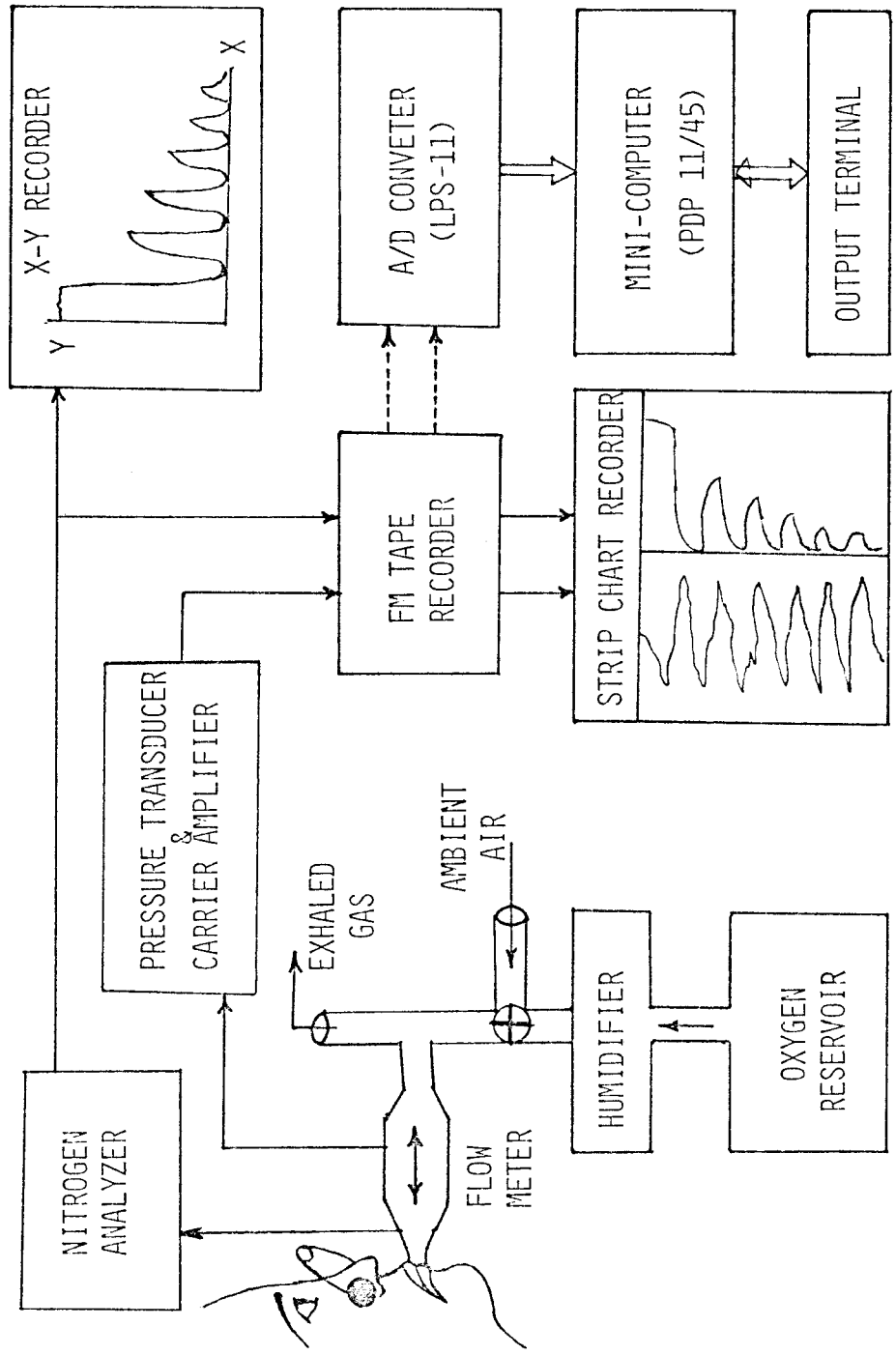


FIGURE 3-1 INSTRUMENT CONFIGURATION FOR MULTIBREATH NITROGEN WASHOUT.

ing of an ionization chamber and a vacuum pump (Welch Model 1410). The typical response time of 50-60 m/sec (Daniel, 1975) and accuracy of ± 0.2% are satisfactory for our studies. The flow meter is a heated screen pneumotachometer coupled to differential pressure transducer (Validyne, MP45) whose output is amplified and demodulated (Validyne CD19). The gain is set at 50 mv/V to keep output signal within ± 1 volt. Both the nitrogen and flow signals are recorded continuously on FM tape. The nitrogen and integrated flow signals are monitored simultaneously on a strip-chart recorder (Gould). In addition, the nitrogen signal is displayed on an X-Y recorder for easier determination of the end of the test.

Sources of Errors

In our experiment, several sources of error are possible. The obvious one is a gas leak, which most likely would occur around the connections and from the ionization chamber of the nitrogen analyzer. Drift, that is a slow change in output level at frequencies below 0.1 Hz, is not a problem because of the good stability of the instruments. Noise, however, is produced directly in the flow signal because of the sensitivity of the pressure transducer to mechanical shock and in the nitrogen signal from variation in the

sampling flow rate because of inconsistent performance of the vacuum pump. A more general source of noise is created by presence of devices run from 60-Hz line source. In addition, the use of a FM magnetic tape recorder introduces noise whose frequency components are higher than the signals of interest.

The measured signals must be synchronous and free of interference and noise. Furthermore, compensation is needed for the various nonlinearities, especially in the flow signal. Although signal filtering, conditioning, and delay compensation may be done by analog hardware, these can be accomplished with more flexibility by digital signal processing. In a later section, we shall discuss the method of error correction.

# CHAPTER IV

## SIGNAL PROCESSING

### Introduction

The nitrogen fraction and flow signals stored on FM tape are digitized with 12-bit accuracy in real time using the LPS-11 system of PDP 11/45 digital computer. Samples of these signals taken at 40 Hz are processed and retained in memory only long enough to compensate for the time-delay between the nitrogen and flow signals. The programs, which occupy only 14K of core memory when used with an overlay technique, consist of a set of subroutines linked by one main routine. The main program processing is controlled through a push-button console switch. This program includes entry of parameters and constants of the experiment, calibration of input signals, manipulation of peripheral devices, and control of data processing. The RSX-11M operating system facilitates the procedures.

Figure 4-1 presents the functional diagram of data processing which includes the following blocks:

1. Input: calibration factors and sampled

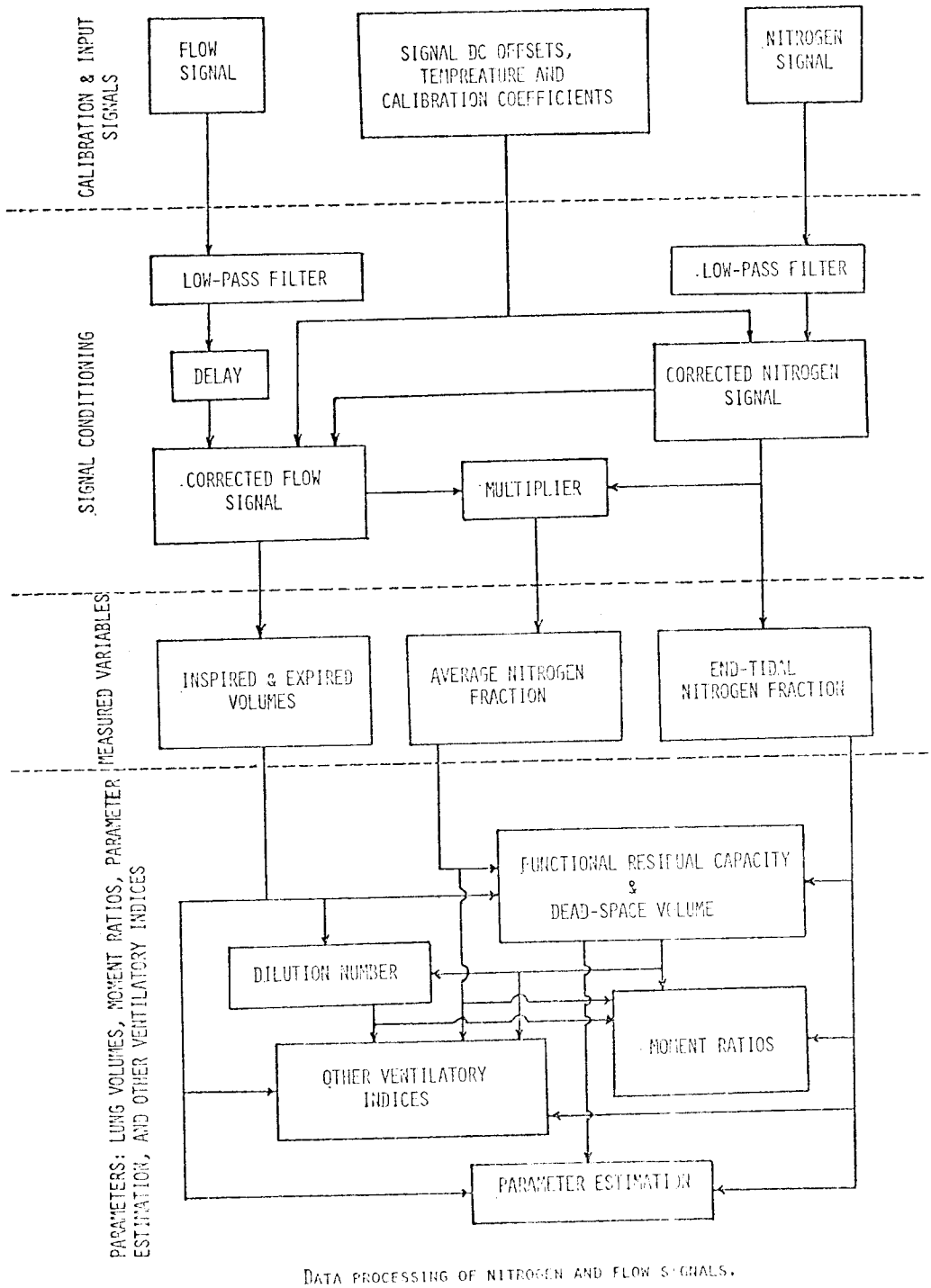


DATA PROCESSING OF NITROGEN AND FLOW SIGNALS.

Figure 4-1

input signals.

2. Signal conditioning: filtering, delay, and correction.
3. Variables on each breath: tidal volume, end-tidal nitrogen fraction, and average nitrogen fraction.
4. Derived quantities: lung volumes, dilution number, moments, optimal parameters, and other indices.

The main program description and computer flow chart are given in Appendix I.

Signal Conditioning

Calibration. With zero inputs to the nitrogen analyzer and pressure signal amplifier, the outputs are recorded for a few minutes before the washout test in order to compensate for the DC offsets. The nitrogen signal is calibrated by assuming that $N_2$ fraction in the ambient air and in the lung before washout is 0.796 (dry). The measured nitrogen signal is the nitrogen fraction ($F_{N_2}$), which is directly proportional to nitrogen concentration ($C_{N_2}$) by the ideal gas law. Consequently, the normalized nitrogen fraction and nitrogen concentration are identical.

$$\frac{F_{N_2}}{F^0_{N_2}} = \frac{C_{N_2}}{C^0_{N_2}} \equiv X$$

where the superscript zero indicates a reference value, e.g. at the start of experiment. In all calculations involving normalized nitrogen concentrations, the value of nitrogen fraction ratio can be substituted.

The flow signal is calibrated using a reciprocal (Harvard) pump which provides an oscillatory flow of ambient air through a pneumotachometer at 0.25 Hz with a cycle volume ($\Delta V$) of 1.000 Liter. The relationship between the measured pressure drop, $\Delta P(t)$, across the pneumotachometer and the flow rate, $Q(t)$, is given by

$$Q(t) = (K/\eta)\Delta P(t)$$

where K is the volume calibration coefficient and $\eta$ is the viscosity of air at ambient temperature (e.g. $\eta$ = 185.55 $\mu$ poise at 23°C). Integration of this equation over one-half a cycle yields

$$K = \eta\Delta V \; / \; \int \Delta P(t)dt$$

To get an accurate value of K, we calculate its mean value from several cycles. This coefficient is the same for flow in either direction. The criterion of acceptability of the K value is that its coefficient

of variation be less than 1%. If this criterion is not met, it is necessary to clean and dry the pneumotachometer screen and recalibrate. The calibration factors are stored on the disk and automatically become available when they are needed in the main program.

Signal filtering. In converting flow and nitrogen signals from analog to digital form, we can select an appropriate filter to improve the signal-to-noise ratio. For practical purposes, the flow and the nitrogen signals can be considered band limited at 10-20 Hz. Therefore, a low-pass filter with a cut-off frequency in this range is appropriate. This puts a lower bound on the sampling rate. If the sampling rate is too low, important information will be lost. If the sampling rate is too high, however, digital computer storage and processing will be unnecessarily large and time consuming. According to the sampling theorem, we chose the minimum sampling rate to be twice the highest frequency component which in this case would be 40 Hz. For the flow and nitrogen signals, we designed a second-order Butterworth low-pass filter with a frequency function H(f) given by

$$|H(f)|^2 = \frac{1}{1+(f/f_c)^4}$$

The cut-off frequency, $f_c$, is taken as 20 Hz. The Laplace transform of this frequency function is

$$H(S)H(-S) = \frac{1}{1+(S/j2\pi f_c)^4}$$

whose poles are equally spaced by $\pi/4$ on a circle of radius $2\pi f_c$ in the S-plane. To construct a stable and causal low-pass filter, we chose poles in the left half-plane of Butterworth circle. Thus, our specified Butterworth filter has the form

$$H(S) = \Omega_c^2/[S^2+ \sqrt{2}\,\Omega_c S + \Omega_c^2 ]$$

where $\Omega_c = 2\pi f_c$. The analog transfer function, H(S), is transformed into a digital transfer function D(Z), by the bilinear transformation:

$$S = \frac{2}{T}\,\frac{1 - Z^{-1}}{1 + Z^{-1}}$$

where T is the interval between the samples. Consequently, we find

$$D(Z) = \frac{a_0(1+2Z^{-1}+Z^{-2})}{1 + a_1Z^{-1}+a_2Z^{-2}}$$

where

$$a_0 = \Omega_c^2/\ (4/T^2+2\sqrt{2}\,\Omega_c/T + \Omega_c^2)$$

$$a_1 = (-8/T^2+2\Omega_c^2)/\ (4/T^2+2\sqrt{2}\Omega_c/T+\Omega_c^2)$$

$$a_2 = (4/T^2 - 2\sqrt{2}\,\Omega_c/T+\Omega_c^2)\ /\ (4/T^2 + 2\sqrt{2}\,\Omega_c/T+\Omega_c^2)$$

Now, let us define

$$D(Z) = Y(Z)/X(Z)$$

where Y (Z) represent the Z transform of filtered (output) samples and X(Z) represent the Z transform of unfiltered (input) samples. Taking the inverse of D (Z), we get the algorithm relating the unfiltered signal X(K) and the filtered signal Y(K):

$$Y(K) = a_0[X(K) + 2X(K-1)+X(K-2)] - [a_1Y(K-1) + a_2Y(K-2)]; \quad K=2,3, \ldots$$

where

$$Y(0)=Y(1)=0 \ , a_0=0.9048, a_1=1.6155, \text{ and } a_2=0.5853$$

Delay time compensation and starting identification. The response time of the nitrogen analyzer to a sudden change in nitrogen concentration can be divided into two parts: delay time and rise time. The time delay for sampled gas to travel from the sampling valve to the ionization chamber and become ionized is approximately 75 msec. Since we use the nitrogen signal for flow signal correction and must obtain the product of nitrogen and volume flow rate at the same time, it is important that the two signals be synchronous. Consequently, we delay the flow signal also by 75 msec.

The nitrogen signal may be used to find the beginning of the washout test. When the subject starts

inhaling pure oxygen, the nitrogen fraction drops precipitously. Processing of that washout test starts when this drop between two successive samples is greater than a given threshold, TH1. Taking into account the input signal range and number of bits in the A/D converter, we set TH1=3000/sampling rate.

Flow signal correction. The accurate measurement of volume flow rate at the mouth is essential in our data analysis. The calibration of the pressure signal is highly dependent on the composition and temperature of the gas passing through the pneumotachometer. The differences are particularly noticeable between inspired and expired gases. While the inspired gas consists of humidified oxygen at ambient temperatures, the gas leaving the mouth is saturated with water close to body temperature. Unless the screen of the pneumotachometer is heated, water vapor can condense on it to cause a change in resistance, i.e., a change in the calibration coefficient of the pressure signal.

Provided the flow is laminar, we can relate the volume flow rate Q(t) and pressure difference $\Delta P(t)$ across the pneumotachometer screen by

$$Q(t) = K \frac{\Delta P(t)}{\eta(\underline{X}, \overline{T})}$$

where $\eta$, the gas viscosity is function of temperature,

T, and gas composition, $\underline{X} = (N_2, O_2, H_2, CO_2)$ and K is a geometrical constant. Since the mixture of gas species can be considered an ideal gas, the viscosity of the mixture can be formulated as the linear combination of viscosities of pure gas weighted by their fractional concentrations $F_\alpha$:

$$\eta(T) = \sum_\alpha F_\alpha \eta_\alpha(t)$$

where $\alpha = N_2, O_2, H_2O, CO_2$.

The temperature changes are sufficiently small to allow the viscosities of $O_2$, $N_2$, $H_2O$, and $CO_2$ to be related linearly to temperature (Blumenfeld, 1973):

$$\eta(T) = \begin{pmatrix} \eta_{N_2}(T) \\ \eta_{O_2}(T) \\ \eta_{H_2O}(T) \\ \eta_{CO_2}(T) \end{pmatrix} = \begin{pmatrix} 43.93 + 0.453T \\ 118.50 + 0.298T \\ -23.0 + 0.570\ T \\ 16.25 + 0.455\ T \end{pmatrix} 10^{-6} \text{ poise}$$

where T is absolute temperature. The fractional concentration of $H_2O$ and $CO_2$ in inspired gas, expired gas, and ambient air are assigned reasonable values (Table 4-1). We assume that the fractions of nitrogen and oxygen sum to a constant value. The inspired gas has the ambient temperature of approximately $T_I = 23°C$, while the expired gas is cooled from body temperature to mean value of $T_E = 34°$ C at the pneumotachometer

Table 4-1. The fractional concentration of inspired gas, expired gas, and ambient air.

| SPECIES FRACTION | INSPIRATION | EXPIRATION | AMBIENT AIR |
|---|---|---|---|
| $^{*}F_{N_2}$ | $F_{N_2}(t)$ | $F_{N_2}(t)$ | 0.790 |
| $F_{O_2}$ | $0.972-F_{N_2}(t)$ | $0.896-F_{N_2}(t)$ | 0.200 |
| $^{+}F_{H_2O}$ | 0.028 | 0.062 | 0.007 |
| $F_{CO_2}$ | 0 | 0.041 | 0.003 |

*At the beginning of inspiration, there is some nitrogen left from previous expiration in our instrumental dead space. Therefore $F_{N_2}(t)$ is not zero until the dead space is cleared.

+The fractional concentration of water vapor, assuming complete saturation, may be approximated by $F_{H_2O} = (13.20-0.61T+0.04T^2)/P$, where temperature, T, is in centigrade and pressure, P is in mm Hg.

screen. This was found by direct experimental measurement with a thermistor. Consequently, the volume flow rate at body temperature can be given by

$$Q(t) = K\left(\frac{T_B}{T_p}\right) \frac{\Delta P(t)}{(A(T_p) - B(T_p)\, F_{N_2}(t))}$$

where during inspiration, $T_p = T_I$ , $A(T_I) = 205.3$, and $B(T_I) = 28.9$, and during expiration $T_p = T_E$ , $A(T_E) = 204.7$, and $B(T_E) = 27.0$.

Variables and Parameters

Measured variables. A zero-crossing technique is applied to discriminate inspiration from expiration as shown in Figure 4-2. Integration (by the trapezoid method) of the flow signal allows computation of maximum expiratory volume, maximum inspiratory volume, and also tidal volume during the washout test. The inspiratory and expiratory volumes over the breath K are given by

$$\Delta V(K,I) = \int_{I(K)} Q(t)\,dt \quad , \quad \Delta V(K,E) = \int_{E(K)} Q(t)\,dt$$

where $\Delta V(K,I)$ and $\Delta V(K,E)$ are the magnitudes of the volume changes on inspiration and expiration. The end-tidal nitrogen fraction, $F(K)$, is determined by searching for the maximum point in nitrogen signal during K-th period, as shown in Figure 4-2. Multiplication

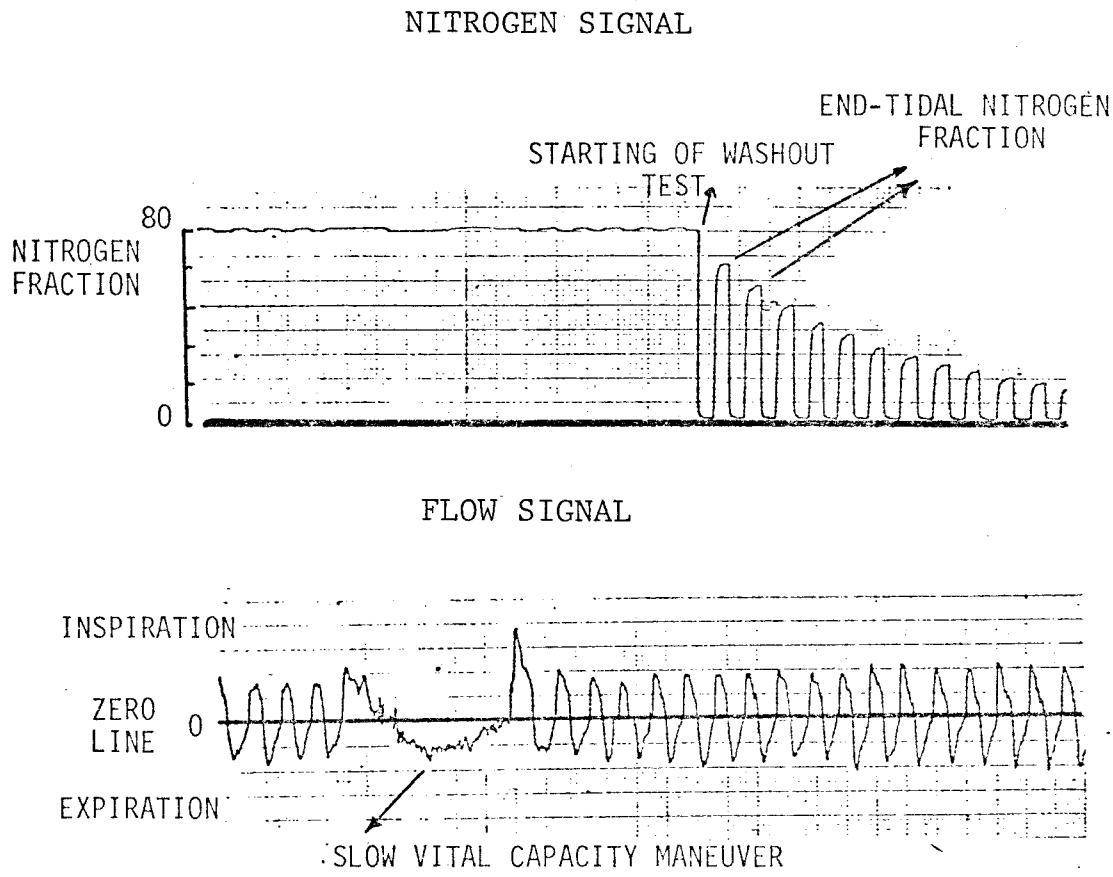


Figure 4-2 Flow and nitrogen signals

of the synchronized nitrogen and flow signals leads to an estimation of averaged expired nitrogen fraction, $\langle F \rangle_K$, in breath K:

$$\langle F \rangle_K = \int_{E(K)} F(t)Q(t)dt/\Delta V(K,E)$$

The accuracy of computer calculation of variables (F(K), $\langle F \rangle_K$, $\Delta V(K,I)$, and $\Delta V(K,E)$) were independently verified by several techniques. In particular, F(K) was directly measured from the X-Y recorder. Volume amplitudes were checked with pump volumes, and the total amount of nitrogen expired over several breaths was measured from a collection bag. We find that the difference between computer and measured variables is typically ± 1%.

Lung Volumes. The dead-space volume may be estimated for any breath K as

$$V_D = \Delta V(K,E)(1-\langle F \rangle_K/F(K))$$

For typical tidal volumes (400-700 ml.) and breathing frequencies (8-20 breaths/min.) during spontaneous breathing the change in dead-space volume is not large. Nevertheless, to get a reliable estimate of $V_D$, we average $V_D$ over the first five breaths for which the expired nitrogen signal has a large signal-to-noise ratio. Experimentally, the dead-space volume

is actually the sum of anatomical dead space and instrumental dead space between the mouth and nitrogen sampling point. The latter, measured directly by water volume, is found to be 50 ml.

Functional residual capacity (FRC) is derived from the measured variables:

$$FRC \equiv V(0,E) = \sum_{J=1}^{K} \langle F_J \rangle \, \Delta V(J,E) / [F(0)-F(K)]$$

$$+ \sum_{J=1}^{K} [\Delta V(J,I)-\Delta V(J,E)] / [F(0)/F(K)-1]$$

Once we estimate the FRC, the alveolar-space volume after breath K is given by

$$V_A(K,E) = FRC-V_D + \sum_{J=1}^{K} [\Delta V(J,I)-\Delta V(J,E)]$$

In addition to the FRC, we compute the following volume parameters: vital capacity (VC), residual volume (RV), and total lung capacity (TLC).

As the number of breaths increase, the calculated value of FRC on each breath K asymptotically approaches the final value. The asymptotic value takes more breaths to approximate when the ventilation and mixing in the lung is less uniform. For practical purposes, we assume that sufficient mixing occurs when the cumulative expired volume (CEV) is 10 times FRC. Ending washout tests before CEV/FRC is sufficiently

large can cause a significant loss of information. When CEV/FRC becomes too large, undue emphasis is given to the tail region of washout curve which has a low signal-to-noise ration. Qualitatively, the ratio CEV/FRC indicates the number of times the resting lung volume (FRC) has been diluted with an equal amount of $N_2$-free inspired gas. We call this ratio the dilution number $\eta$. Its value after breath K is

$$\eta_K = \sum_{J=1}^{K} \Delta V(J,E)/FRC$$

Moments. Over the domain $0 \leq \eta_K \leq 10$, a moment analysis is performed. The moments in discrete form are computed by

$$M_r = \sum_{K=1}^{N} (\eta_K)^r \delta_K [\eta_K - \eta_{K-1}]$$

where

$$\delta_k = F(K)/F(0) \text{ or } \langle F \rangle_K / F(0)$$

Since the experimental procedure is stopped when $F(N)/F(0) = 0.025$, it may happen that $\eta_N$ does not reach 10. For that special case, we extrapolate the washout curve by assuming $F(N)/F(0) = 0$ at $\eta_K = 10$; hence, we compute

$$M_r = (10)^r \cdot \delta_N [10 - \eta_N]/2$$

The correction term is usually less than 2% of $M_r$.

From the moments $M_0$, $M_1$, and $M_2$, we compute the ratio $M_1/M_0$ and $M_2/M_0$ and the coefficient of variation

$$CV = [M_2 M_0 / M_1^2 - 1]^{\frac{1}{2}}$$

Other indices. Computational algorithms of the other ventilation indices are as follows:

Lung clearance index (LCI). This is computed as the dilution number up to breath N at which the normalized end-tidal nitrogen fraction is $X(N) \equiv F(N)/F(0) = 0.025$:

$$LCI = \eta_N$$

Mixing ratio (MR). This is the ratio of the actual number (N) of breaths to the ideal number (NI) of breaths at which the normalized nitrogen fraction X(N) is 0.025:

$$MR = (N/NI)\Big|_{X(N)=0.025}$$

where

$$NI = -\ell n[F(N)/F(0)] \; / \ell n[1+(\langle V_T \rangle - V_D)/FRC]$$

and

$$\langle V_T \rangle = \sum_{J=1}^{N} [\Delta V(J,I) + \Delta V(J,E)]/2N$$

Ventilatory efficiency ($E_{90\%}$). This is the ratio of the ideal cumulative expired volume to the actual cumulative expired volume up to breath N at which X (N)= 0.1.

$$E_{90\%} = \langle V_T \rangle \, NI / \sum_{J=1}^{N} \Delta V(J,E)$$

Note, NI is calculated from the ideal lung model which includes the dead space.

Index of alveolar ventilation (ICC/MCC). This index is computed as the ratio of the ideal clearance coefficient (ICC) to the measured clearance coefficient (MCC) up to breath N at which X(N) = 0.025.

$$ICC = \langle V_T \rangle \, NI / [1-F(N)]FRC$$

and

$$MCC = \sum_{J=1}^{N} \Delta V(K,I) / \sum_{K=1}^{N} \langle F \rangle_K \, \Delta V(K,E)$$

Note, NI is calculated from the ideal lung model which includes the dead space.

Becklake index (BI). This is the ratio of the actual cumulative expired volume up to breath N at which X (N) = 0.125 to 90% of FRC.

$$BI = \sum_{J=1}^{N} \Delta V(J,E) / [1-F(N)] \, FRC$$

Five breath index (5BI). This is the ratio of the actual nitrogen expired to the nitrogen ideally expired in the first five breaths of washout, which is computed as

$$5BI = \sum_{J=1}^{5} \langle F \rangle_J \Delta V(J,E) / \sum_{J=1}^{5} \hat{F}(J)[\Delta V(J,E) - V_D]$$

where

$$\hat{F}(J) = \frac{F(J-1)\left[\sum_{K=1}^{J-1}[\Delta V(K,I) - \Delta V(K,E)] + FRC\right]}{FRC + \Delta V(J,I) - V_D + \sum_{K=1}^{J-1}[\Delta V(K,I) - \Delta V(K,E)]}$$

for $J = 1,2, \ldots ,5$. Note that the sum is zero for $J = 1$.

Model parameter evaluation. To estimate the model parameters, $f_2$ and $v_2$, we use the following modified Gauss-Newton algorithm to minimize the objective function:

1. Make an initial guess (i=0) of the unknown parameters within the feasible region, $\underline{\theta}^o = [.3, .8]^T$, select appropriate initial values of the constraint vector, $\underline{\lambda} = [10^{-3}, 10^{-3}, 10^{-3}]^T$, and choose the Marquardt factor, $\gamma = 10^{-2}$.

2. Solve the model equations,

3. Evaluate the objective function.

4. Compute the components of the gradient vector and the approximated elements of hessian matrix.

5. Solve for the next estimate of the parameter vector.

$$\underline{\theta}^{i+1} = \underline{\theta}^i - \hat{H}_i^{-1} \underline{q}_i$$

6. For the new value of parameters, $\underline{\theta}^{i+1}$, solve the model equations and evaluate the objective function.

7. If $\Phi(\underline{\theta}^i) - \Phi(\underline{\theta}^{i+1}) < 10^{-3}$, reset $\gamma$ and $\lambda$ to

zero and go to step 9; otherwise

8. Replace the old value of parameter, $\underline{\theta}^i$, by new values, $\underline{\theta}^{i+1}$. Reset $\gamma$ by $\gamma/i^2$, and $\lambda$ by $\lambda/i^2$ on each iteration (i). Then, return to step 4.

9. If

$$\Phi(\underline{\theta}^i)-\Phi(\underline{\theta}^{i+1})>10^{-5}$$

and

$$|\theta_j^{i+1}-\theta_j^i|/(\theta_j^i+10^{-4}) >10^{-3} \; ; \; j=1,2$$

hold true, replace $\underline{\theta}^i$ by $\underline{\theta}^{i+1}$ and return to step 4; otherwise we take $\underline{\theta}^i$ to be the optimal solution, $\underline{\theta}^*$.

# CHAPTER V

## EVALUATION OF INDICES

In the evaluation of indices of ventilation inhomogeneity, we examine the sensitivity of the indices to the degree of abnormality and the variability of the indices for a given subject and among subjects in a given diagnostic group. For each subject, we have two values of all parameters and indices denoted by $Z_1(I,J,L)$ and $Z_2(I,J,L)$ where I is the parameter or index, J is the diagnostic group, and L is the subject in the diagnostic group J. For each subject, we compute an average

$$AZ(I,J,L) = (Z_1 + Z_2)/2$$

and a relative difference

$$RD(I,J,L) = |Z_1 - Z_2|/AZ$$

As measures of sensitivity among diagnostic groups, we can define for each group J, having Q(J) subjects, a mean

$$MZ(I,J) = \sum_{L=1}^{Q(J)} AZ(I,J,L)/Q(J)$$

and a standard deviation

$$SDZ(I,J) = \left[\sum_{L=1}^{Q(J)} [AZ-MZ]^2/Q(J)\right]^{\frac{1}{2}}$$

The variability of the parameters and indices are characterized for all subjects by a mean and standard deviation of the relative difference:

$$MRD(I) = \sum_{J=1}^{P} \sum_{L=1}^{Q(J)} RD \Big/ \sum_{J=1}^{P} Q(J)$$

$$SDRD(I) = \left[ \sum_{J=1}^{P} \sum_{L=1}^{Q(J)} [RD-MRD]^2 \Big/ \sum_{J=1}^{P} Q(J) \right]^{\frac{1}{2}}$$

In the sections following, we discuss lung volume ratios, moment ratios, and flow-volume distribution index. Furthermore, other indices given in the literature are compared to moment ratios.

Volume Ratios. The estimated values of functional residual capacity (FRC) computed on each breath approach an asymptote at a rate which depends on the uniformity of mixing in the lung. In abnormal lungs, in which mixing between inspired and residual gases tends to be less than in normal lungs, it takes more breaths or a greater dilution number to approximate the value of FRC (Fig. 5-1). The mean variability (MRD) of FRC is 6.4%. From the five-breath estimate of the dead-space volume, $V_D$, the mean variability is 12.1%.

From FRC and maximal inspiratory and expiratory volumes, we can compute other lung volumes, such as residual volume (RV), vital capacity (VC), and total

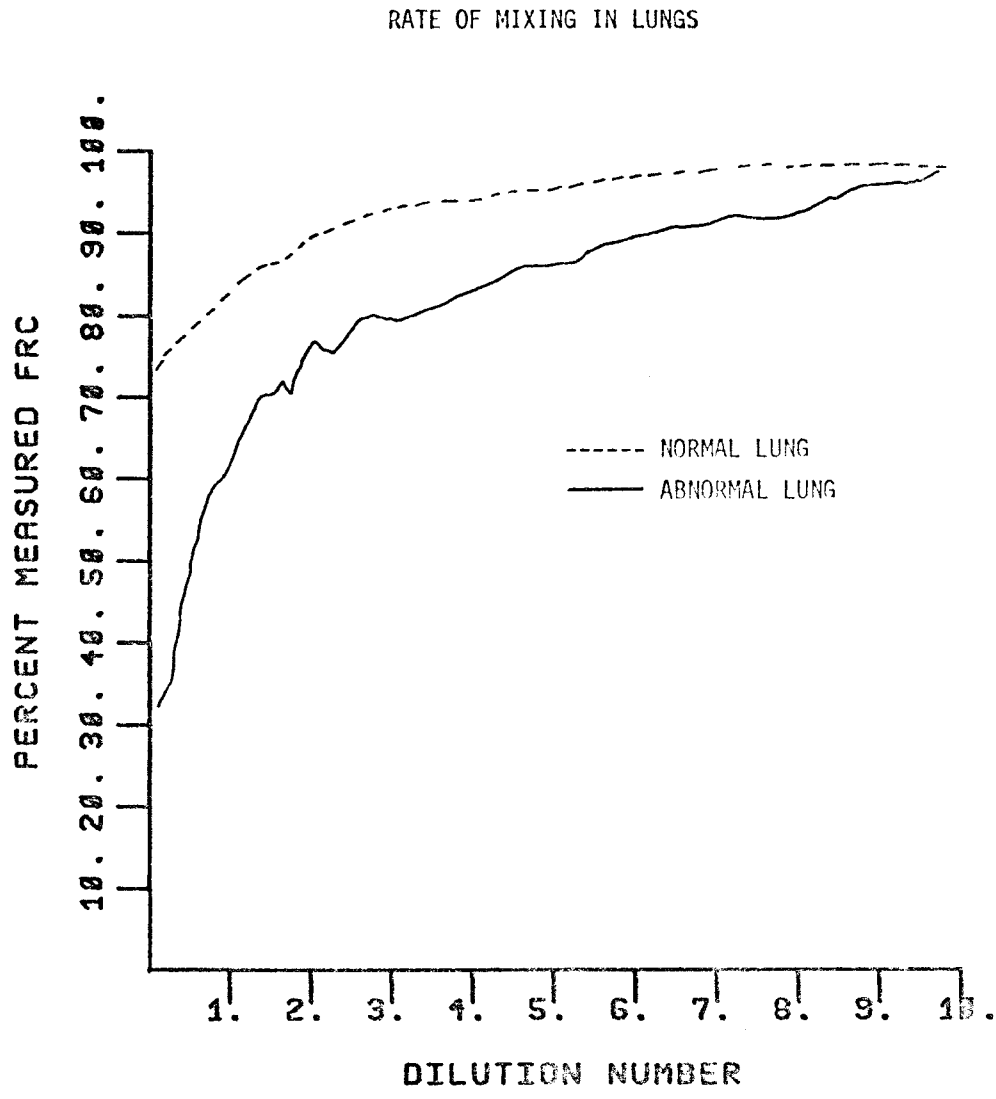
RATE OF MIXING IN LUNGS
PERCENT MEASURED FRC
10. 20. 30. 40. 50. 60. 70. 80. 90. 100.
NORMAL LUNG
ABNORMAL LUNG
1. 2. 3. 4. 5. 6. 7. 8. 9. 10.
DILUTION NUMBER

Figure 5-1

lung capacity (TLC). Although these volume parameters are useful in the diagnosis of certain abnormalities, they are highly dependent on the size, sex, age, and other characteristics of an individual. Volume ratios, e.g., FRC/TLC and VC/FRC, reduce the effects of these factors. A comparison among different volume ratios is illustrated in Figure 5-2, with the subjects in our study. We find that FRC/TLC or VC/FRC tends to separate the COPD group from other diagnostic groups, but the other volume ratios do not display diagnostic clustering.

Moment ratios. From the normalized end-tidal and average-expired nitrogen concentrations $(X_K, \langle X \rangle_K)$ as functions of dilution number $(n_k)$, we compute moment ratios $M_1/M_0$ and $M_2/M_0$ which characterize the shape of washout. The mean (MZ) and standard deviation (SDZ) of the moment ratios are given in Table 5-1. A comparison among moment ratios (Figure 5-3) shows $(M_1/M_0)_x$ is nearly linearly related to $(M_2/M_0)_x$, $(M_1/M_0)_{\langle x \rangle}$, and $(M_2/M_0)_{\langle x \rangle}$. As given in Table 5-1, $(M_1/M_0)_x$ has the least variability among the moment ratios. The variability of second moment ratios are greater because higher weighting is given to the tail of washout which has a lower signal-to-noise ratio. Since $(M_1/M_0)_x$ has the least variability among

DIAGNOSTIC SENSITIVITY COMPARISON OF VC/FRC
VERSUS FRC/TLC

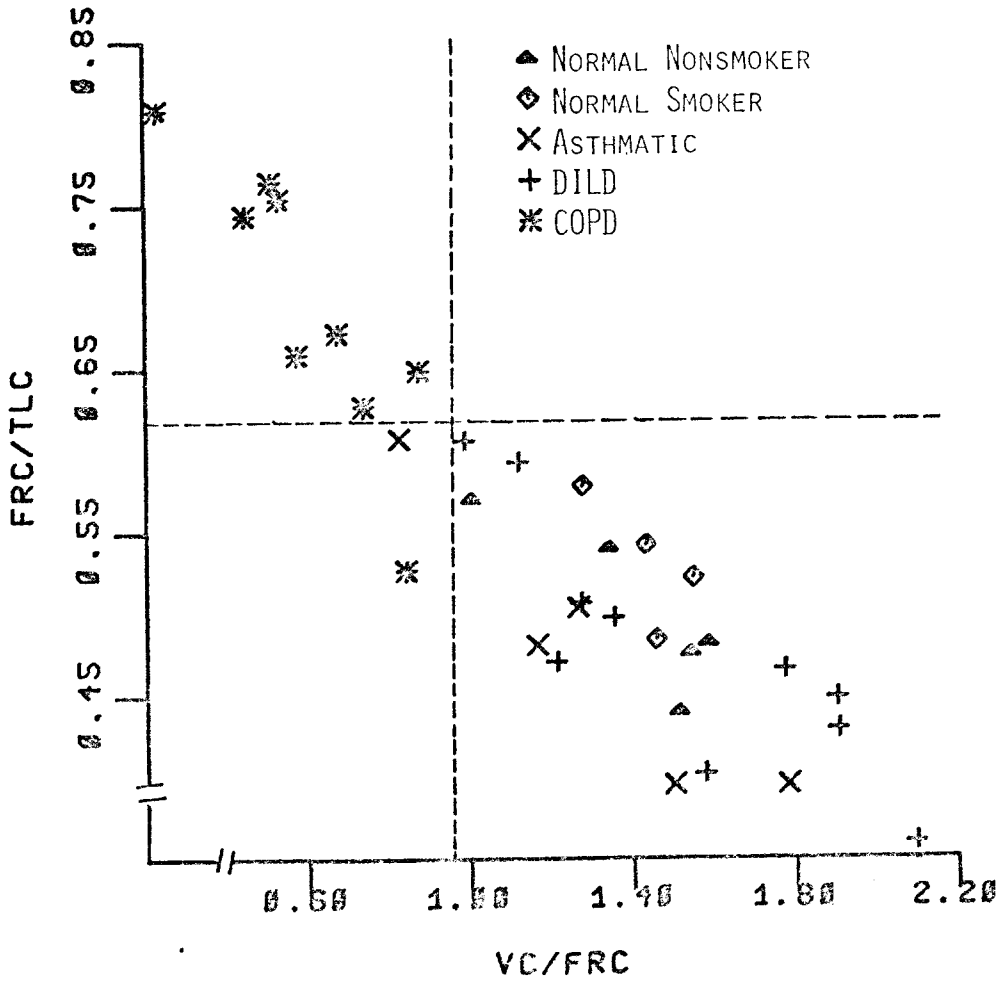


Figure 5-2A

DIGNOSTIC SENSITIVITY COMPARISON OF RV/VC
VERSUS RV/TLC

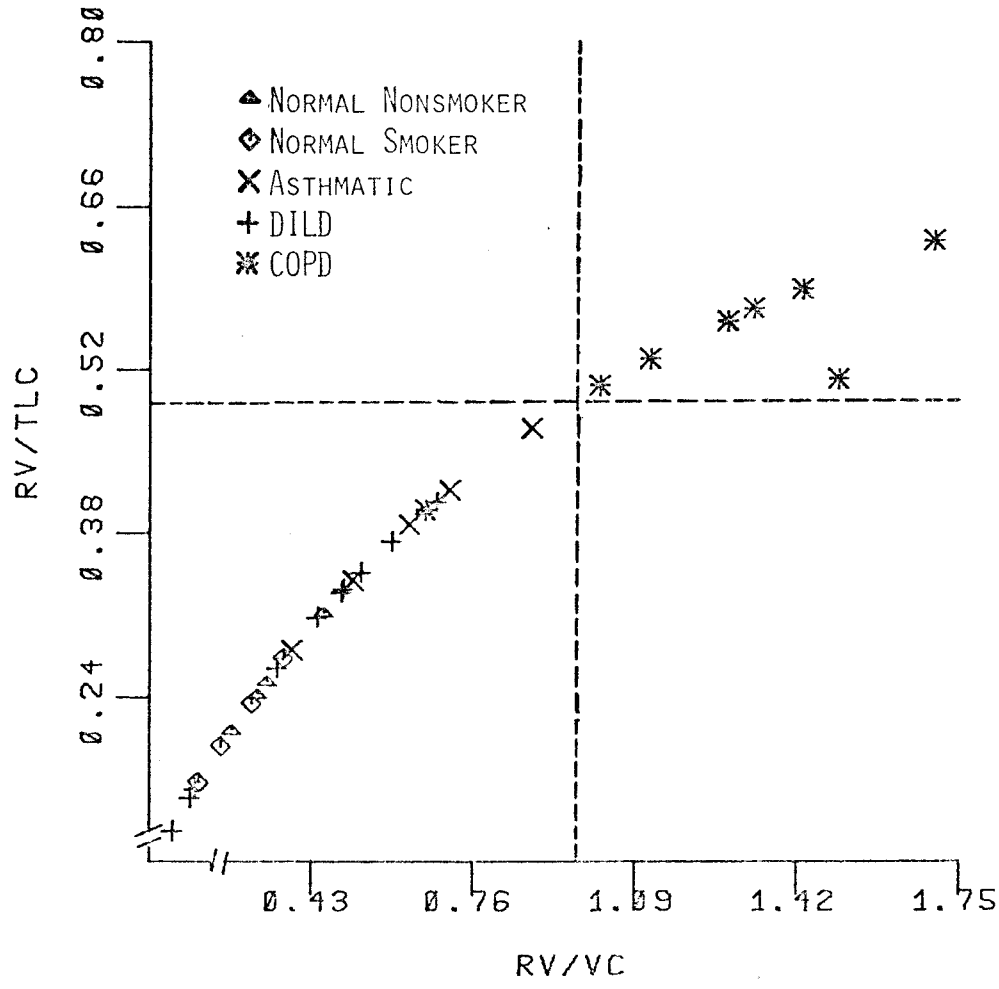


Figure 5-2B

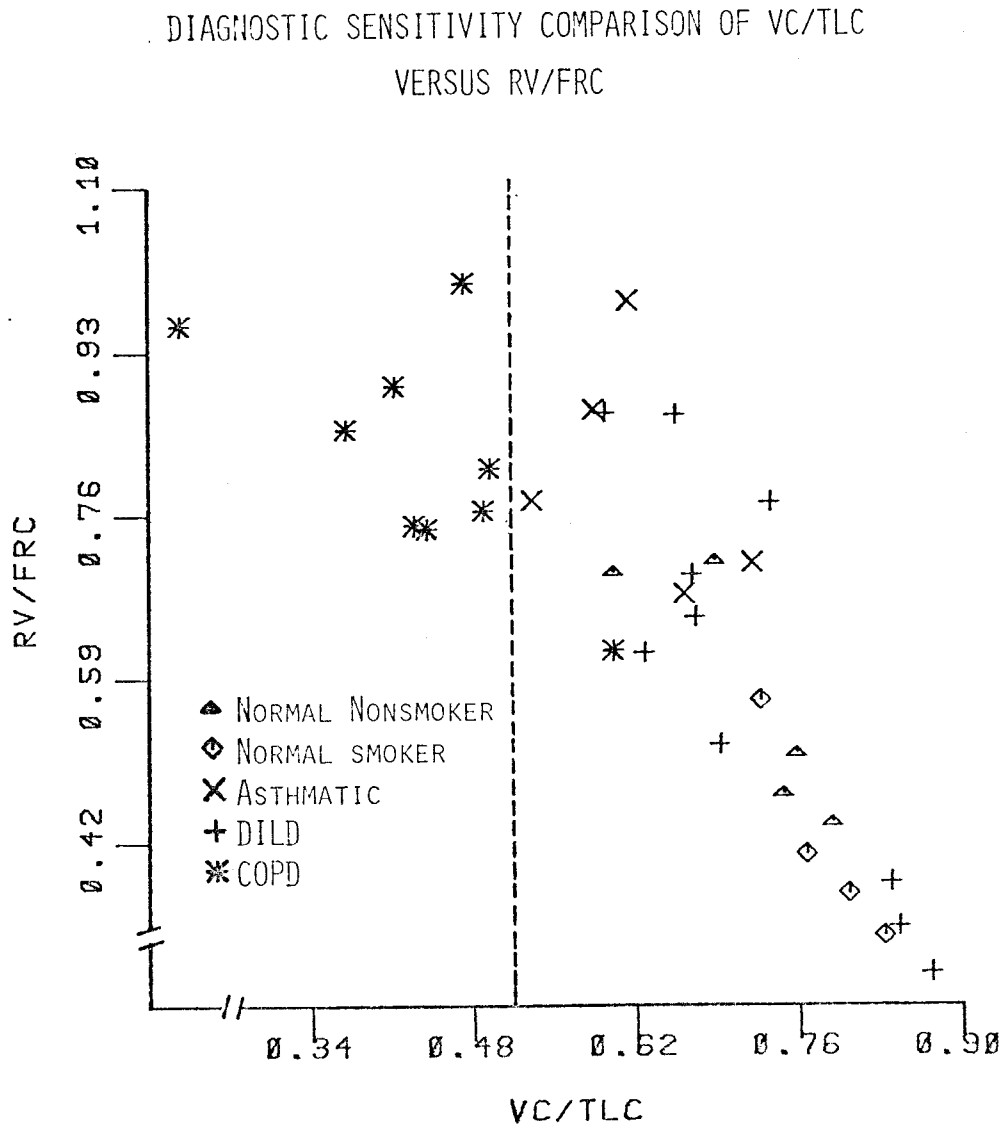
DIAGNOSTIC SENSITIVITY COMPARISON OF VC/TLC
VERSUS RV/FRC
RV/FRC
1.10
0.93
0.76
0.59
0.42
NORMAL NONSMOKER
NORMAL SMOKER
ASTHMATIC
DILD
COPD
0.34
0.48
0.62
0.76
0.90
VC/TLC

Figure 5-2C

Table 5-1 Sensitivity and variability of moment ratios for diagnostic groups.

| | $(M_1/M_0)_x$ | | | $(M_2/M_0)_x$ | | | $(M_1/M_0)_{<x>}$ | | | $(M_2/M_0)_{<x>}$ | | |
|---|---|---|---|---|---|---|---|---|---|---|---|---|
| | MZ | SDZ | Range | MZ | SDZ | Range | MZ | SDZ | Range | MZ | SDZ | Range |
| Normal Nonsmokers | 2.01 | 0.12 | 1.77-2.19 | 7.57 | 1.02 | 5.56-8.90 | 1.84 | 0.12 | 1.61-2.04 | 6.66 | 0.96 | 4.84-8.05 |
| Normal Smokers | 2.34 | 0.12 | 2.18-2.49 | 10.08 | 0.72 | 8.90-10.83 | 2.16 | 0.16 | 1.98-2.41 | 9.24 | 0.96 | 8.12-10.76 |
| Asthmatics | 2.55 | 0.24 | 2.40-2.98 | 11.78 | 2.06 | 9.85-15.25 | 2.28 | 0.17 | 2.13-2.56 | 10.26 | 1.47 | 8.97-12.63 |
| COPD Subjects | 3.10 | 0.28 | 2.65-3.55 | 16.45 | 2.62 | 13.04-20.65 | 2.80 | 0.22 | 2.40-3.09 | 14.48 | 2.09 | 11.23-17.57 |
| DILD Subjects | 2.73 | 0.25 | 2.28-3.07 | 13.09 | 2.06 | 9.44-15.86 | 2.41 | 0.22 | 2.13-2.67 | 11.21 | 1.62 | 8.54-14.27 |
| VARIABILITY MRD ± SDRD% | 5.05 ± 3.24 | | | 10.01 ± 8.12 | | | 6.40 ± 4.68 | | | 12.10 ± 9.06 | | |

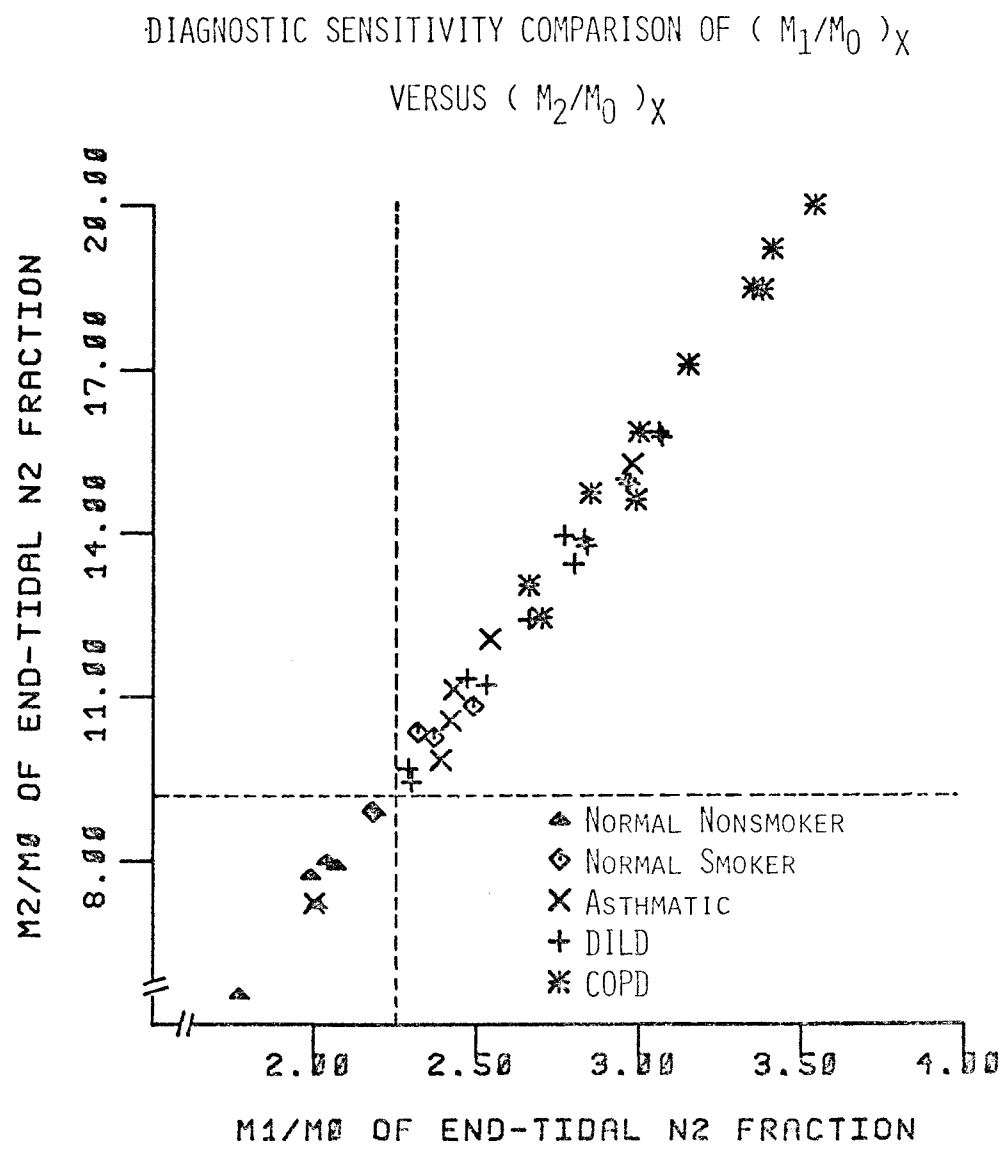
DIAGNOSTIC SENSITIVITY COMPARISON OF ( M1/M0 )X
VERSUS ( M2/M0 )X
M2/M0 OF END-TIDAL N2 FRACTION
8.00
11.00
14.00
17.00
20.00
NORMAL NONSMOKER
NORMAL SMOKER
ASTHMATIC
DILD
COPD
2.00
2.50
3.00
3.50
4.00
M1/M0 OF END-TIDAL N2 FRACTION

Figure 5-3A

DIAGNOSTIC SENSITIVITY COMPARISON OF $( M_1/M_0 )_X$
VERSUS $( M_1/M_0 )_{<X>}$

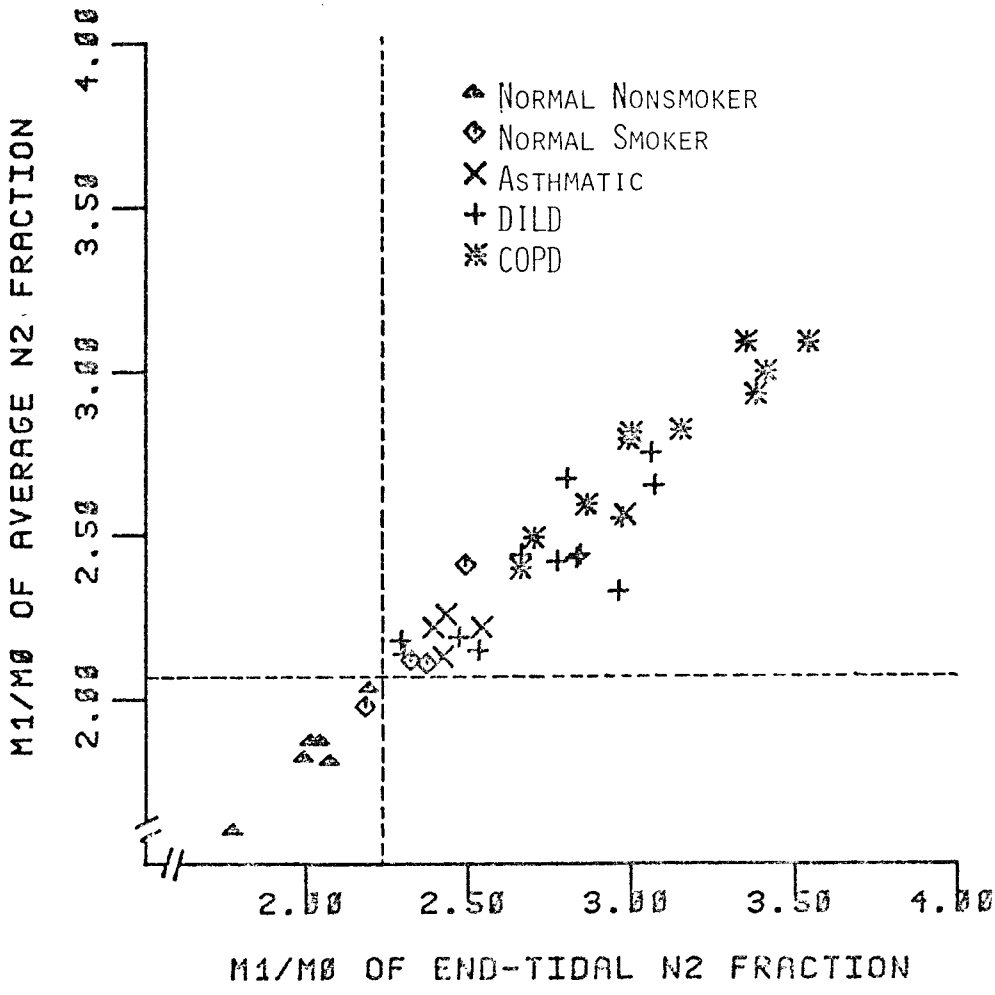


Figure 5-3B

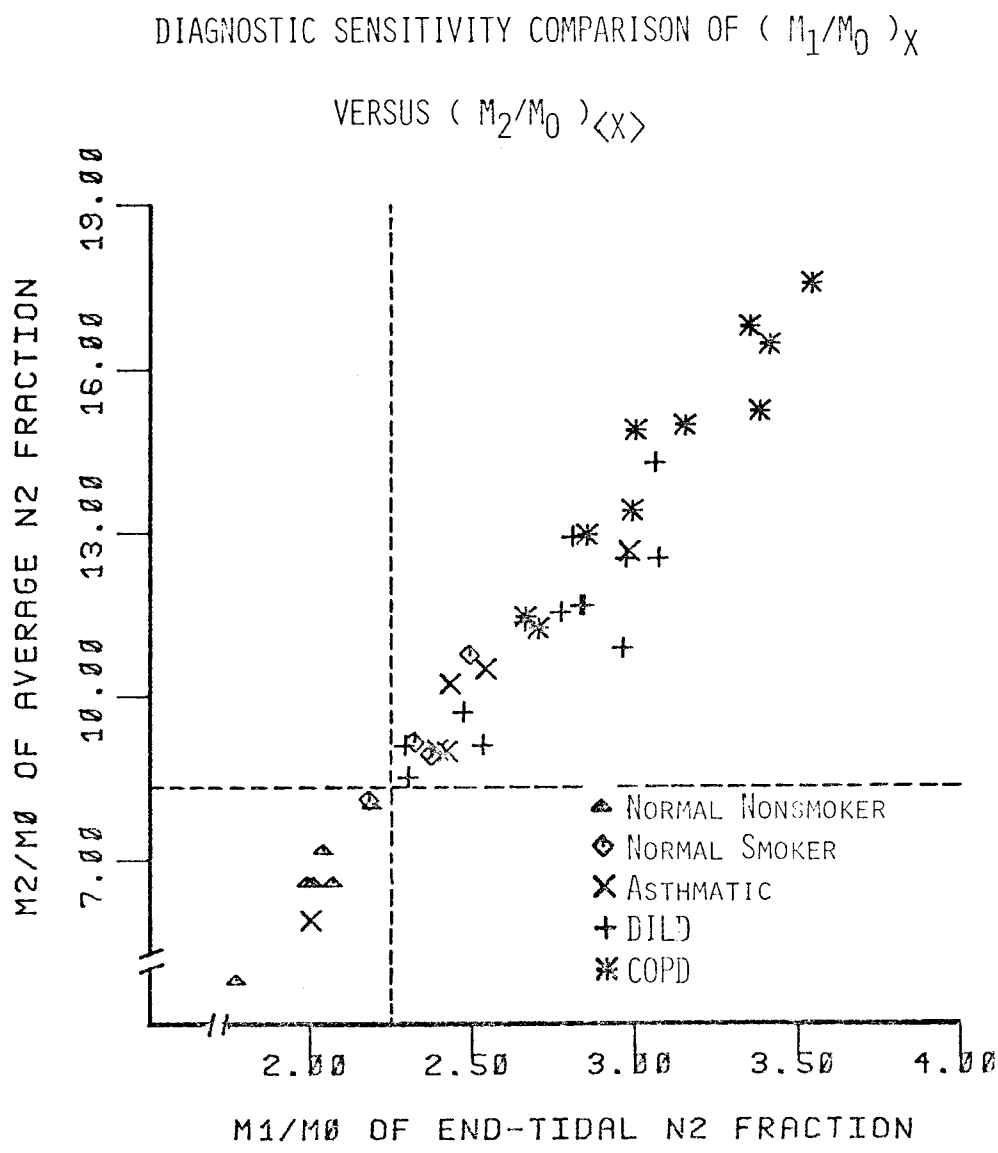
DIAGNOSTIC SENSITIVITY COMPARISON OF ( $M_1/M_0$ )$_X$
VERSUS ( $M_2/M_0$ )$_{\langle X \rangle}$
M2/M0 OF AVERAGE N2 FRACTION
7.00
10.00
13.00
16.00
19.00
2.00
2.50
3.00
3.50
4.00
M1/M0 OF END-TIDAL N2 FRACTION
NORMAL NONSMOKER
NORMAL SMOKER
ASTHMATIC
DILD
COPD

Figure 5-3 C

the moment ratios and is almost linearly related to the others, we take it the index of choice among the moment ratios.

With respect to normal non-smokers, the mean values (MZ) of $(M_1/M_0)_x$ are 16% greater for normal smokers, 27% greater for asthmatics, 36% greater for DILD subjects, and 54% greater for COPD subjects. By the moment ratios, abnormal subjects including the normal smokers are well discriminated from the normal non-smokers. The symptomatic asthmatics have moment ratios higher than normals; in remission, however, asthmatics have have normal values for all the pulmonary function tests applied including the indices of $N_2$ washout. Although the mean of $(M_1/M_0)_x$ for COPD subjects is higher than the means for asthmatics and DILD subjects by 27% and 18% respectively, some asthmatics and DILD subjects have moment ratios as high COPD subjects. To distinguish COPD subjects from subjects in other diagnostic groups, we can plot $(M_1/M_0)_x$ versus VC/FRC (Figure 5-4).

Flow-Volume distribution index. The model parameters, alveolar volume fraction $v_2$ and flow fraction $f_2$, are estimated by minimizing the residuals between the model solution and washout data. Even for a given individual, the values of the parameters $v_2$ and $f_2$ vary greatly on repeated washouts. The absolute

DIAGNOSTIC SENSITIVITY COMPARISON OF $( M_1/M_0 )_X$ VERSUS VC/FRC

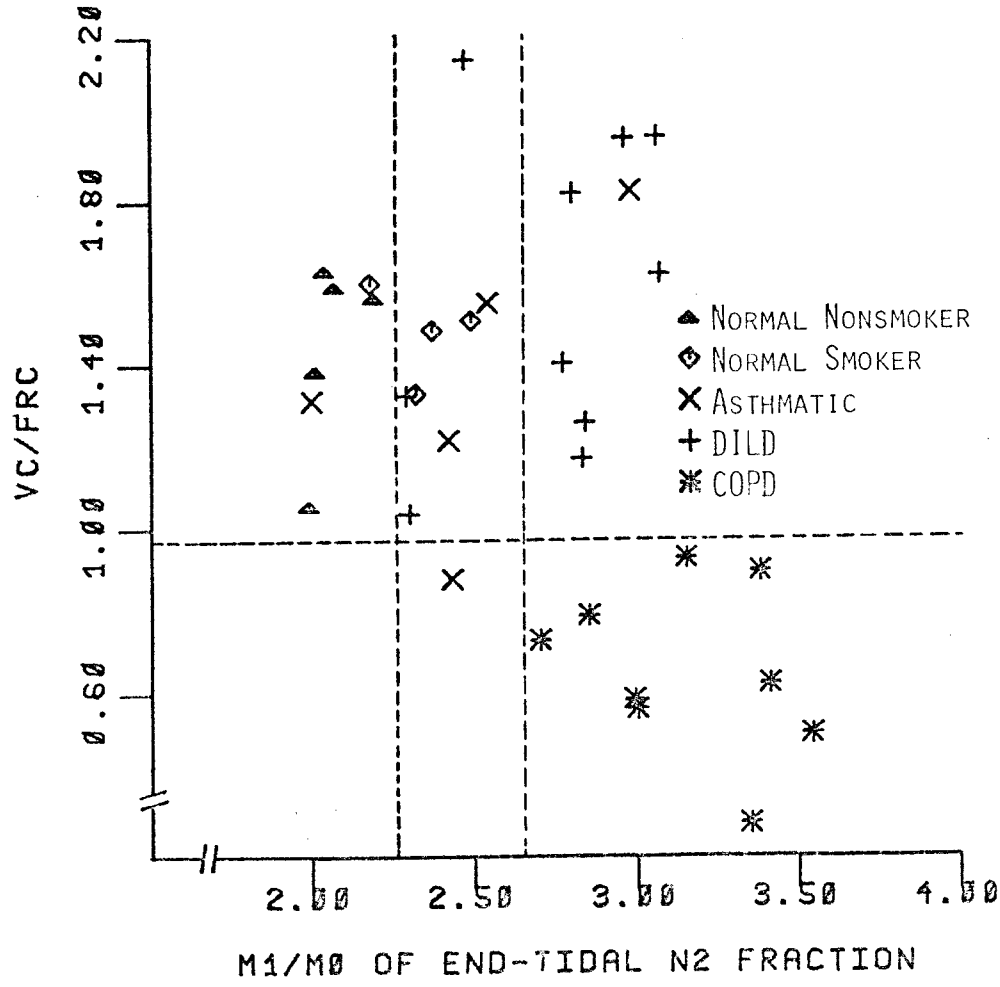


Figure 5-4

difference of these parameter values $|f_2-v_2|$, however, is much more reproducible. Yet, the mean relative difference of $|f_2-v_2|$ is 11%, which is not satisfactory. Noise in the data can account for some of the variability, but the inadequacy of the model may also be a factor. For some data sets, we could not estimate the optimal parameters, which might be a limitation of our optimization algorithm. Optimization for parameter estimation requires more computational time than evaluation of moments or other indices of ventilatory dysfunction. Graphically, the $(M_1/M_0)_x$ and flow-volume distribution index are compared in Figure 5-5. From these data, the flow-volume distribution index does not appear to yield additional information.

4. Comparison of ventilatory indices. We estimated and compared the values of the following indices: Becklake Index (BI), lung clearance index (LCI), ventilatory efficiency ($E_{90\%}$), mixing ratio (MR), index of alveolar ventilation (IAV), and five-breath index (5BI). The mean values (MZ) and standard deviation (SDZ) of these indices for the various diagnostic groups are given in Table 5-2. Furthermore, the mean values of these indices were normalized in reference to normal subjects and illustrated in Figure 5-6 for comparison with moment ratios. The various indices

DIAGNOSTIC SENSITIVITY COMPARISON OF ( $M_1/M_0$ )$_X$
VERSUS FLOW-VOLUME DISTRIBUTION INDEX

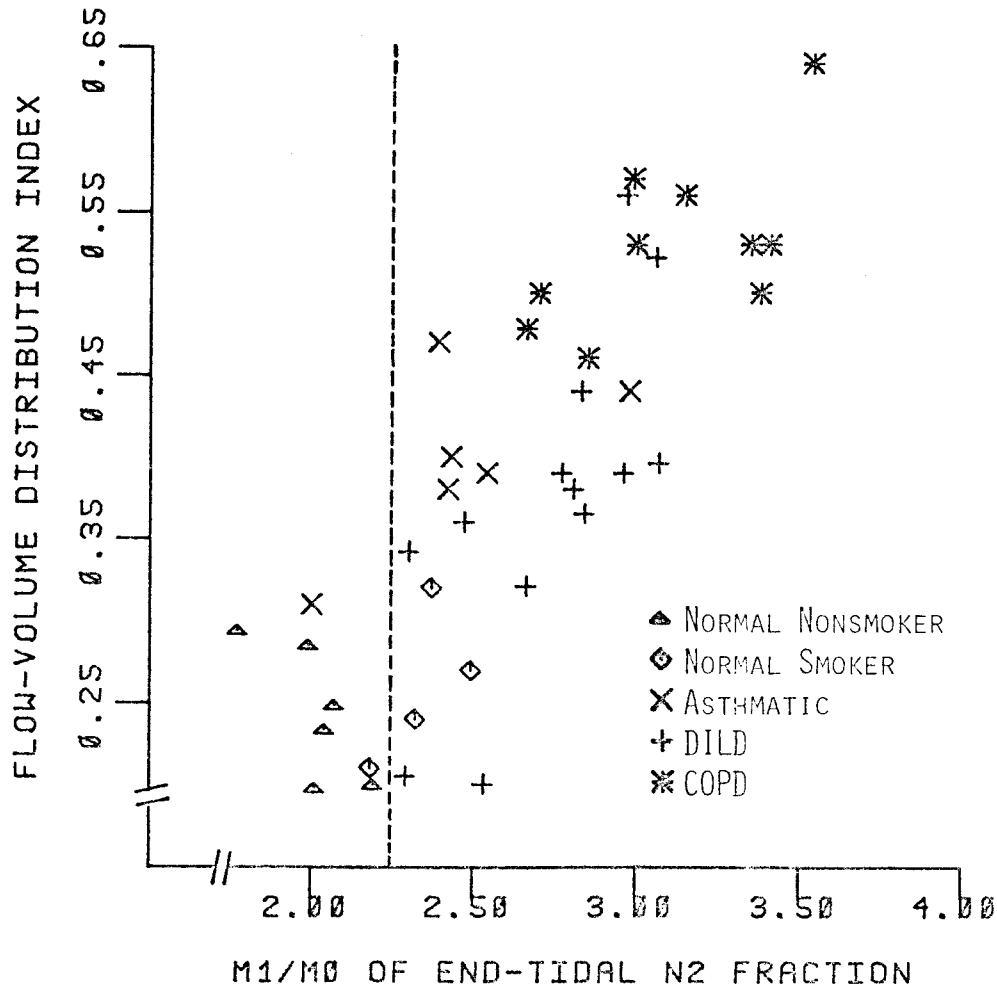


Figure 5-5

Table 5-2 Sensitivity of ventilatory indices for diagnostic groups.

| | Normal Nonsmokers | Normal Smokers | Asthmatics | DILD Subjects | COPD Subjects |
|---|---|---|---|---|---|
| Index of Alveolar Ventilation | | | | | |
| Mean (MZ) | 85.10 | 78.60 | 65.70 | 71.50 | 56.30 |
| Standard dev. (SDZ) | 2.30 | 4.20 | 1.52 | 2.82 | 3.66 |
| Range | 74.6-93.7 | 68.5-91.3 | 62.0-67.7 | 58.7-89.8 | 34.5-63.7 |
| Lung Clearance Index | | | | | |
| Mean (MZ) | 8.40 | 9.78 | 13.54 | 13.30 | 18.96 |
| Standard dev. (SDZ) | 0.15 | 0.26 | 2.05 | 0.71 | 2.47 |
| Range | 7.70-8.85 | 9.12-10.31 | 10.30-18.50 | 8.70-17.33 | 11.40-32.80 |
| Mixing Ratio | | | | | |
| Mean (MZ) | 1.50 | 1.65 | 1.98 | 1.89 | 2.65 |
| Standard dev. (SDZ) | 0.04 | 0.09 | 0.06 | 0.08 | 0.33 |
| Range | 1.37-1.68 | 1.40-1.87 | 1.89-2.12 | 1.42-2.24 | 1.44-4.76 |
| Ventilatory Efficiency | | | | | |
| Mean (MZ) | 76.60 | 73.43 | 65.90 | 67.20 | 55.50 |
| Standard dev. (SDZ) | 1.86 | 3.83 | 3.15 | 2.52 | 3.83 |
| Range | 71.6-83.8 | 63.2-82.0 | 59.3-76.4 | 53.2-88.2 | 37.25-78.57 |
| Five Breath Index | | | | | |
| Mean (MZ) | 88.78 | 85.43 | 84.98 | 83.66 | 68.67 |
| Standard dev. (SDZ) | 2.04 | 3.02 | 4.69 | 5.58 | 5.57 |
| Range | 85.9-91.4 | 81.2-89.2 | 78.9-91.3 | 75.52-90.75 | 60.5-78.29 |
| Becklake Index | | | | | |
| Mean (MZ) | 4.25 | 5.01 | 4.62 | 6.17 | 6.54 |
| Standard dev. (SDZ) | 0.30 | 0.65 | 0.95 | 0.94 | 1.45 |
| Range | 3.92-4.68 | 4.32-5.78 | 4.30-6.84 | 4.75-7.38 | 5.04-8.77 |

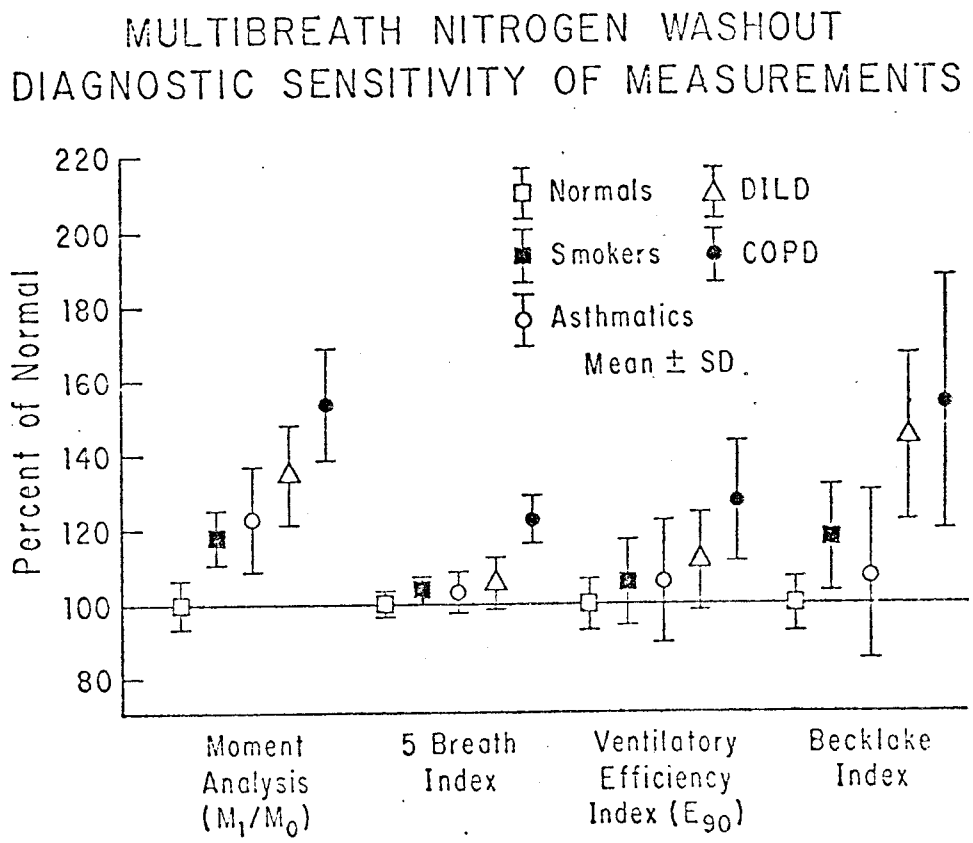
MULTIBREATH NITROGEN WASHOUT
DIAGNOSTIC SENSITIVITY OF MEASUREMENTS
Percent of Normal
220
200
180
160
140
120
100
80
Normals
DILD
Smokers
COPD
Asthmatics
Mean ± SD.
Moment Analysis ($M_1/M_0$)
5 Breath Index
Ventilatory Efficiency Index ($E_{90}$)
Becklake Index

Figure 5-6A

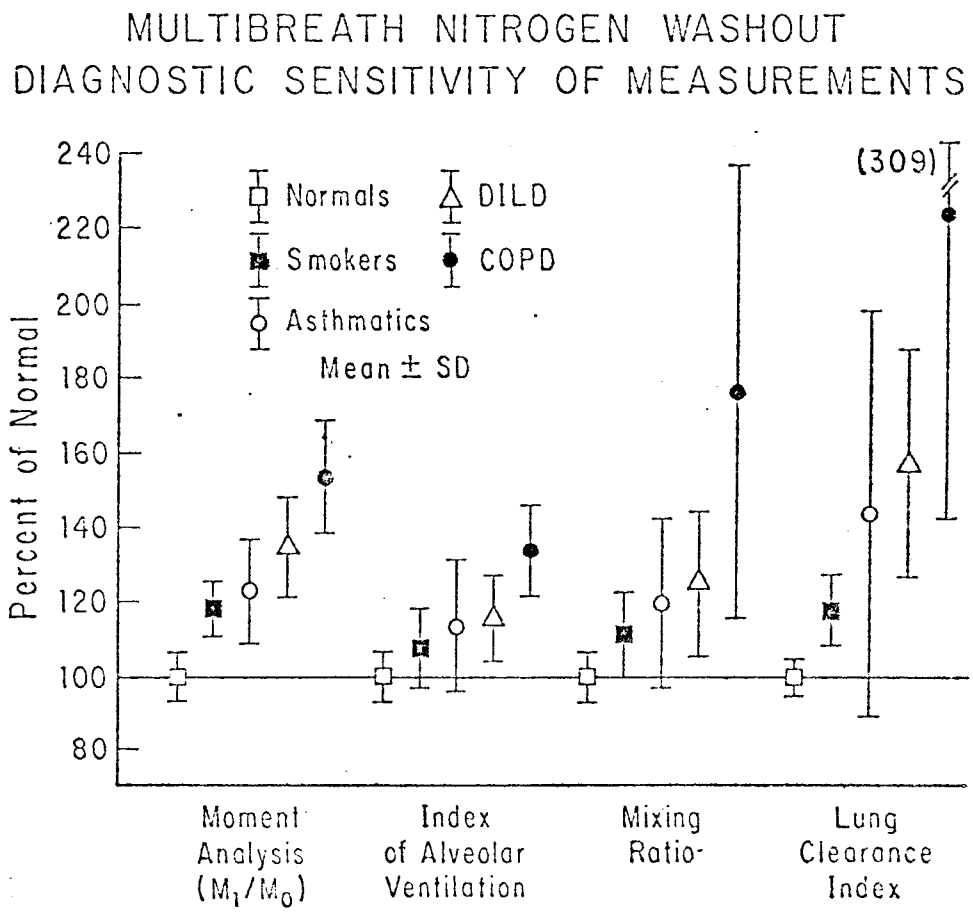
MULTIBREATH NITROGEN WASHOUT
DIAGNOSTIC SENSITIVITY OF MEASUREMENTS
Percent of Normal
240
220
200
180
160
140
120
100
80
Normals
Smokers
Asthmatics
DILD
COPD
Mean ± SD
(309)
Moment Analysis ($M_1/M_0$)
Index of Alveolar Ventilation
Mixing Ratio
Lung Clearance Index

Figure 5-6B

have different termination criteria, requiring different number of breaths and consequently testing times (see Figure 5-7).

Our values of the LCI for normal subjects show agreement within 5% of the values observed by Bouhuys (1963) and Edelman (1968), but not with those of Orzalesi et al (1965), and Prowse and Cumming (1973). Our values of BI fall within 10% of those given by Prowse and Cumming (1973), and even closer to the values given originally by Becklake.

Our values of the MR calculated for normal subjects are within 5% of the values observed by Edelman (1968), but more than 15% higher than those values measured by Cumming (1973). We find values of the IAV index for normal and COPD subjects within 5% of the values given by Lichtneckert et al (1963), although they used the ideal lung model with $V_D=0$ in their calculations. Our $E_{90\%}$ values for normal non-smokers are within 2% of the values observed by Cumming and Prowse (1973) who also assumed $V_D=0$. Since they grouped their abnormal subjects differently, further quantitative comparison is not feasible. For the 5BI, we find normal values within 5% of the values given by Weygandt (1976). In their experiments the tidal volume was maintained constant at one liter, while in our experi-

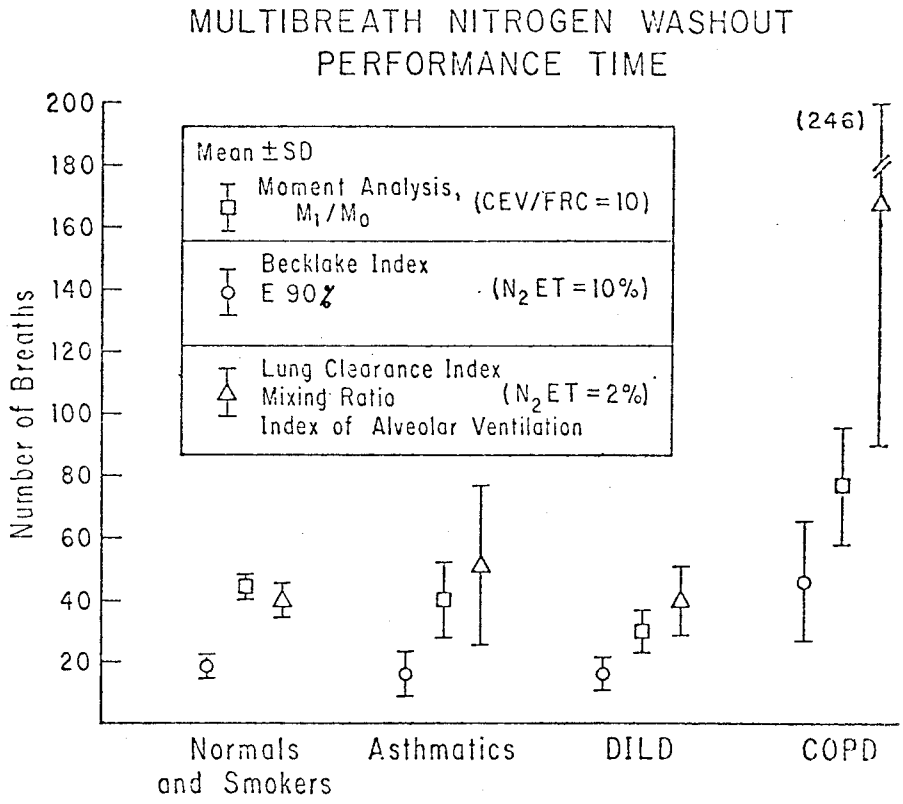
MULTIBREATH NITROGEN WASHOUT
PERFORMANCE TIME
Number of Breaths
200
180
160
140
120
100
80
60
40
20
Mean ± SD
Moment Analysis, M1/M0 (CEV/FRC = 10)
Becklake Index E 90χ (N2ET = 10%)
Lung Clearance Index
Mixing Ratio (N2ET = 2%)
Index of Alveolar Ventilation
(246)
Normals and Smokers
Asthmatics
DILD
COPD

Figure 5-7

ments it varied from 0.5 to 1.2 liter.

A direct comparison among the $(M_1/M_0)_x$ and the other indices is illustrated in Figure 5-8. In each diagnostic group, the values of $(M_1/M_0)_x$ are more tightly clustered than the other indices. The intra-subject variability of BI, LCI, $E_{90\%}$, MR, IAV, and 5BI is higher than $(M_1/M_0)_x$ as shown in Figure 5-9. This relatively large variability and lack of discrimination of these indices may be explained by the following:

1. Inability to account for breathing pattern variations.
2. Imprecise point of evaluation in the presence of noise (e.g., at $F_{N_2} = 0.02$).
3. Insufficient characterization of the form of the washout curve.

In spontaneous breathing we find that the tidal volume may vary as much as 40%; consequently, the values of the indices can be greatly changed. Bouhuys (1963) showed this effect on LCI. Furthermore, with spontaneous breathing, the "ideal" model can not serve as a satisfactory periodic breathing pattern with constant $V_D$, $V_T$, and FRC. The anatomical dead space of a given subject can vary greatly from breath to breath and with changes in breathing pattern. Also, for

DIAGNOSTIC SENSITIVITY COMPARISON OF ( $M_1/M_0$ )$_X$

VERSUS BECKLAKE INDEX

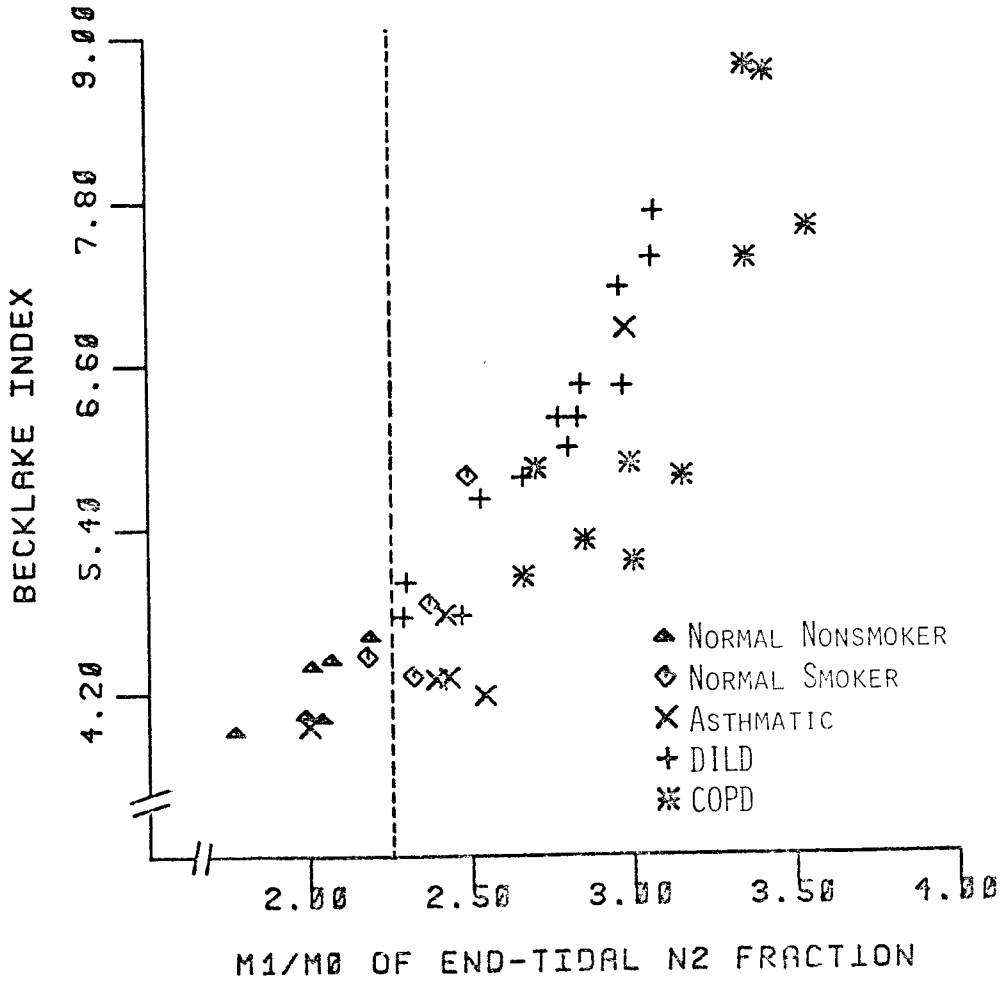


Figure 5-8A

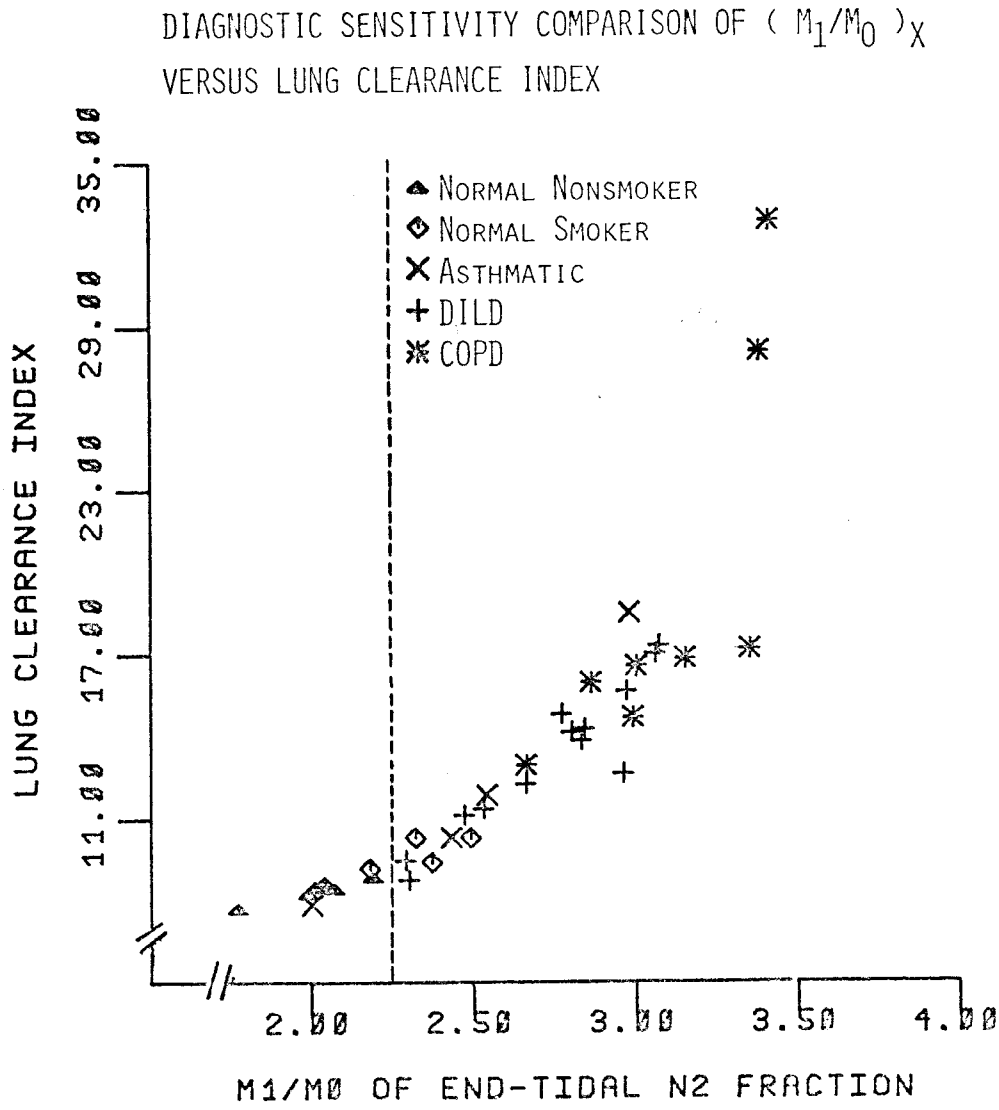
DIAGNOSTIC SENSITIVITY COMPARISON OF ( $M_1/M_0$ )$_X$
VERSUS LUNG CLEARANCE INDEX
NORMAL NONSMOKER
NORMAL SMOKER
ASTHMATIC
DILD
COPD
LUNG CLEARANCE INDEX
11.00
17.00
23.00
29.00
35.00
2.00
2.50
3.00
3.50
4.00
M1/M0 OF END-TIDAL N2 FRACTION

Figure 5-8B

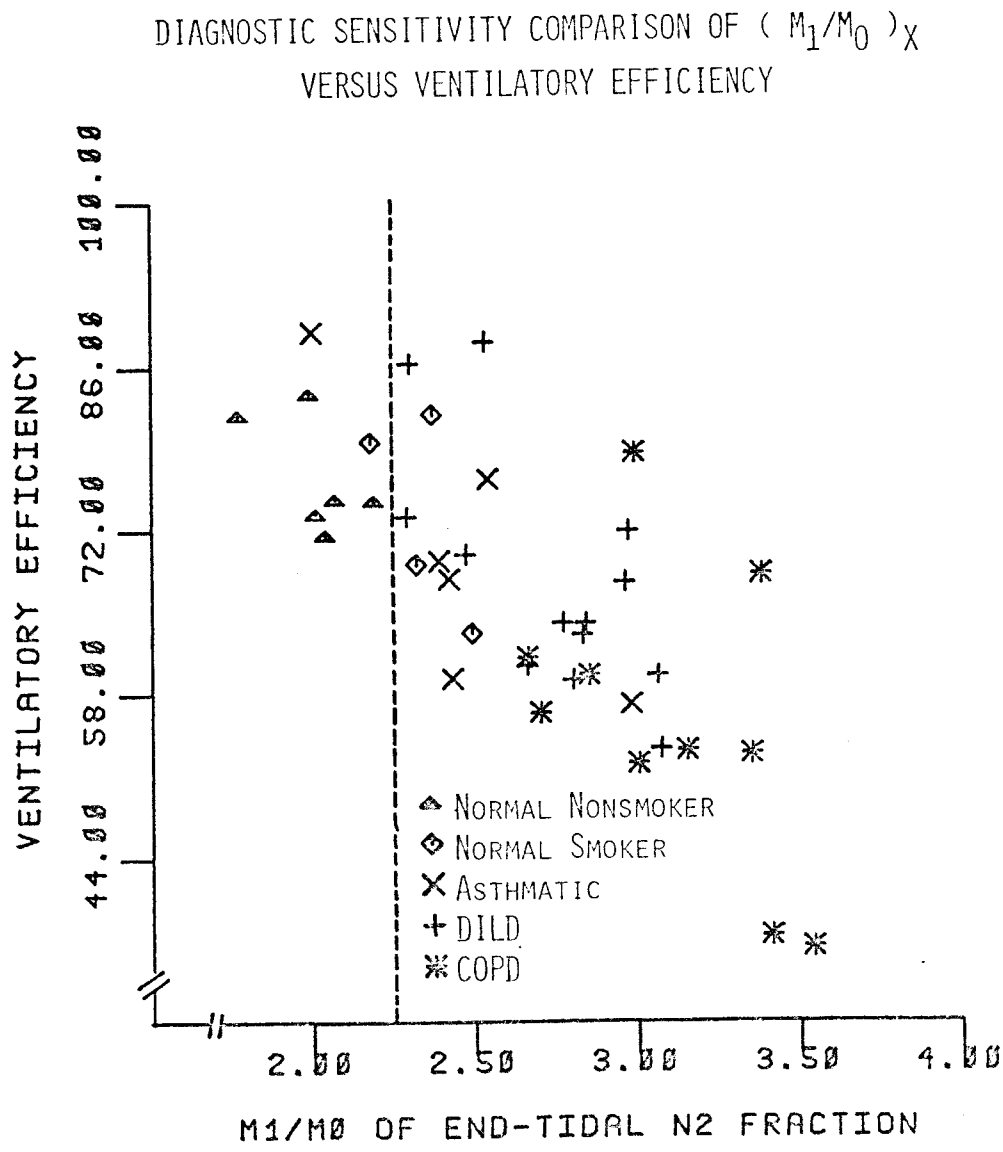
DIAGNOSTIC SENSITIVITY COMPARISON OF ( $M_1/M_0$ )$_X$
VERSUS VENTILATORY EFFICIENCY
VENTILATORY EFFICIENCY
44.00
58.00
72.00
86.00
100.00
NORMAL NONSMOKER
NORMAL SMOKER
ASTHMATIC
DILD
COPD
2.00
2.50
3.00
3.50
4.00
M1/M0 OF END-TIDAL N2 FRACTION

Figure 5-8C

DIAGNOSTIC SENSITIVITY COMPARISON OF ( $M_1/M_0$ )$_X$
VERSUS MIXING RATIO

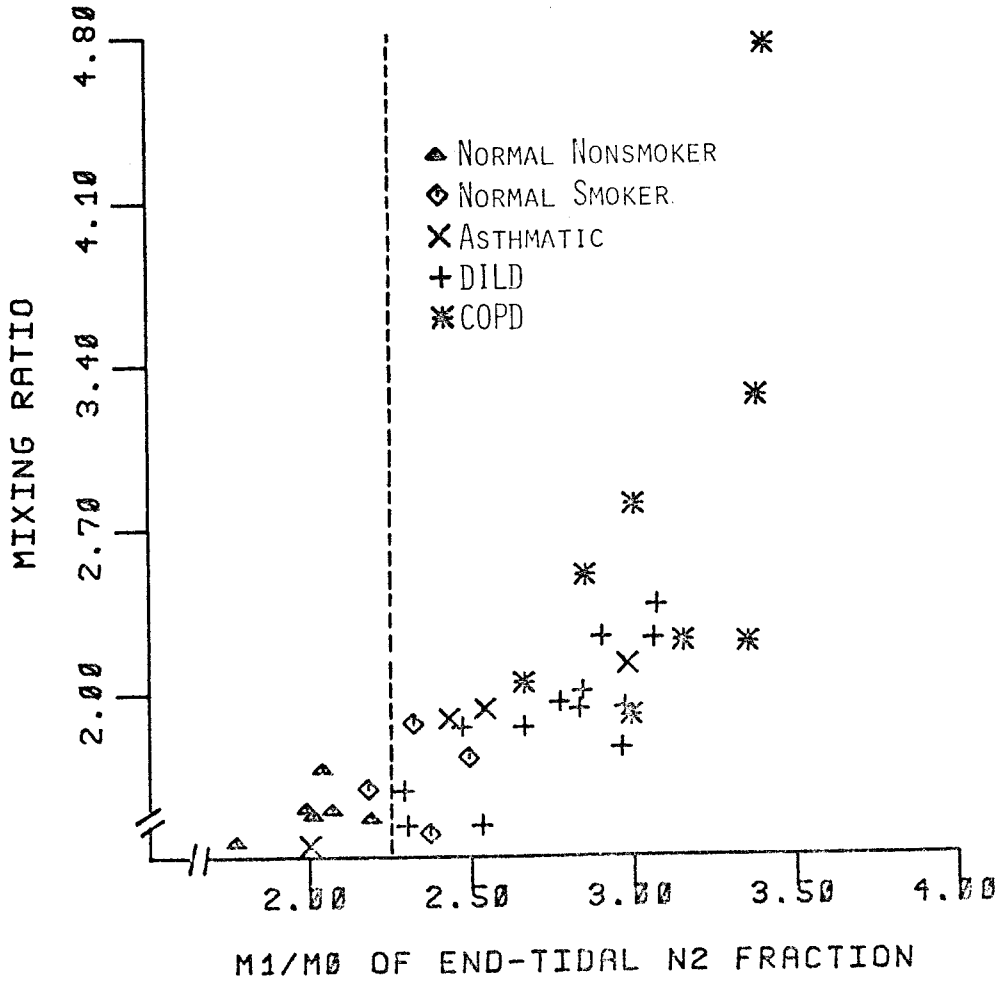


Figure 5-8D

DIAGNOSTIC SENSITIVITY COMPARISON OF ( $M_1/M_0$ )$_X$
VERSUS INDEX OF ALVEOLAR VENTILATION

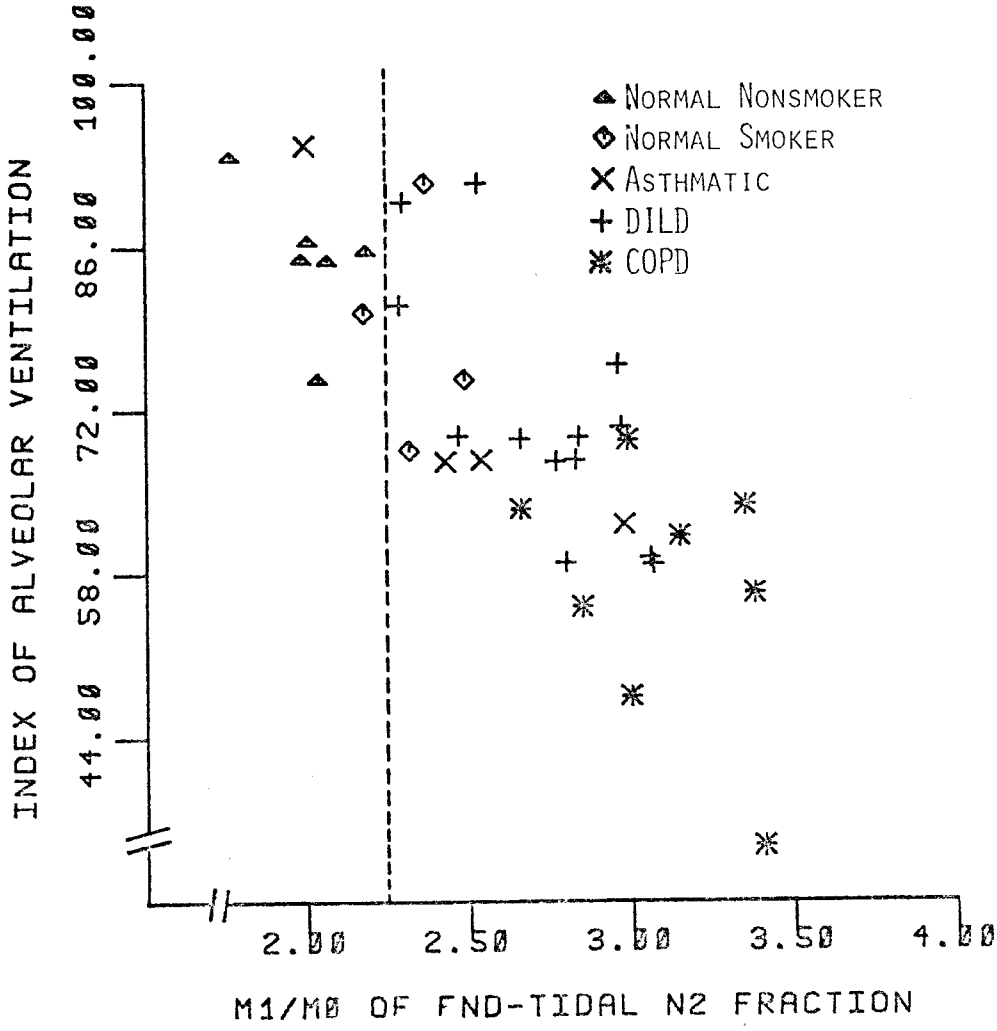


Figure 5-8E

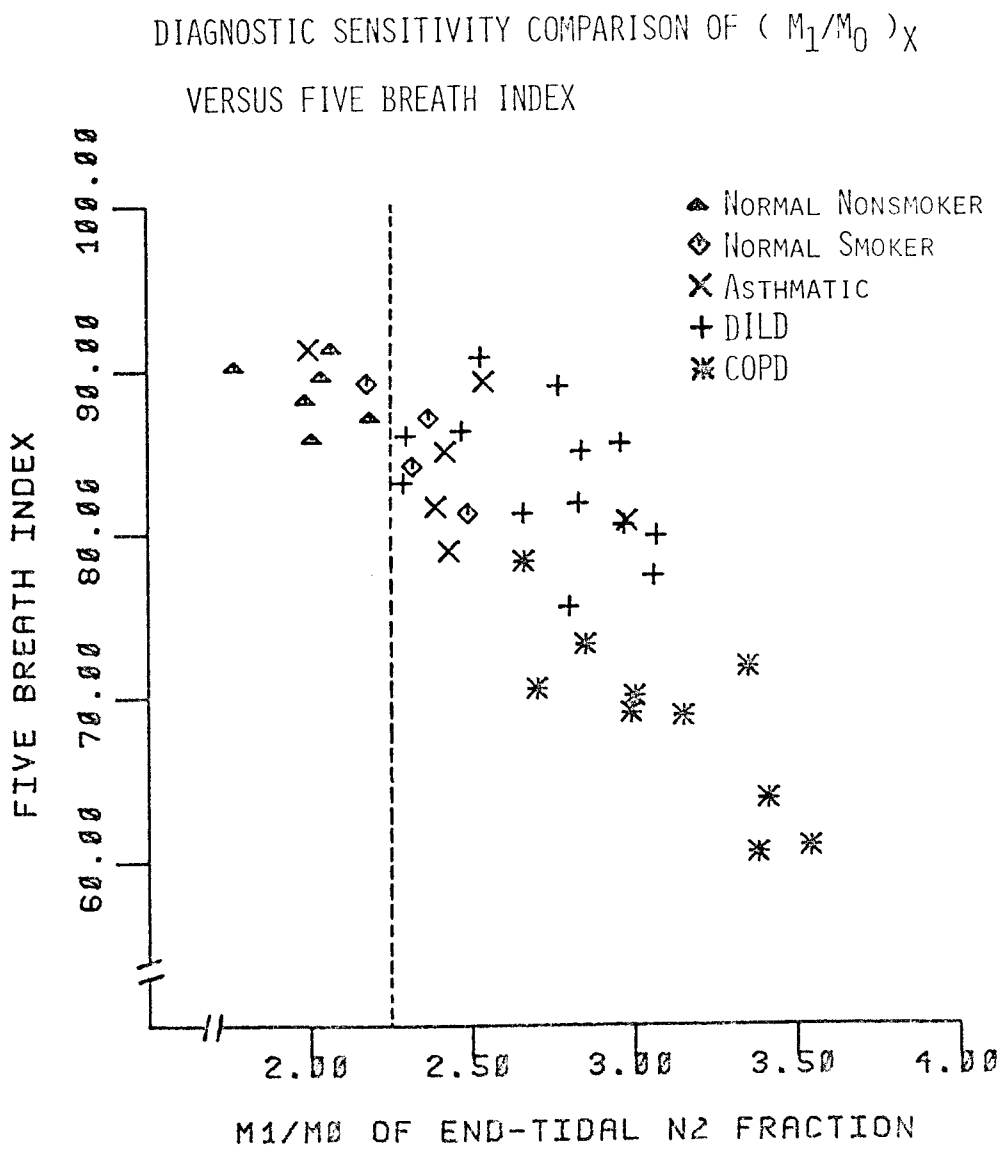
DIAGNOSTIC SENSITIVITY COMPARISON OF ( $M_1/M_0$ )$_X$
VERSUS FIVE BREATH INDEX
NORMAL NONSMOKER
NORMAL SMOKER
ASTHMATIC
DILD
COPD
FIVE BREATH INDEX
60.00
70.00
80.00
90.00
100.00
2.00
2.50
3.00
3.50
4.00
M1/M0 OF END-TIDAL N2 FRACTION

Figure 5-8F

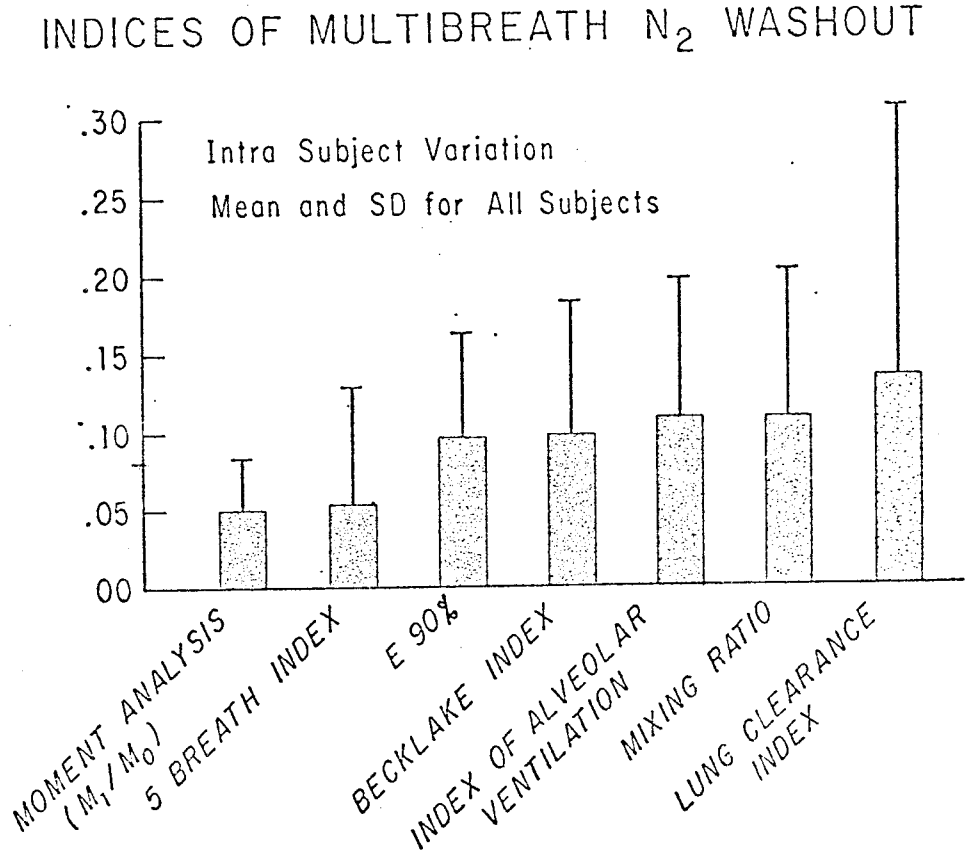
INDICES OF MULTIBREATH $N_2$ WASHOUT
.30
.25
.20
.15
.10
.05
00
Intra Subject Variation
Mean and SD for All Subjects
MOMENT ANALYSIS ($M_1/M_0$)
5 BREATH INDEX
E 90%
BECKLAKE INDEX
INDEX OF ALVEOLAR VENTILATION
MIXING RATIO
LUNG CLEARANCE INDEX

Figure 5-9

spontaneous breathing, use of the breath number as the point of evaluation (e.g., by the 5BI) rather than the number of volume turnovers (or dilution number) is inappropriate. Unless the dilution number is the same, there is not a common basis for comparing different individuals and different breathing patterns. This is the major reason we find the intra-subject variability (MRD) of 5BI (5.4%) to be greater than the observation made by Weygandt (1976). In summary, although all indices discriminate normal subjects from severely abnormals (e.g., COPD subjects), the $(M_1/M_0)_x$ provides the best differentiation among the different disease groups and is more sensitive to mild and moderate ventilation inhomogeneity.

# CHAPTER VI

## CONCLUSIONS

Major findings. The ratio of the first to zeroth moments $(M_1/M_0)_X$ of the end-tidal nitrogen fraction dynamics yields a quantitatively informative and clinically feasible index of ventilation inhomogeneity. It is superior to other ventilatory indices described in this study, since it (1) has a relatively small range of values for normal non-smokers, (2) can even detect mild ventilation inhomogeneity of normal smokers, and (3) can distinguish the greater inhomogeneity of subjects with asthma, diffuse interstitial lung disease, or chronic obstructive pulmonary disease. Our data indicates $(M_1/M_0)_X$ is independent of small measurement errors and random noise. Up to this point, we have found that parameters of a two-alveolar space model are less reproducible and provide less discrimination than the moment ratio. Furthermore, parameter estimation requires more computational time than the other indices.

With proper signal conditioning and corrections incorporated into a computerized analysis, the washout procedure can be done with spontaneous breathing in

minimal time using a simple experimental set up. If the data are collected and analyzed on-line, the results can be available seconds after the completion of wash-out test.

Future developements. Although the results of moment analysis were satisfactory in this study, further evaluations can be pursued to determine:

1. The effects of larger breathing pattern (amplitude and frequency) variations.

2. Whether of a dead-space volume correction for cumulative expired volume can reduce the effects of breathing pattern variation.

3. Whether testing time can be reduced by changing the termination criteria to dilution number less than 10.

Since the model parameters did not yield satisfactory results, additional studies should evaluate:

1. Other parameter combinations, which may be chosen with the same model, to yield a better index of inhomogeneity.

2. Whether the model can fit the data more closely by using a dead-space volume computed on each breath compared to an average dead-space volume.

3. The sensitivity of estimated parameters to

measurment noise and errors.

4. Better optimization algorithm for parameter estimation.

# REFERENCES

Bard, Y., Nonlinear Parameter Estimation, 1974, Academic Press Inc.

Bates, D.V., and R. V. Christie. Intrapulmonary mixing of helium in health and disease. Clin. Sci. 9: 17-27, 1950.

Becklake, M.R. A new index of the intrapulmonary mixture of inspired air. Thorax 7: 111-116, 1952.

Blumenfeld, W., S. Turney, and R. A. Cowley. Mathematical model for flow in the heated Fleisch pneumotachometer. Medical and Biological Engineering. 546-551, 1973.

Bouhuys, A. Pulmonary nitrogen clearance in relation to age in healthy males. J. Appl. Physiol. 18: 297-300, 1963.

Bouhuys, A., S. Lightneckert, C. Lundgren, and G. Lundin. Voluntary changes in breathing pattern and N: clearance from the lungs. J. Appl. Physiol. 16:1010-1042, 1961.

Chiang, S.T., and R. Yang. Volume control and compartment analysis in multiple-breath nitrogen washout. Aerospace Medicine 843-848, August, 1974.

Cournand, A., E. Baldwin, R.C. Darling, and D. W. Richards. Studies of intrapulmonary mixture of gases. IV. The significance of the pulmonary emptying rate and a simplified open circuit measurement of residual air. J. Clin. Invest., 20: 681-689, 1941.

Cumming, G., and J. G. Jones. The construction and repeatability of nitrogen clearance delay curves. Respiration Physiol. 1: 238-248, 1966.

Daniels, A.V., L. A. Couvillon, Jr., and J.M. Lebrizzi. Evaluation of nitrogen analyzers, Sept. 1973, Utah Biomedical Test Laboratory, 520 Wakara Way, Salt Lake City, Utah 84112.

Edelman, N.H., C. Mittman, A. H. Norris, and N. W. Shock. Effects of respiratory pattern on age differences in ventilation uniformity. J. Appl. Physiol. 24: 49-53, 1968.

Fowler, W.S., E. R. Cornish, and S. S. Kety. Lung function studies. VIII. Analysis of alveolar ventilation by pulmonary $N_2$ clearance curves. J. Clin Invest. 31: 40-50, 1952.

Gomez, D., W. A. Brincoe, and G. Cumming. Continuous distribution of specific tidal volume throughout the lung. J. Appl. Physiol. 19:683-692, 1964.

Grenvik, A., Hedstrand, V. and Sjogren, H. (1966) Problems in pneumotachography. Acta. Anaesth. Svand. 10, 1947.

Hashimoto, T., A. C. Young, and C. J. Martin. Compartmental analysis of the distribution of ages in the lungs. J. Appl. Physiol. 23: 293-209, 1967.

Hogman, C. D., West, R.C., Shankland, R.S. and Selby, S. M. (Eds.). Handbook of Chemistry and Physics 5th edn., Chemical Rubber Publishing Co., Cleveland, Ohio U.S.A.

Liehineckert, S.J.A., and G.E.G. Lundgren, An index of alveolar ventilation. J. Appl. Physiol. 18: 639-645, 1963.

Nakamura, T., T. Takishima, J. Okubo, T. Sasaki, and N. Takahashi. Distribution function of the clearance time constant in lungs. J. Appl. Physiol. 21: 227-232, 1966.

Orzalesi, M.M., M. C. Hart, and C. D. Cook. Distribution of ventilation in normal subjects from 7 to 45 years of age. J. Appl. Physiol. 20: 77-78, 1965.

Paiva, M., and M. Demeester. Gas transport in the air phase of the lung simulated by a digital computer. Computers Biomd. Res. 3: 675-689, 1971.

Prowse, K., and G. Cumming. Effects of lung volume and disease on the lung nitrogen decay curve. J. Appl. Physiol. 34:23-33, 1973.

Roos, A., H. Dahlstrom, and J. P. Murphy. Distribution of inspired air in the lungs. J. Appl. Physiol. 7: 645-659, 1955.

Saidel, G. M., T. C. Militano, and E. H. Chester. Pulmonary gas transport characterization by a dynamic model. Respiration Physiol. 12:305-328, 1971.

Saidel, G.M., R. B. Salmon, and E. H. Chester (1975) Moment analysis of multibreath lung washout. J. Appl. Physiol. 38:328

Turney, S. and Blumenfeld, W. The heated Fleisch pneumotachometer: a calibration procedure. J. Appl. Physiol. 34, 117-121, 1973.

Weygandt, G. R. A sensitive five-breath $N_2$ washout test of distribution of ventilation. J. Appl. Physiol. Vol. 40, 464-467, March 1976.

# APPENDIX I

## COMPUTER PROGRAMS

### Main Program Description

This program and its associated subroutines are designed for the purpose of real-time data processing of nitrogen washout test. Signals are sampled at a rate of 40 Hz and digitally filtered with the Butterworth second order low-pass filter with cutoff frequency of 20 Hz. Data processing on each breath involves the determination of the inspired and expired volumes, the amount of nitrogen expired and the end-tidal nitrogen fraction. The volume flow rate is integrated to obtain the volume change using a continuously revised calibration factor, which accounts for changing gas composition and temperature during breathing. Allowing for the difference in signal delay time, the product of volume flow rate and nitrogen molar fraction is integrated. From each of the first five breaths, the dead space volume is computed. Functional residual capacity is measured at the end of each breath. Dilution number is computed at each breath and recomputed for all previous breaths at the end of the test. Vital capacity maneuver leads to estimates of total lung capacity and residual volume. Furthermore, this program evaluates all

the other ventilatory indices. Finally, the flow and volume fractions are estimated by modified Gauss-Newton parameter estimation program (PARST). Main program block diagram is illustrated in Fig. A-1.

Main Program Symbols

1. Input Parameters

   DF: Flow signal DC offset
   DN: Nitrogen signal DC offset
   CC: Volume calibration coefficient
   N(I): Nitrogen sample
   NF(I): Flow sample

2. Preset Parameters

   Body temperature, 310K
   Expired gas temperature, 307K
   Inspired gas temperature, 300K
   Sampling Rate (SR), 40Hz.
   Delay between nitrogen and flow signals (DE), 75 MSEC.
   Low-pass filter cutoff frequency (CF), 20 Hz.
   Threshold value (TH1) for tape the start of data processing, 3000/SR.

3. List of Subroutines

   ASLSLN: Assigns a logical unit number (LUN) to the laboratory peripheral system (LPS 11)

   RTS: Subroutine which initiates synchronous A/D at fix sampling rate, whose parameters are IBF, INTVL, IEFN, IERR, and NBF.

   WAITER: Subroutine which waits for half buffer to be filled

   CLREF: Subroutine which clears event flag

   LED: LED display subroutine

   READSW: Reads the contents of the switch register

3. List of Subroutines-continued

FREEB: Fortran subroutine which frees half buffer, adjusts buffer index for more data and check if another half buffer of data is available

FILTER: Fortran subroutine which filters the input data. PI, A0, A1, A2, B0, B1, B2 are parameters of the low pass

DELAY: Fortran subroutine which compensate the delay and DC offsets

PAREST: Fortran subroutine which estimates the optimal parameters (f2,v2)

PLOT: Plot subroutine

4. Measured Variables

IC: Maximal inspiratory capacity
VC: Vital capacity
RV: Residual volume
FRC: Functional residual capacity
TLC: Total lung capacity
VI(K): Volume of gas inspired at breath K
VE(K): Volume of gas expired at breath K
X(K): End-tidal nitrogen fraction at breath K
AVX(K): Average nitrogen fraction at breath K
J: Number of breaths at which X(J)<.02
VL(K): Estimated lung volume after breath K
CLV(K): Volume change of lung after breath K
SAV(K): Cumulative expired nitrogen after breath K
VD(K): Estimated value of anatomical dead space from breath K
AVD(K): Mean value of anatomical dead space from the first five breaths
DI(K): Dilution number up to breath K
MX(r): r-th moment of normalized end-tidal $N_2$ fraction
CVX: Coefficient of variation of normalized end-tidal $N_2$ fraction
MAVX(r): r-th moment of normalized average $N_2$ fraction
CVAVX: Coefficient of variation of normalized $N_2$ fraction
MVL(r): r-th moment of normalized estimated lung volume
CVVL: Coefficient if variation of normalized estimated lung volume

4. Measured variables - continued

| | |
|---|---|
| NX(K): | Normalized $N_2$ fraction at breath K |
| NAVK(K): | Normalized average $N_2$ fraction of breath K |
| NVL(K): | Normalized estimated lung volume at breath K |
| FBI: | Five breath index by G.R. Weygandt (1976) |
| IAV: | Index of alveolar ventilation by Lichtneckert (1963) |
| LCI: | Lung clearance index by Bouhuys (1963) |
| VEF: | Ventilatory efficiency by Prowse (1973) |
| BI: | Becklake Index (1952) |
| MR: | Mixing ratio by Edelman (1968) |
| BCI: | Bate and Christie Index (1950) |

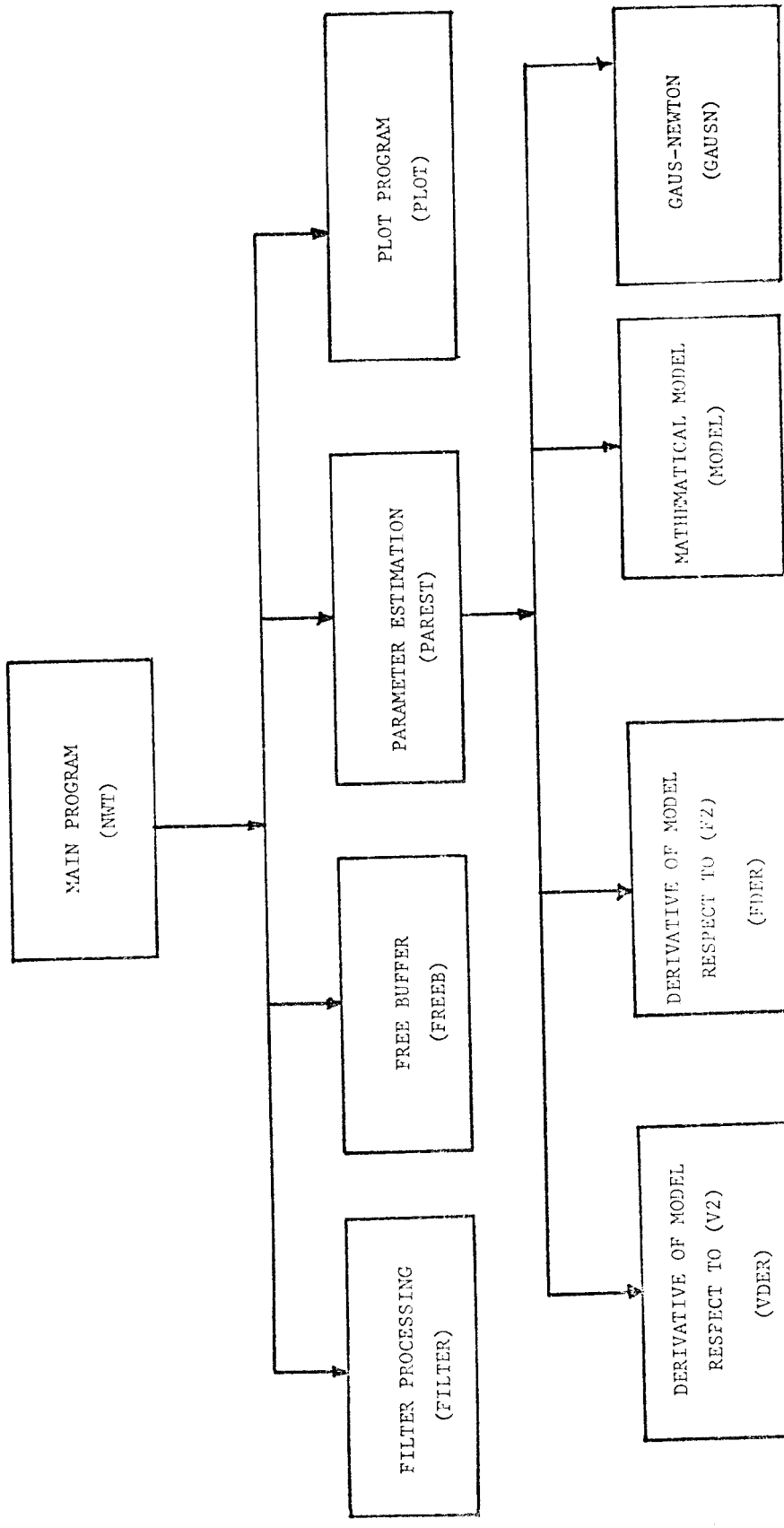


Figure A-1. Main program block diagram

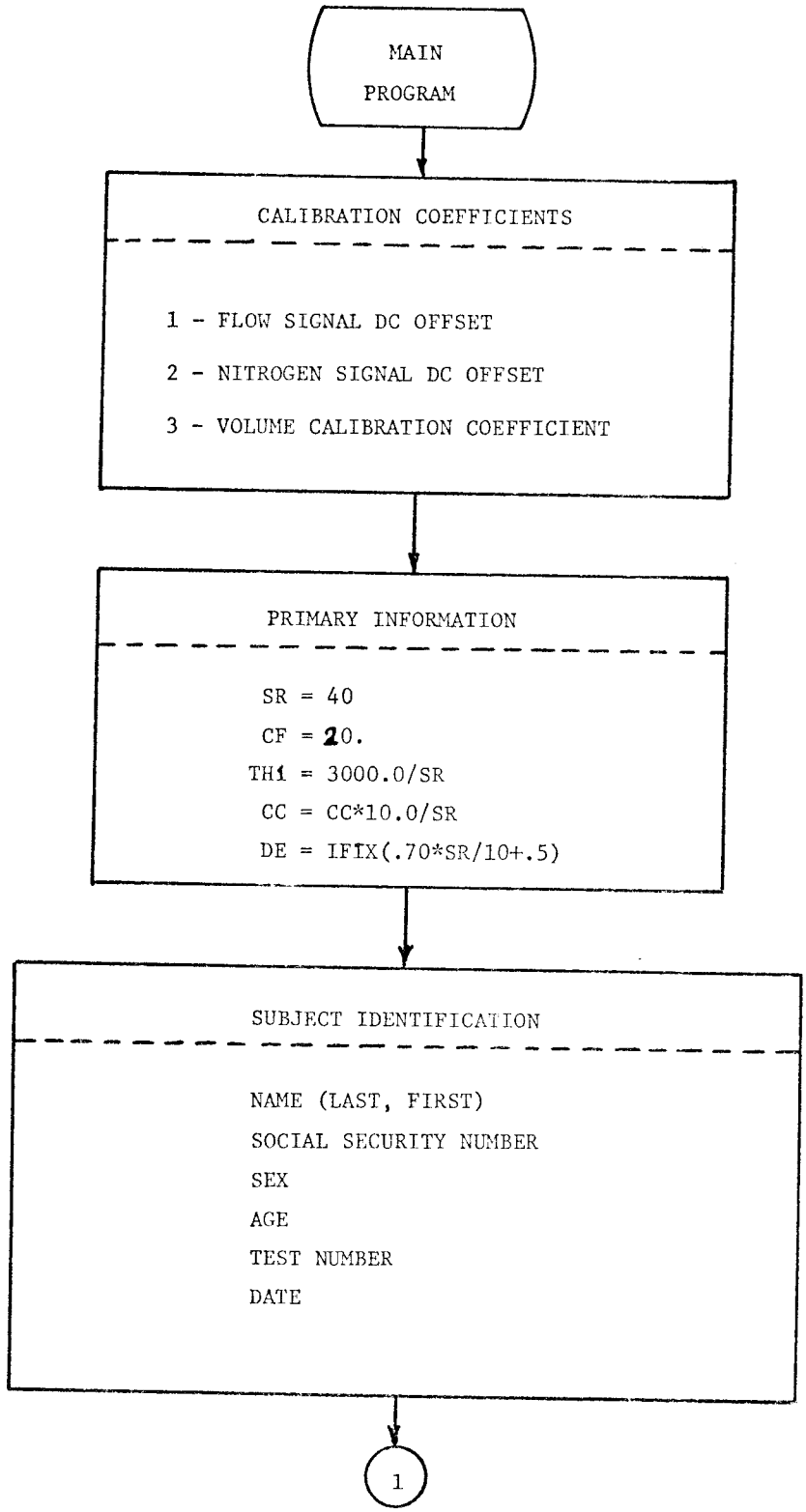
MAIN
PROGRAM
CALIBRATION COEFFICIENTS
1 - FLOW SIGNAL DC OFFSET
2 - NITROGEN SIGNAL DC OFFSET
3 - VOLUME CALIBRATION COEFFICIENT
PRIMARY INFORMATION
SR = 40
CF = 20.
TH1 = 3000.0/SR
CC = CC*10.0/SR
DE = IFIX(.70*SR/10+.5)
SUBJECT IDENTIFICATION
NAME (LAST, FIRST)
SOCIAL SECURITY NUMBER
SEX
AGE
TEST NUMBER
DATE
1

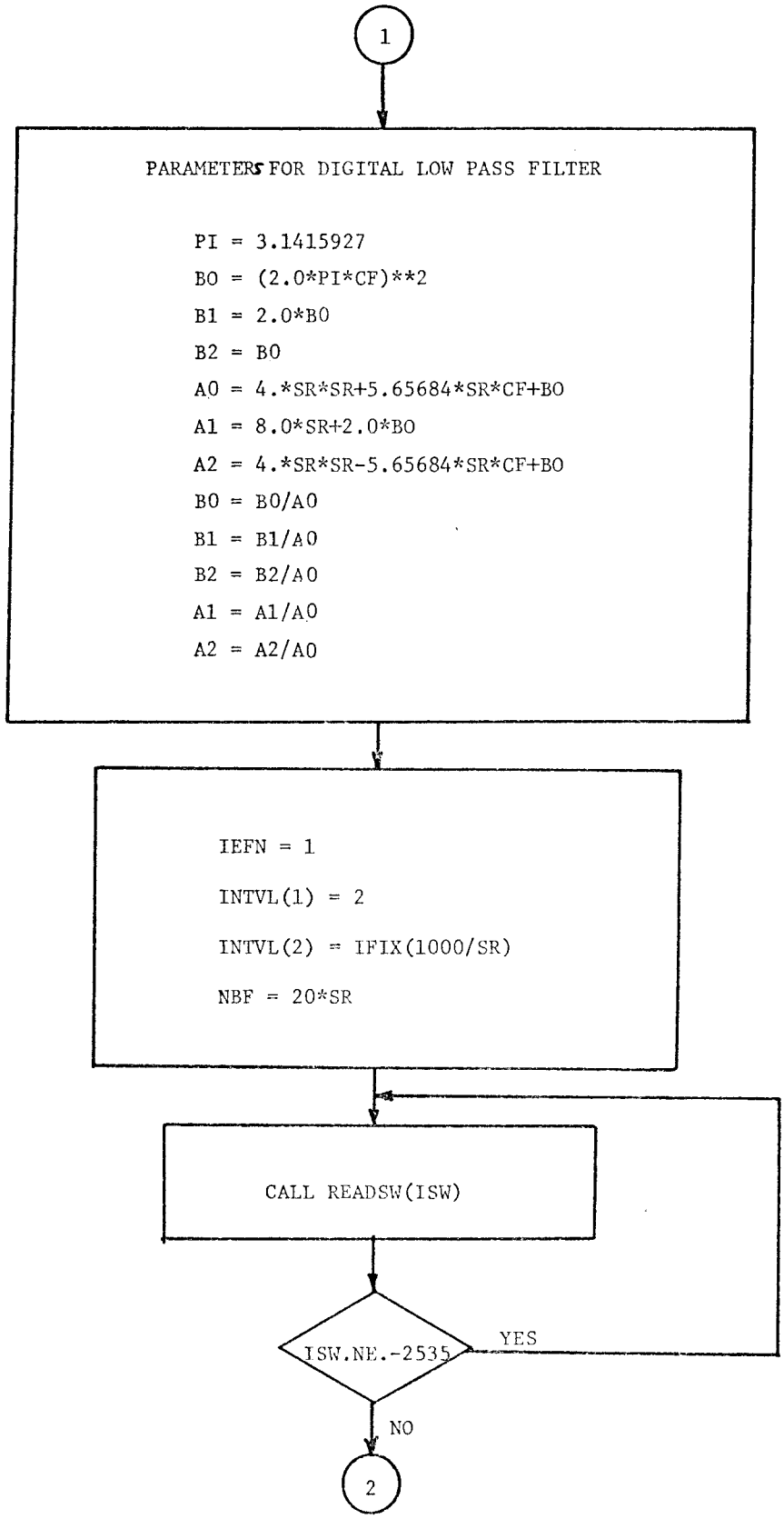
1
PARAMETERS FOR DIGITAL LOW PASS FILTER
PI = 3.1415927
BO = (2.0*PI*CF)**2
B1 = 2.0*BO
B2 = BO
A0 = 4.*SR*SR+5.65684*SR*CF+BO
A1 = 8.0*SR+2.0*BO
A2 = 4.*SR*SR-5.65684*SR*CF+BO
BO = BO/AO
B1 = B1/AO
B2 = B2/AO
A1 = A1/AO
A2 = A2/AO
IEFN = 1
INTVL(1) = 2
INTVL(2) = IFIX(1000/SR)
NBF = 20*SR
CALL READSW(ISW)
ISW.NE.-2535
YES
NO
2

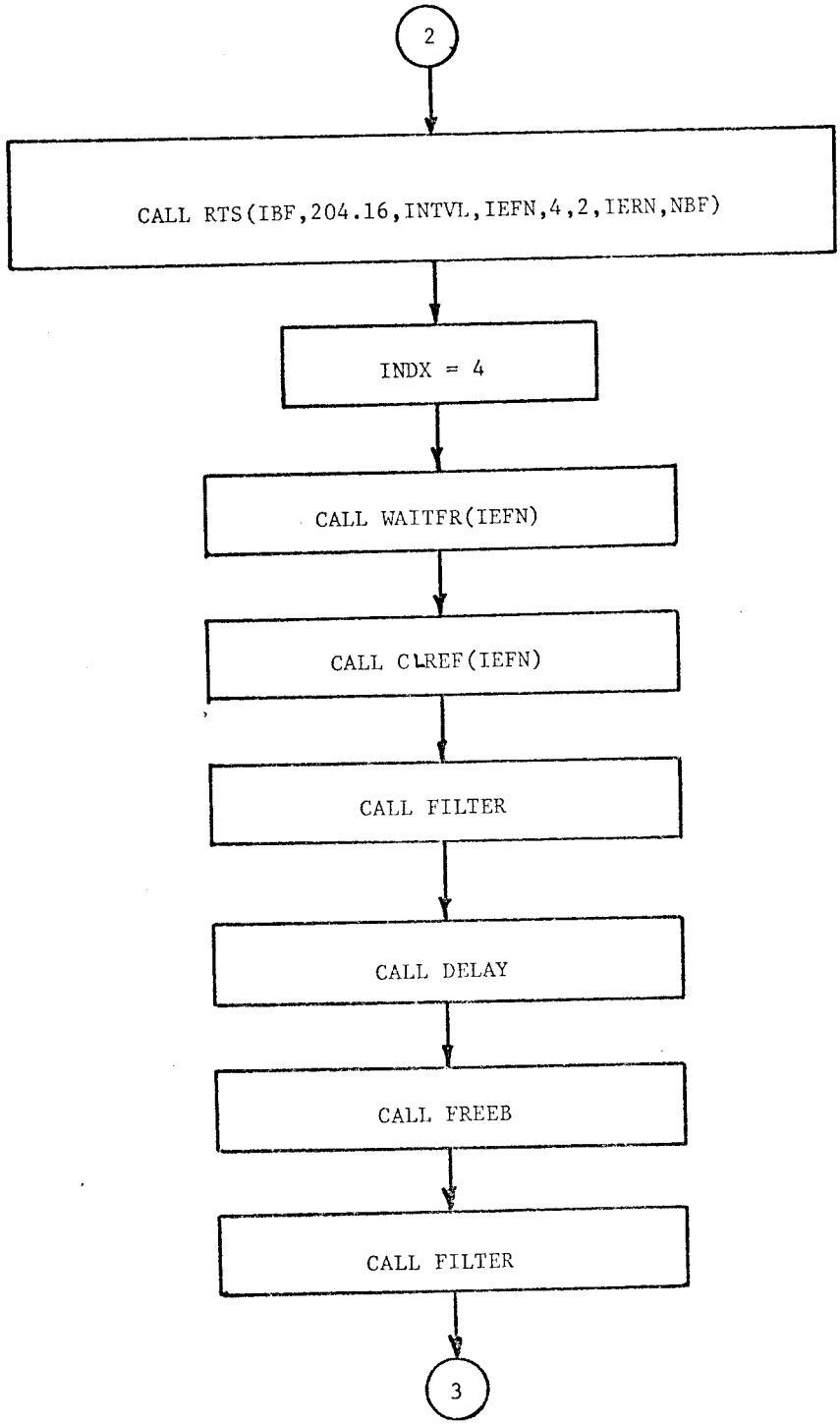
2
CALL RTS(IBF,204.16,INTVL,IEFN,4,2,IERN,NBF)
INDX = 4
CALL WAITFR(IEFN)
CALL CLREF(IEFN)
CALL FILTER
CALL DELAY
CALL FREEB
CALL FILTER
3

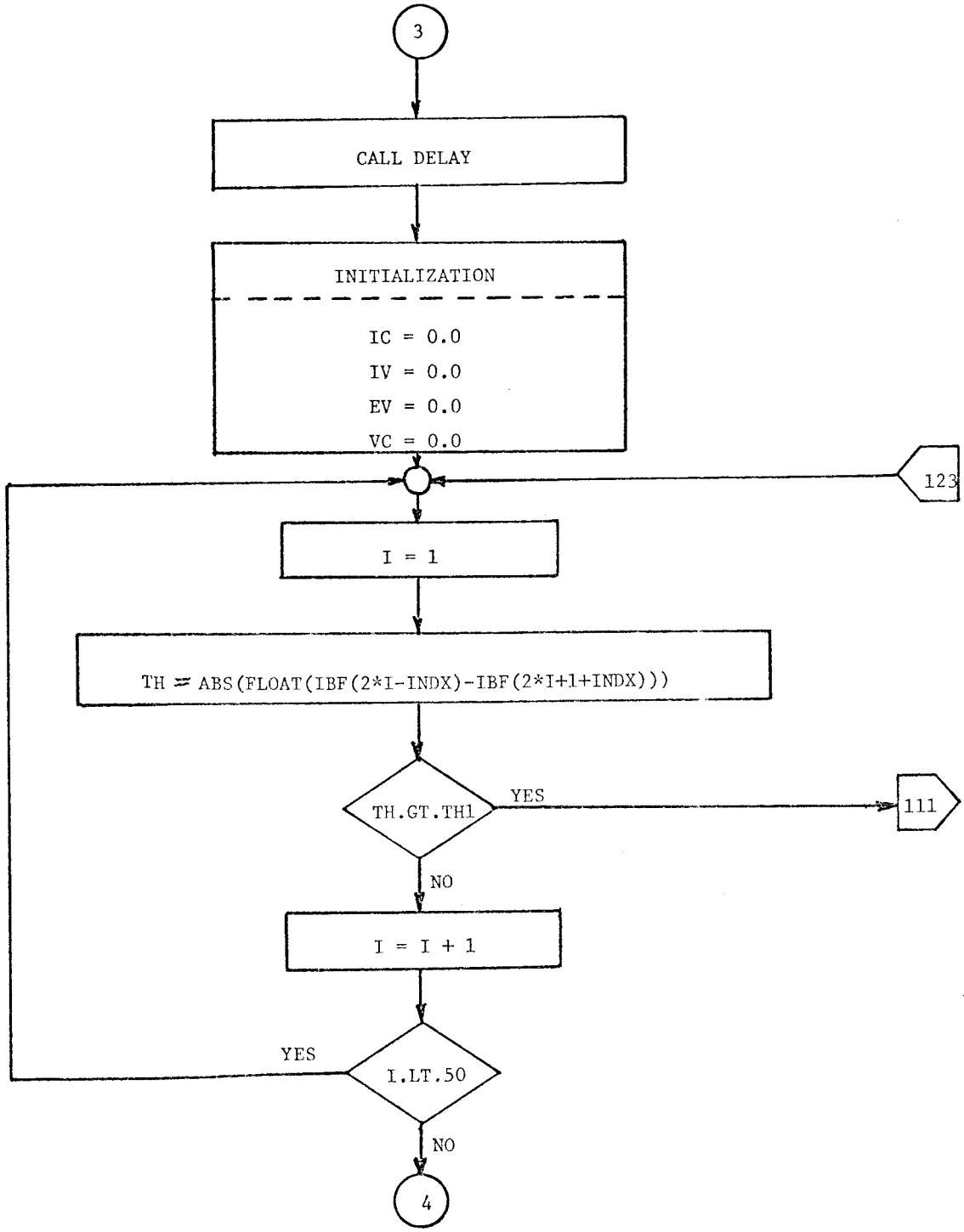
3
CALL DELAY
INITIALIZATION
IC = 0.0
IV = 0.0
EV = 0.0
VC = 0.0
123
I = 1
TH = ABS(FLOAT(IBF(2*I-INDX)-IBF(2*I+1+INDX)))
TH.GT.TH1
YES
111
NO
I = I + 1
I.LT.50
YES
NO
4

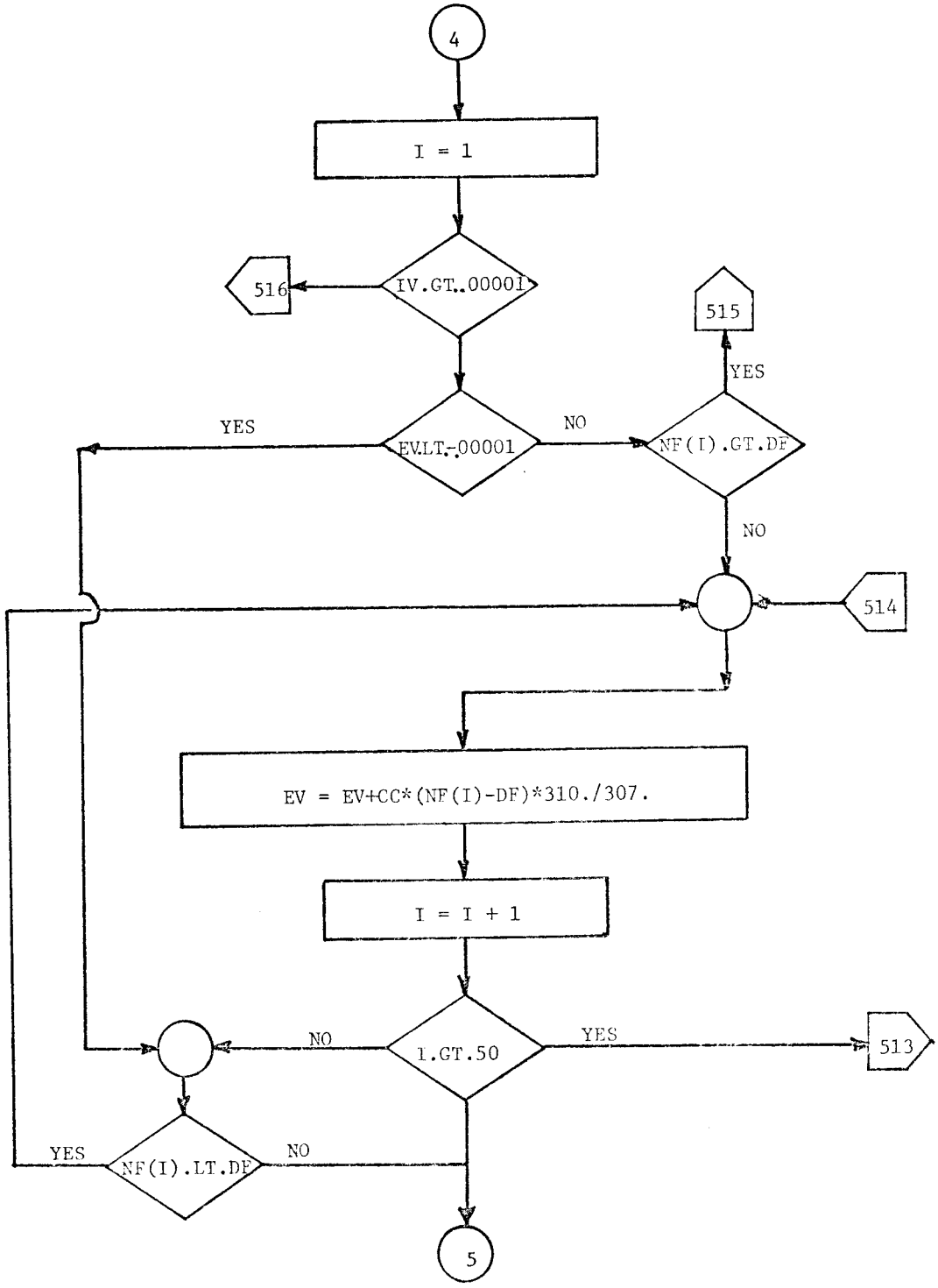
4
I = 1
IV.GT..00001
516
515
YES
YES
EV.LT..00001
NO
NF(I).GT.DF
NO
514
EV = EV+CC*(NF(I)-DF)*310./307.
I = I + 1
NO
I.GT.50
YES
513
YES
NF(I).LT.DF
NO
5

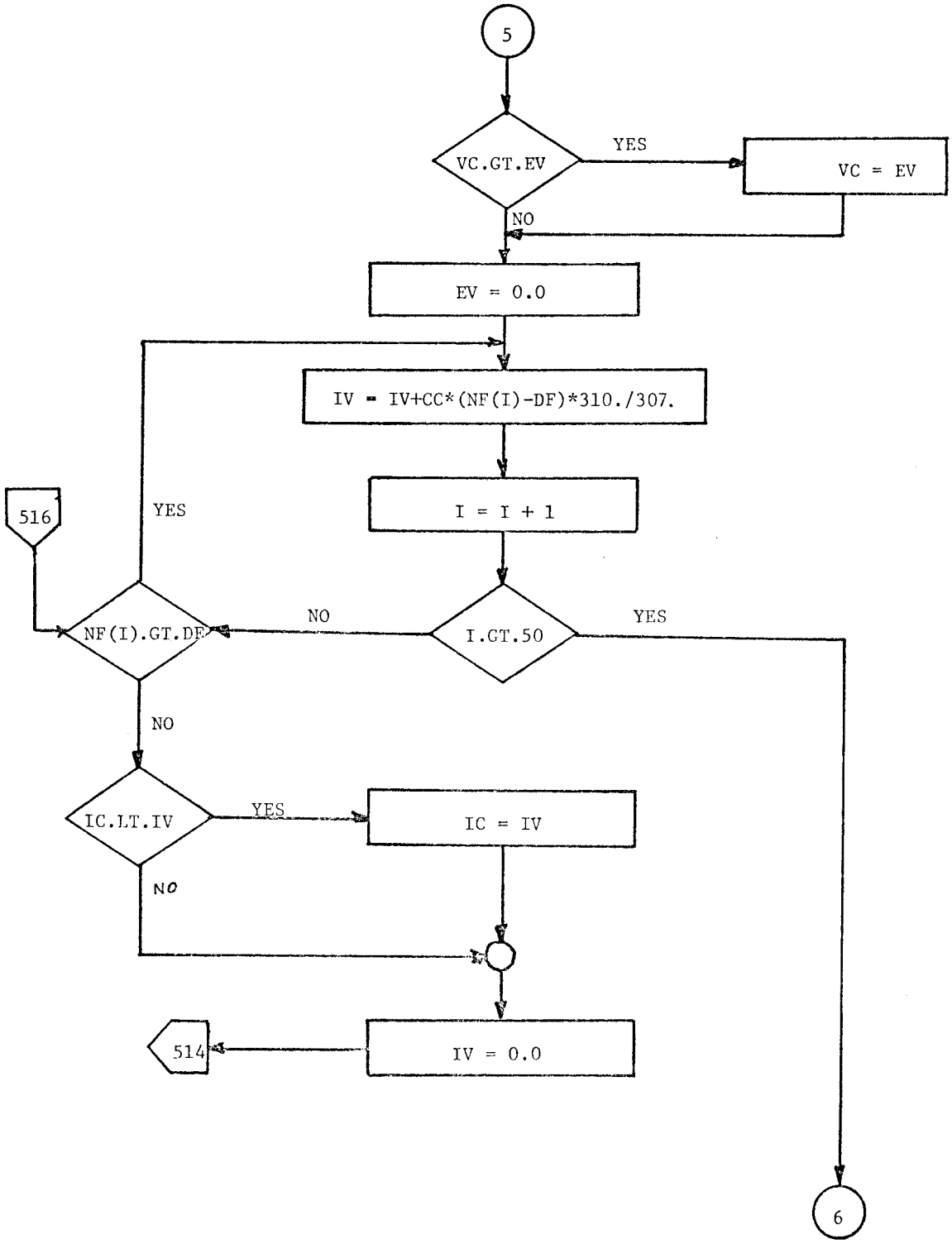
5
VC.GT.EV
YES
VC = EV
NO
EV = 0.0
IV = IV+CC*(NF(I)-DF)*310./307.
I = I + 1
516
YES
NF(I).GT.DF
NO
I.GT.50
YES
NO
IC.LT.IV
YES
IC = IV
NO
514
IV = 0.0
6

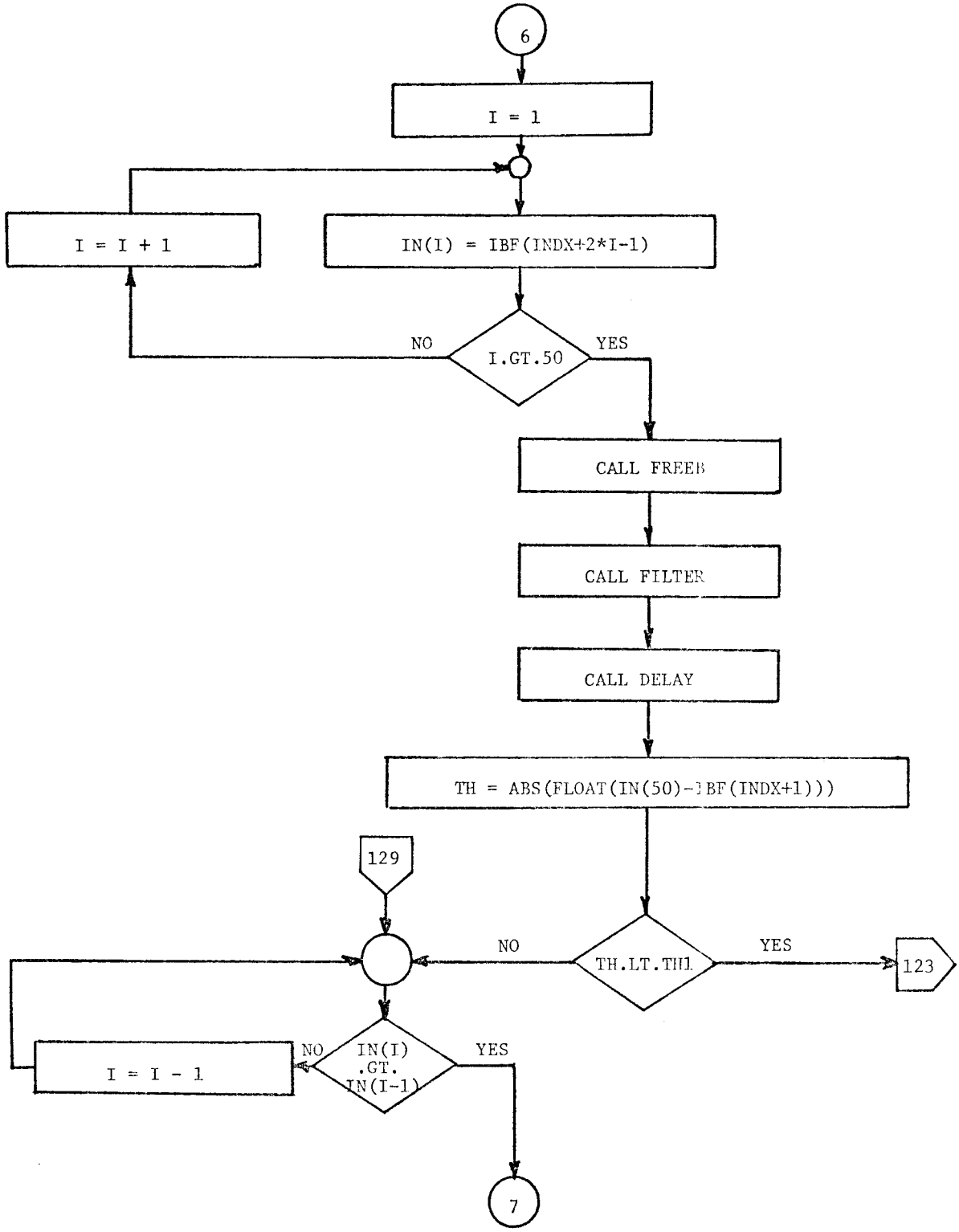
6
I = 1
I = I + 1
IN(I) = IBF(INDX+2*I-1)
NO
I.GT.50
YES
CALL FREEB
CALL FILTER
CALL DELAY
TH = ABS(FLOAT(IN(50)-IBF(INDX+1)))
129
NO
TH.LT.THL
YES
123
I = I - 1
NO
IN(I)
.GT.
IN(I-1)
YES
7

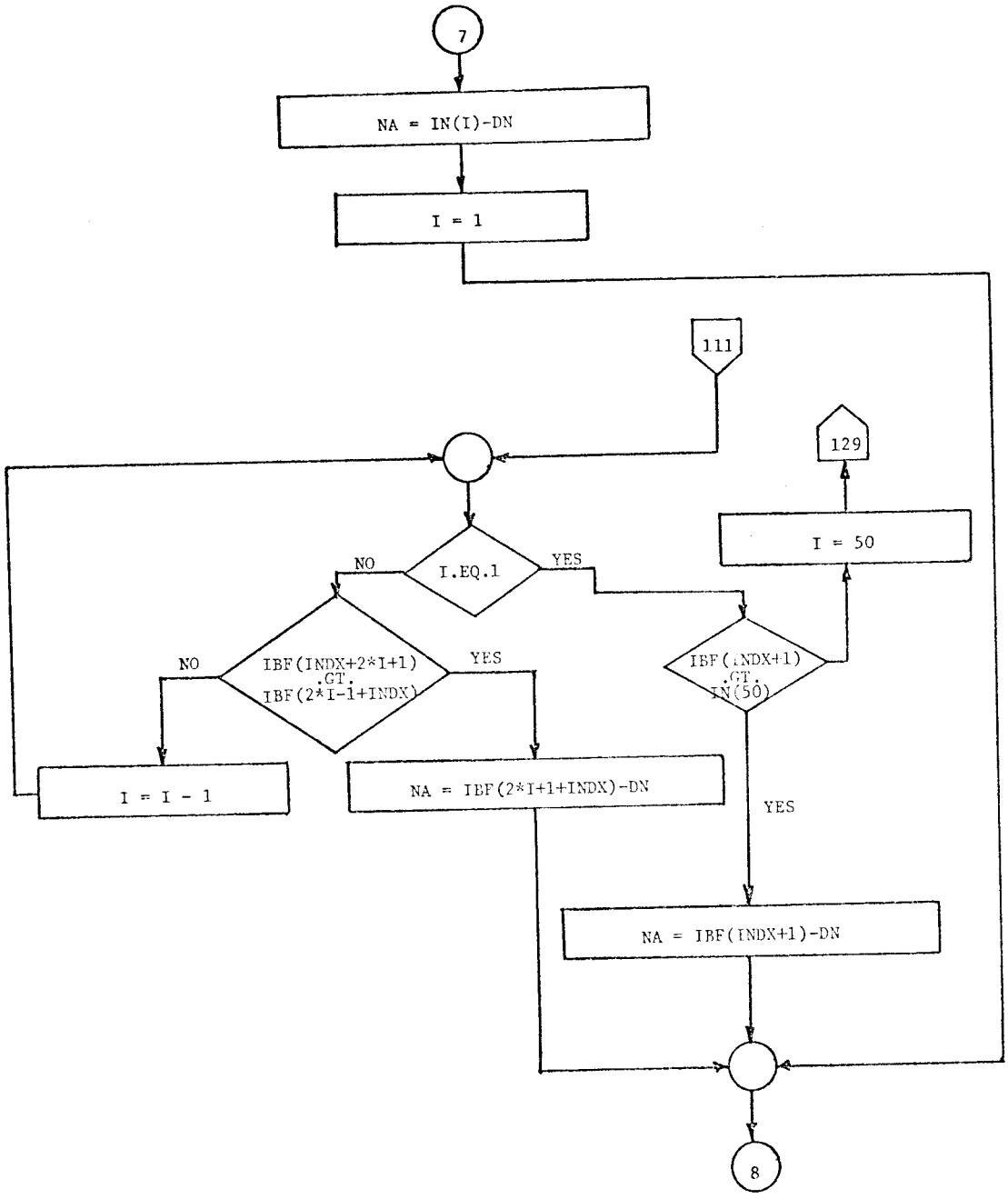
7
NA = IN(I)-DN
I = 1
111
129
I = 50
NO
I.EQ.1
YES
NO
IBF(INDX+2*I+1) .GT. IBF(2*I-1+INDX)
YES
IBF(INDX+1) .GT. IN(50)
I = I - 1
NA = IBF(2*I+1+INDX)-DN
YES
NA = IBF(INDX+1)-DN
8

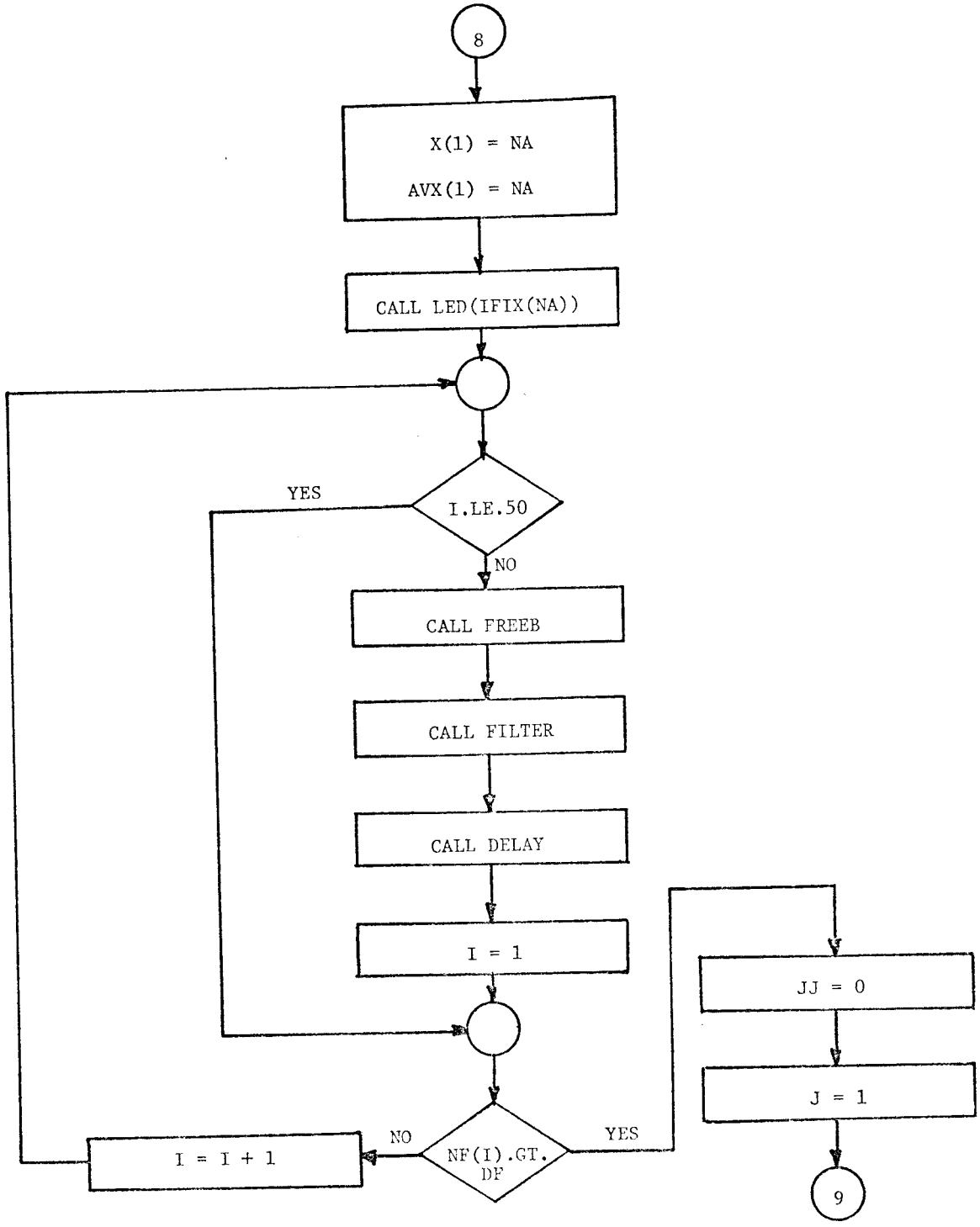
8
X(1) = NA
AVX(1) = NA
CALL LED(IFIX(NA))
YES
I.LE.50
NO
CALL FREEB
CALL FILTER
CALL DELAY
I = 1
JJ = 0
J = 1
9
NO
NF(I).GT.
DF
YES
I = I + 1

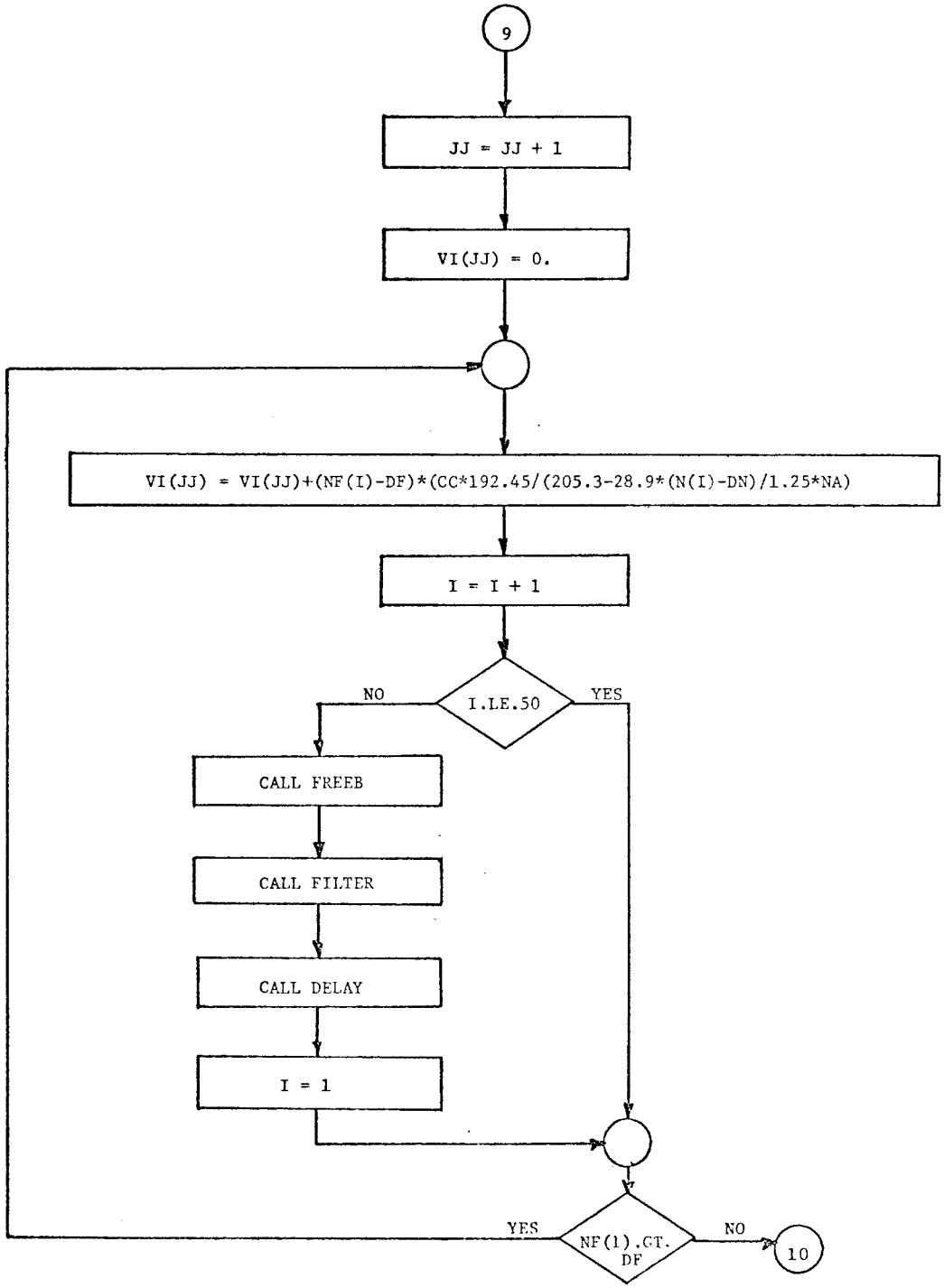
9
JJ = JJ + 1
VI(JJ) = 0.
VI(JJ) = VI(JJ)+(NF(I)-DF)*(CC*192.45/(205.3-28.9*(N(I)-DN)/1.25*NA)
I = I + 1
I.LE.50
NO
YES
CALL FREEB
CALL FILTER
CALL DELAY
I = 1
NF(1).GT. DF
YES
NO
10

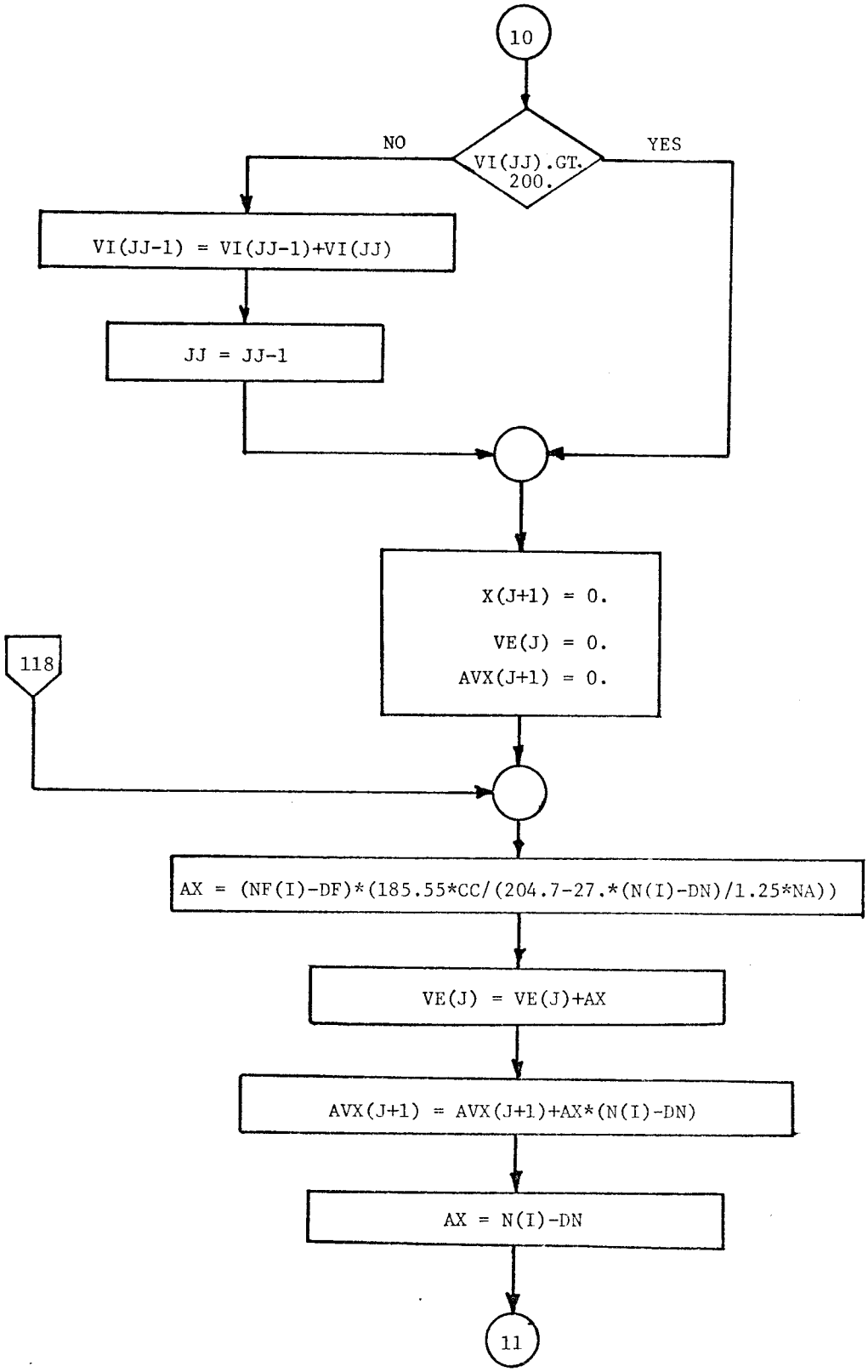
10
VI(JJ).GT.
200.
NO
YES
VI(JJ-1) = VI(JJ-1)+VI(JJ)
JJ = JJ-1
X(J+1) = 0.
VE(J) = 0.
AVX(J+1) = 0.
118
AX = (NF(I)-DF)*(185.55*CC/(204.7-27.*(N(I)-DN)/1.25*NA))
VE(J) = VE(J)+AX
AVX(J+1) = AVX(J+1)+AX*(N(I)-DN)
AX = N(I)-DN
11

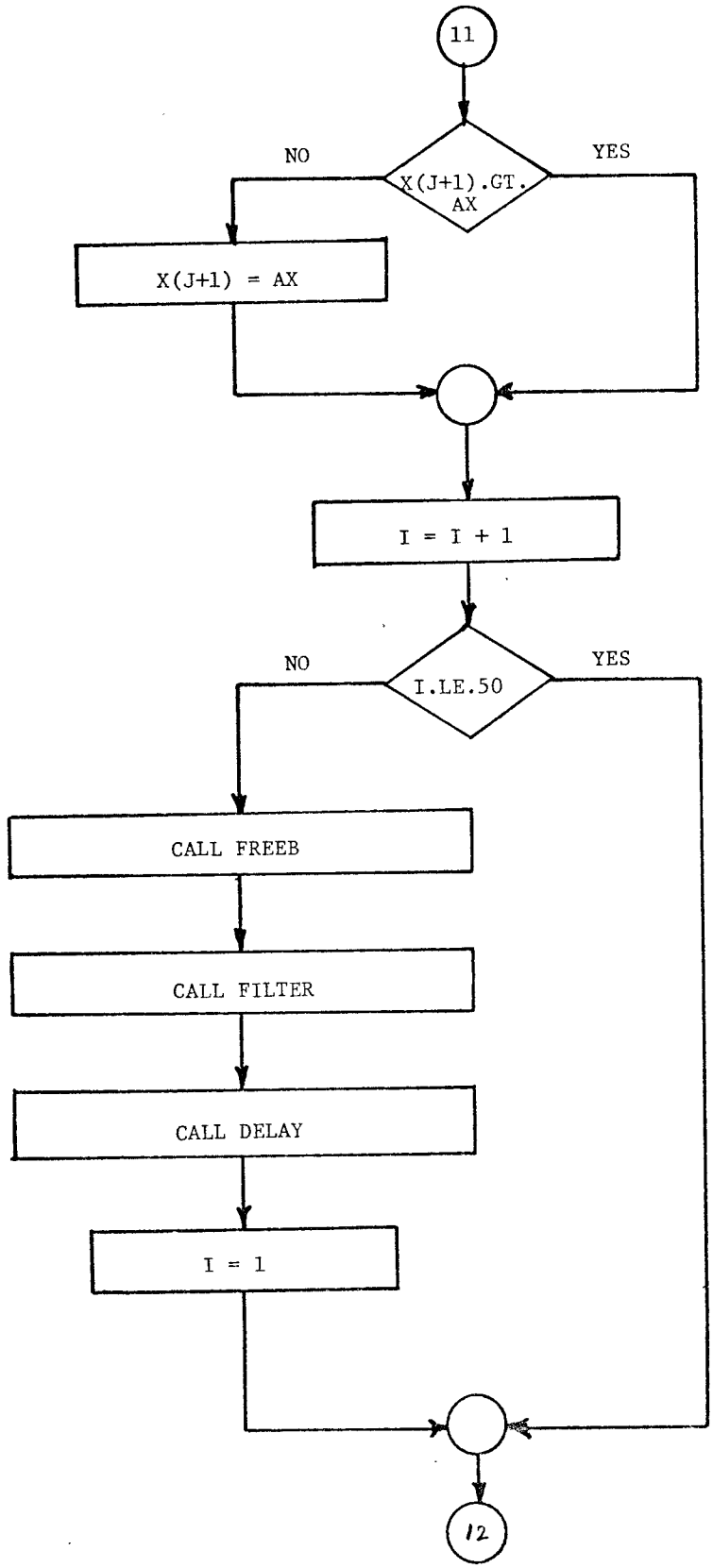
11
NO
X(J+1).GT.
AX
YES
X(J+1) = AX
I = I + 1
NO
I.LE.50
YES
CALL FREEB
CALL FILTER
CALL DELAY
I = 1
12

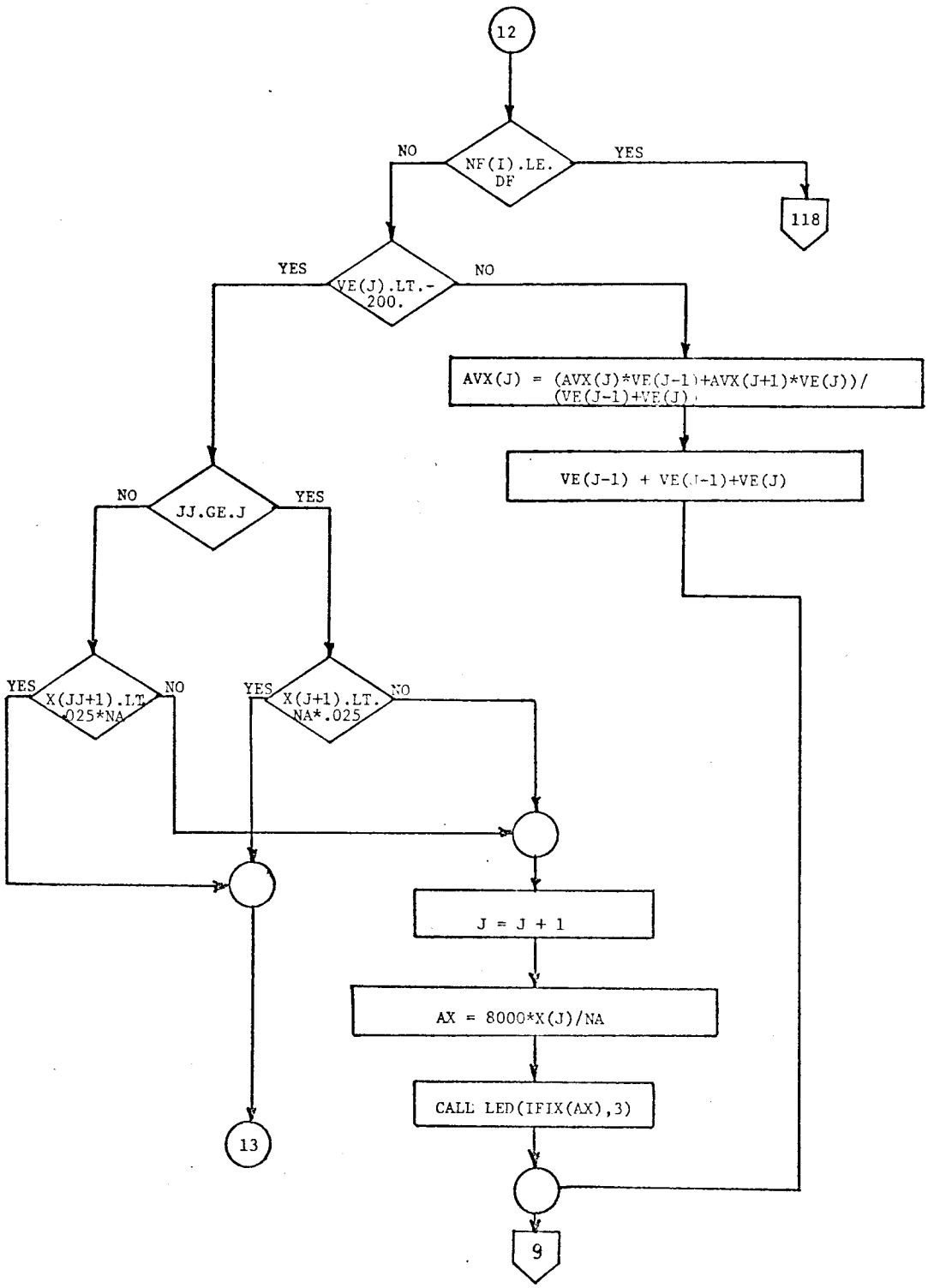
12
NF(I).LE. DF
NO
YES
118
VE(J).LT.-200.
YES
NO
AVX(J) = (AVX(J)*VE(J-1)+AVX(J+1)*VE(J))/(VE(J-1)+VE(J))
VE(J-1) + VE(J-1)+VE(J)
JJ.GE.J
NO
YES
X(JJ+1).LT. .025*NA
YES
NO
X(J+1).LT. NA*.025
YES
NO
J = J + 1
AX = 8000*X(J)/NA
CALL LED(IFIX(AX),3)
13
9

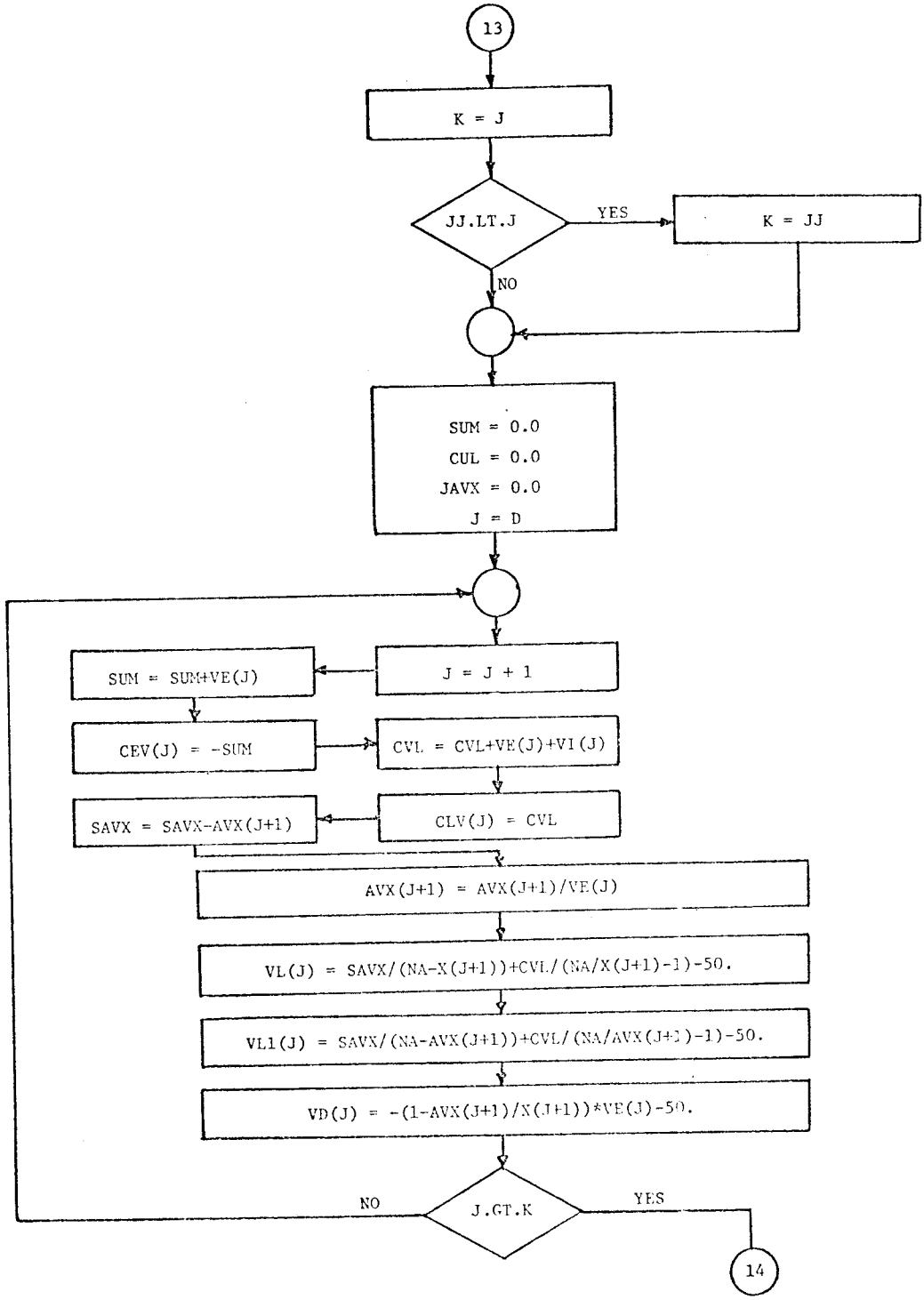
13
K = J
JJ.LT.J
YES
K = JJ
NO
SUM = 0.0
CUL = 0.0
JAVX = 0.0
J = D
J = J + 1
SUM = SUM+VE(J)
CEV(J) = -SUM
CVL = CVL+VE(J)+VI(J)
SAVX = SAVX-AVX(J+1)
CLV(J) = CVL
AVX(J+1) = AVX(J+1)/VE(J)
VL(J) = SAVX/(NA-X(J+1))+CVL/(NA/X(J+1)-1)-50.
VL1(J) = SAVX/(NA-AVX(J+1))+CVL/(NA/AVX(J+1)-1)-50.
VD(J) = -(1-AVX(J+1)/X(J+1))*VE(J)-50.
J.GT.K
NO
YES
14

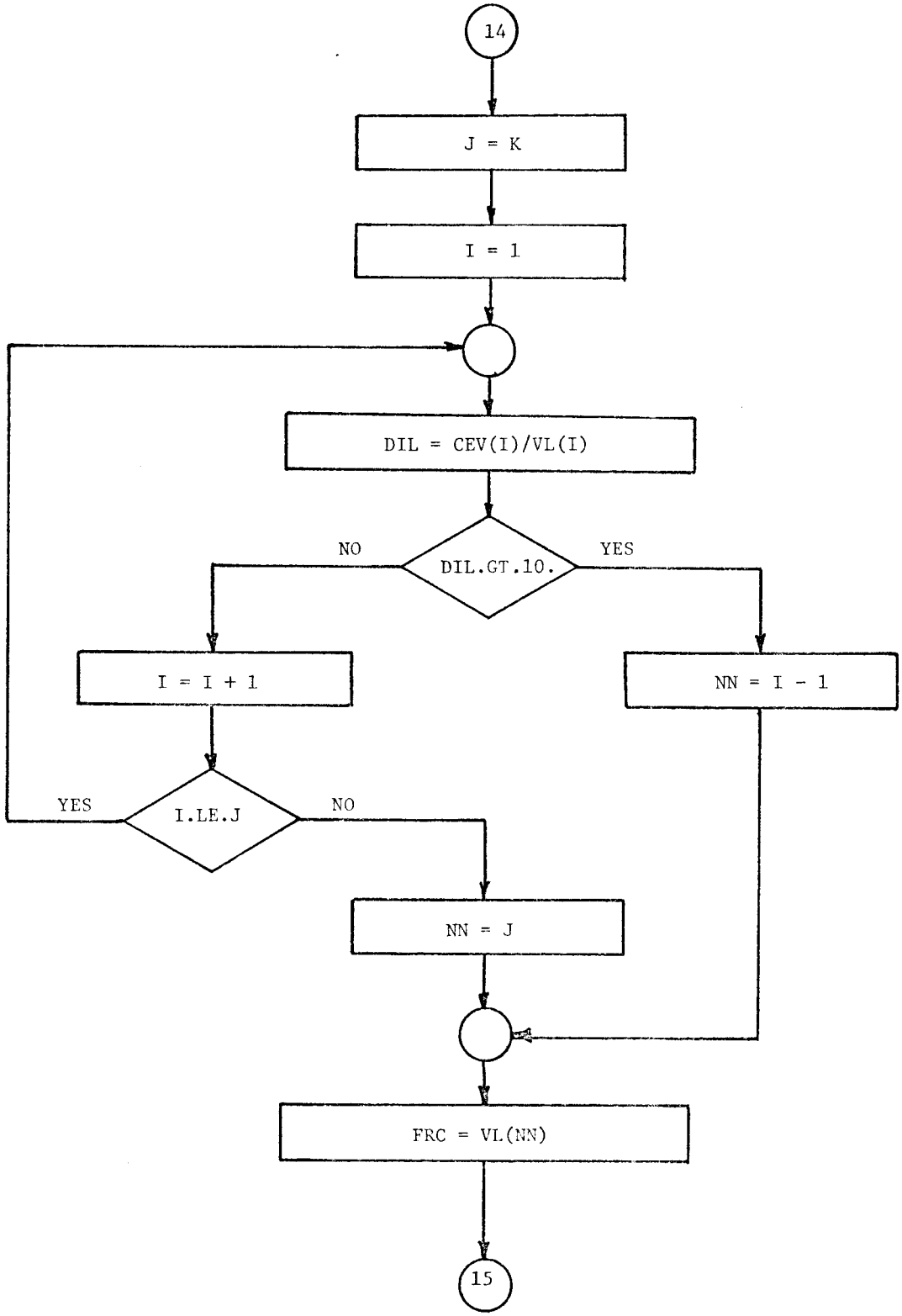
14
J = K
I = 1
DIL = CEV(I)/VL(I)
DIL.GT.10.
NO
YES
I = I + 1
NN = I - 1
I.LE.J
YES
NO
NN = J
FRC = VL(NN)
15

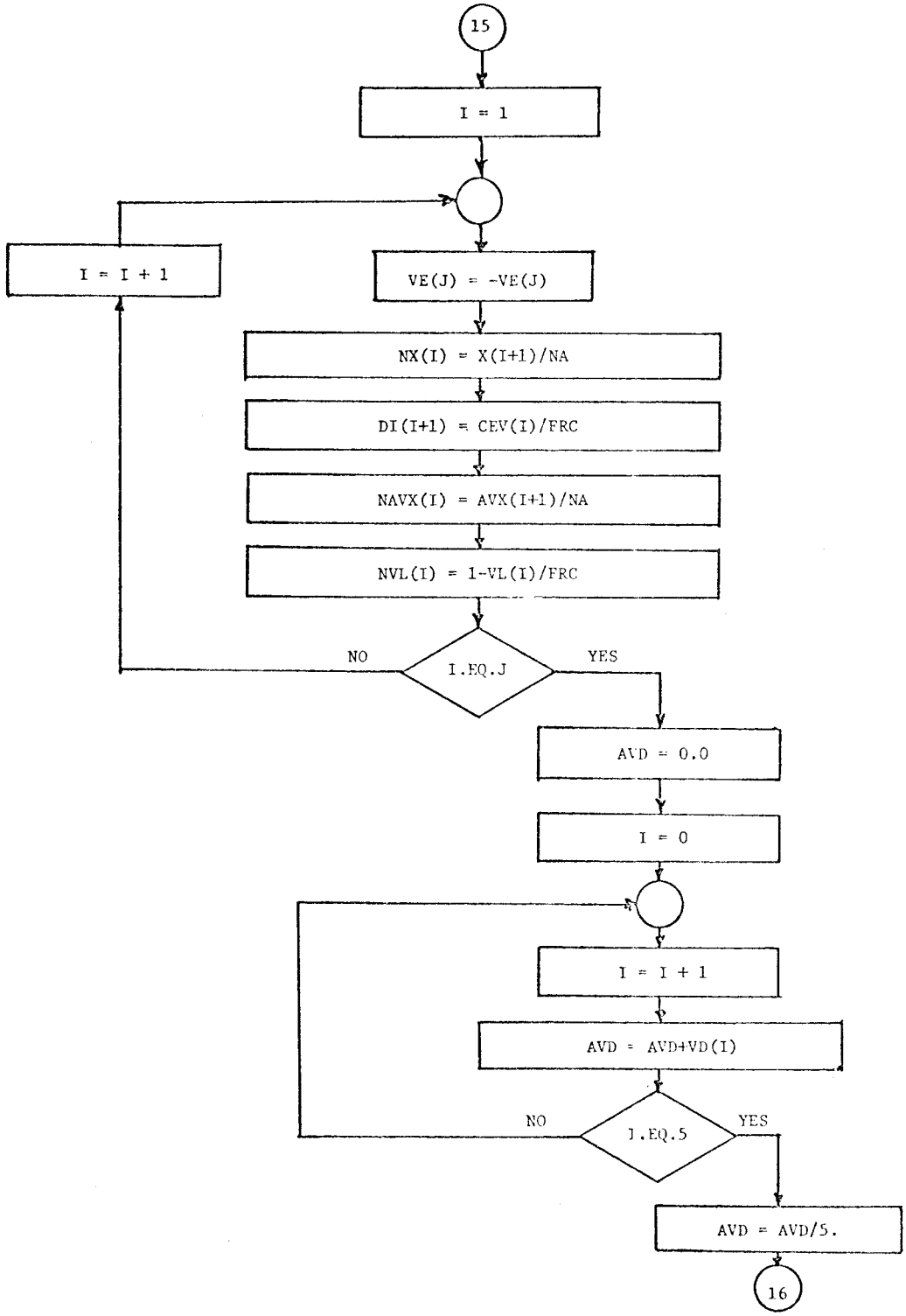
15
I = 1
I = I + 1
VE(J) = -VE(J)
NX(I) = X(I+1)/NA
DI(I+1) = CEV(I)/FRC
NAVX(I) = AVX(I+1)/NA
NVL(I) = 1-VL(I)/FRC
NO
I.EQ.J
YES
AVD = 0.0
I = 0
I = I + 1
AVD = AVD+VD(I)
NO
I.EQ.5
YES
AVD = AVD/5.
16

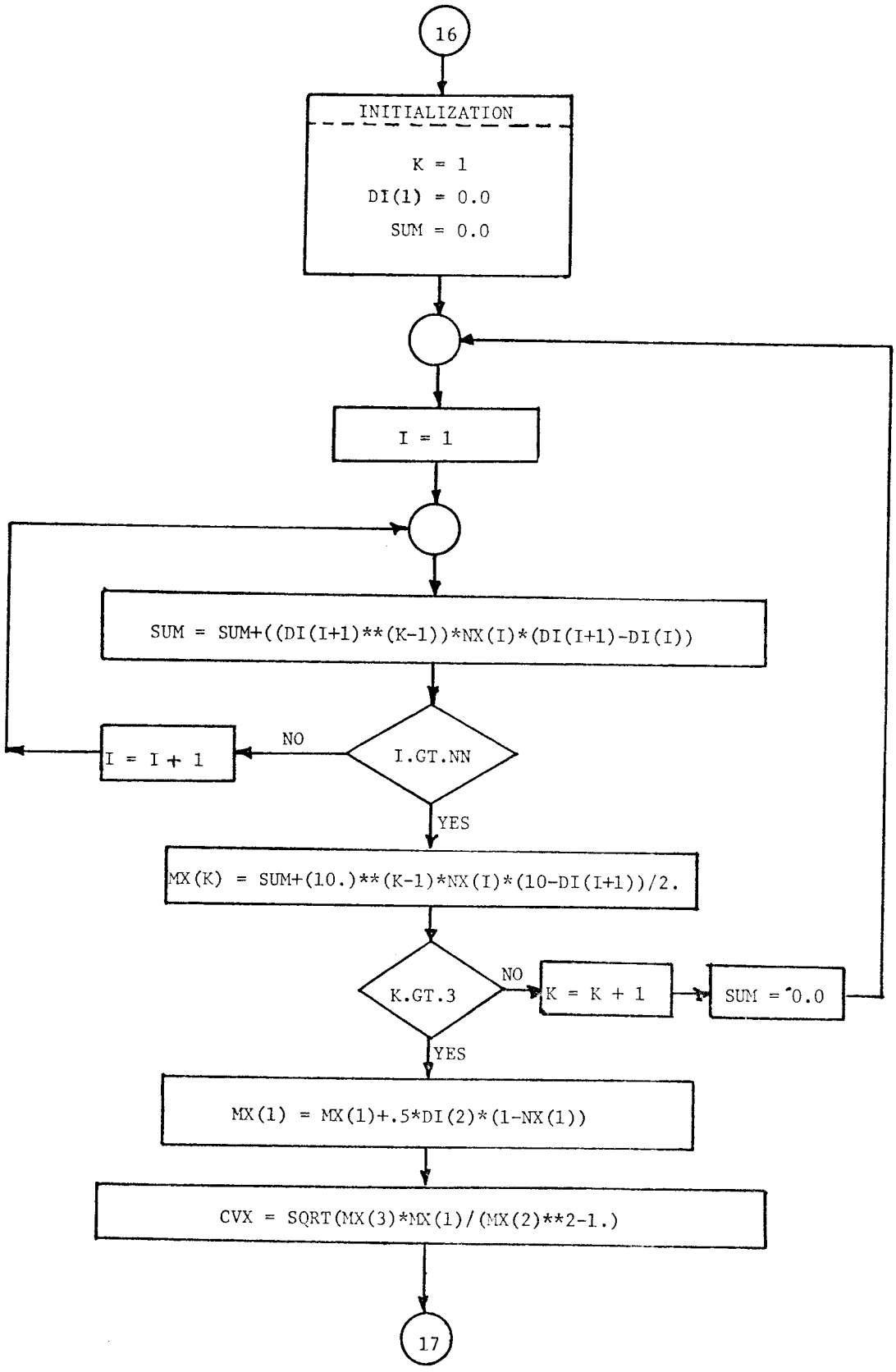
16
INITIALIZATION
K = 1
DI(1) = 0.0
SUM = 0.0
I = 1
SUM = SUM+((DI(I+1)**(K-1))*NX(I)*(DI(I+1)-DI(I))
I.GT.NN
NO
I = I + 1
YES
MX(K) = SUM+(10.)**(K-1)*NX(I)*(10-DI(I+1))/2.
K.GT.3
NO
K = K + 1
SUM = 0.0
YES
MX(1) = MX(1)+.5*DI(2)*(1-NX(1))
CVX = SQRT(MX(3)*MX(1)/(MX(2)**2-1.)
17

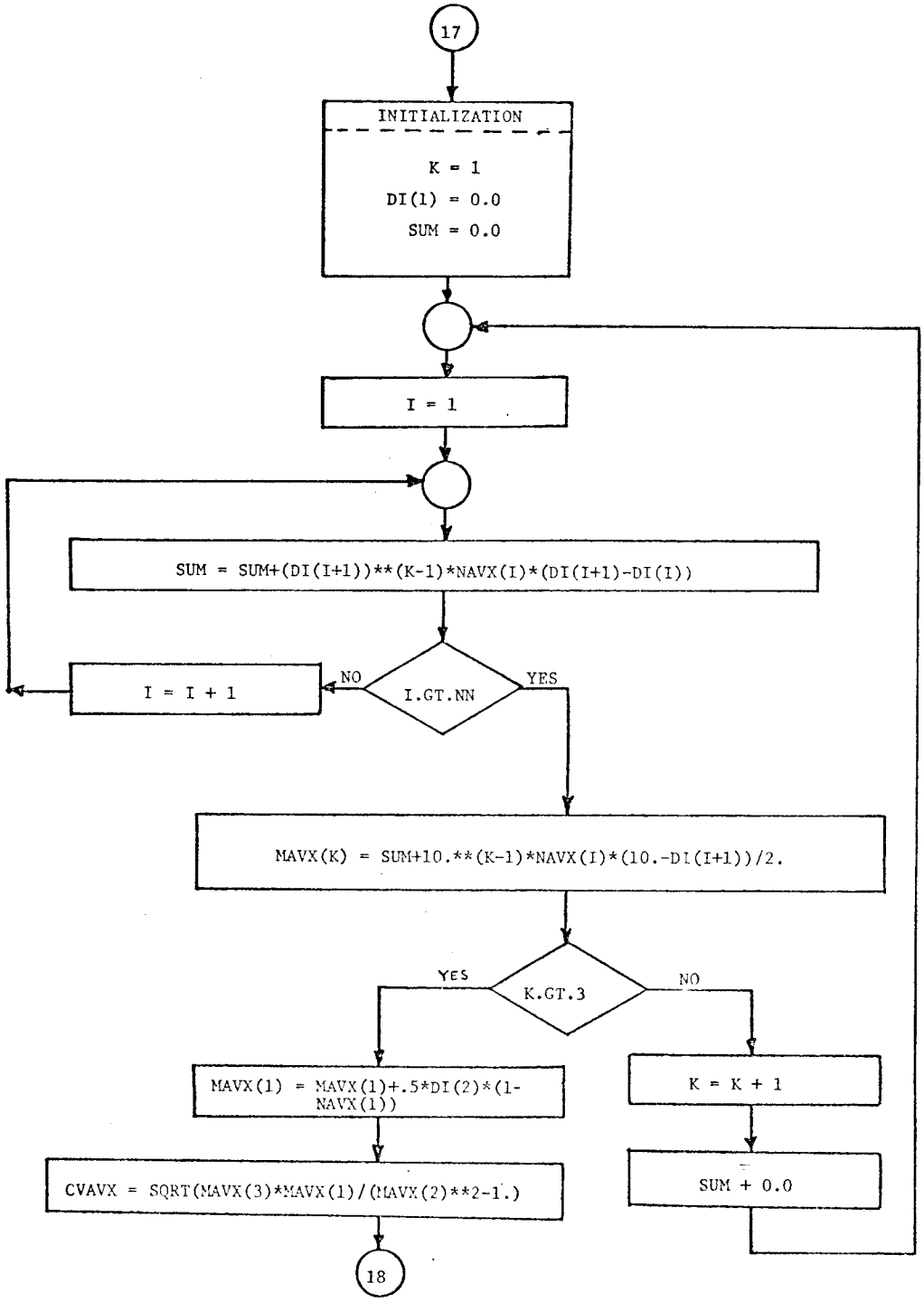
17
INITIALIZATION
K = 1
DI(1) = 0.0
SUM = 0.0
I = 1
SUM = SUM+(DI(I+1))**(K-1)*NAVX(I)*(DI(I+1)-DI(I))
I.GT.NN
NO
YES
I = I + 1
MAVX(K) = SUM+10.**(K-1)*NAVX(I)*(10.-DI(I+1))/2.
K.GT.3
YES
NO
MAVX(1) = MAVX(1)+.5*DI(2)*(1-NAVX(1))
CVAVX = SQRT(MAVX(3)*MAVX(1)/(MAVX(2)**2-1.)
18
K = K + 1
SUM + 0.0

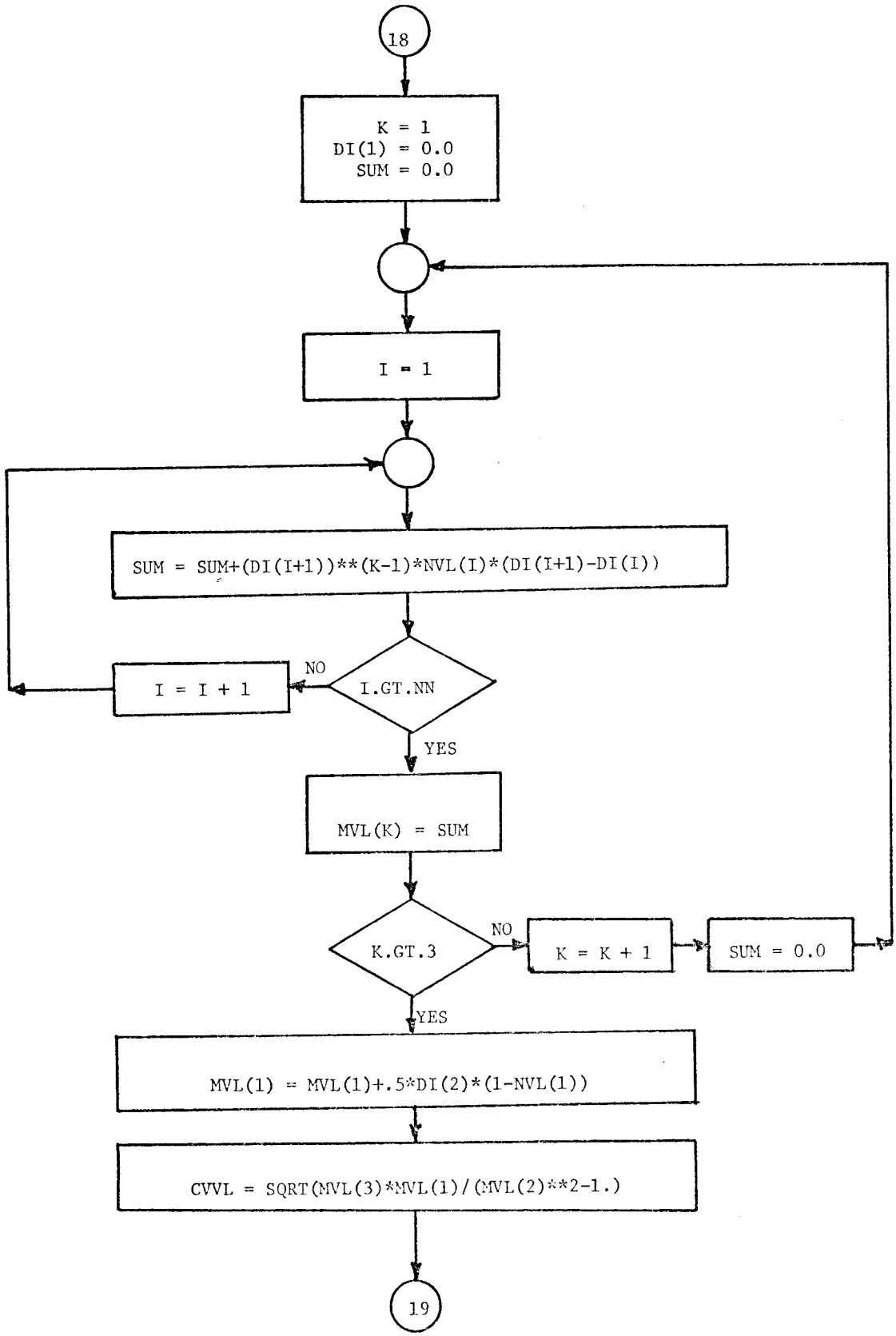
18
K = 1
DI(1) = 0.0
SUM = 0.0
I = 1
SUM = SUM+(DI(I+1))**(K-1)*NVL(I)*(DI(I+1)-DI(I))
I.GT.NN
NO
I = I + 1
YES
MVL(K) = SUM
K.GT.3
NO
K = K + 1
SUM = 0.0
YES
MVL(1) = MVL(1)+.5*DI(2)*(1-NVL(1))
CVVL = SQRT(MVL(3)*MVL(1)/(MVL(2)**2-1.)
19

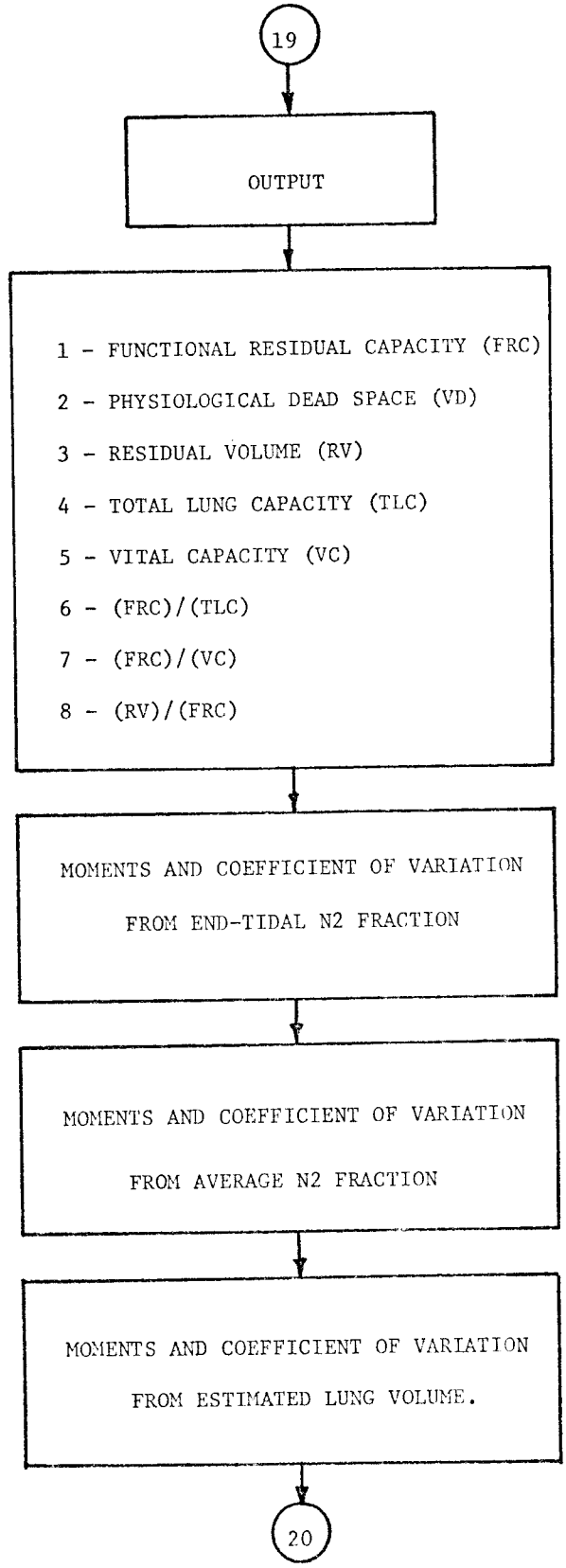
19
OUTPUT
1 - FUNCTIONAL RESIDUAL CAPACITY (FRC)
2 - PHYSIOLOGICAL DEAD SPACE (VD)
3 - RESIDUAL VOLUME (RV)
4 - TOTAL LUNG CAPACITY (TLC)
5 - VITAL CAPACITY (VC)
6 - (FRC)/(TLC)
7 - (FRC)/(VC)
8 - (RV)/(FRC)
MOMENTS AND COEFFICIENT OF VARIATION
FROM END-TIDAL N2 FRACTION
MOMENTS AND COEFFICIENT OF VARIATION
FROM AVERAGE N2 FRACTION
MOMENTS AND COEFFICIENT OF VARIATION
FROM ESTIMATED LUNG VOLUME.
20

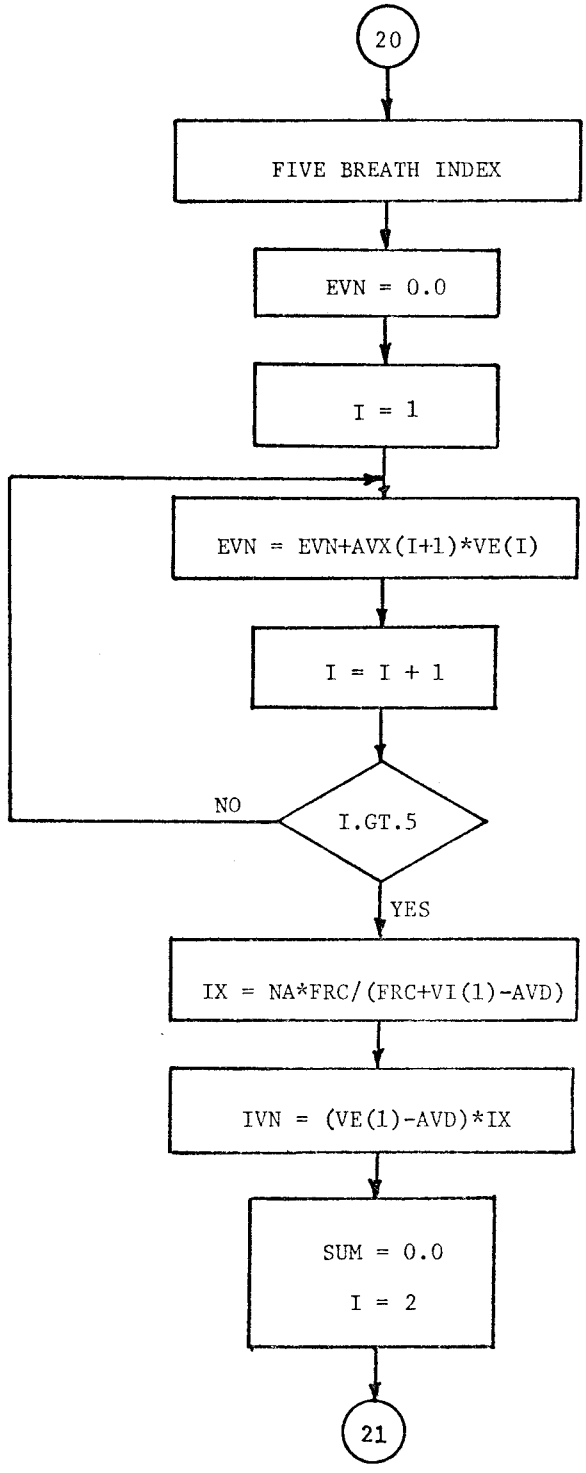
20
FIVE BREATH INDEX
EVN = 0.0
I = 1
EVN = EVN+AVX(I+1)*VE(I)
I = I + 1
I.GT.5
NO
YES
IX = NA*FRC/(FRC+VI(1)-AVD)
IVN = (VE(1)-AVD)*IX
SUM = 0.0
I = 2
21

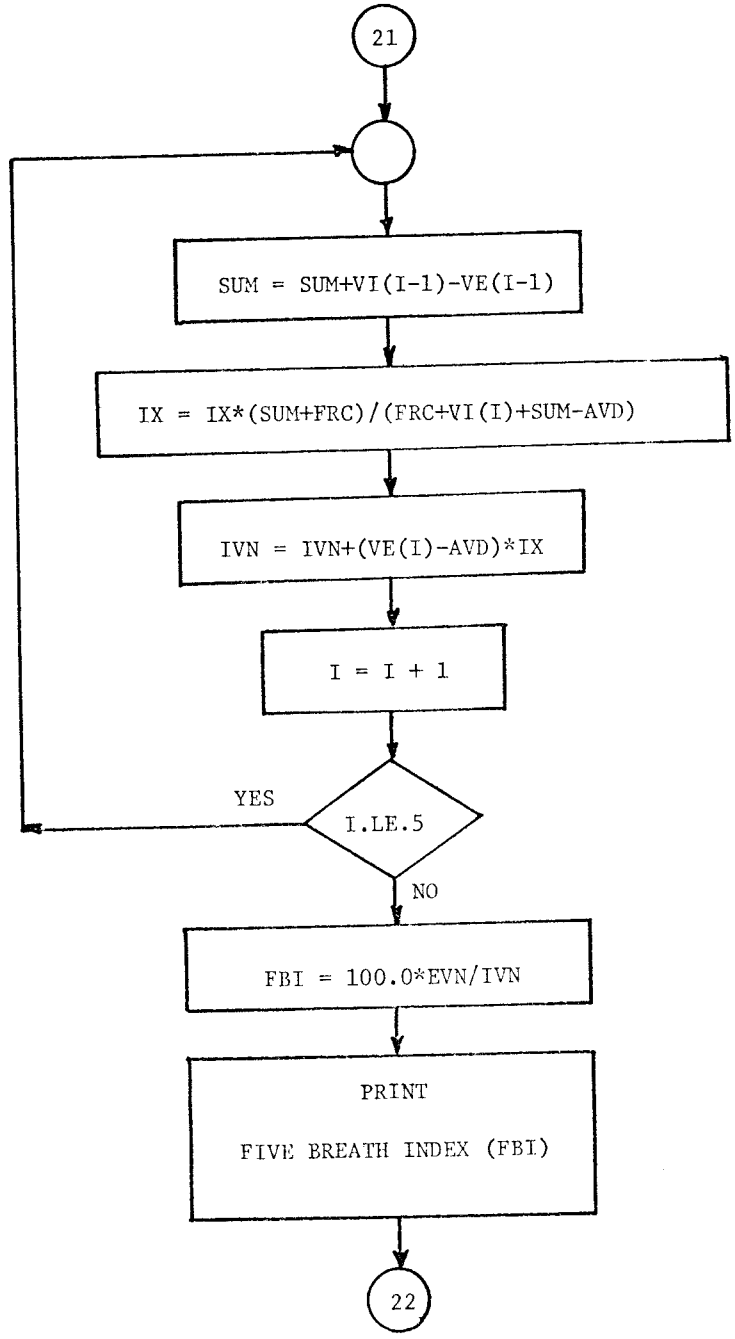
21
SUM = SUM+VI(I-1)-VE(I-1)
IX = IX*(SUM+FRC)/(FRC+VI(I)+SUM-AVD)
IVN = IVN+(VE(I)-AVD)*IX
I = I + 1
YES
I.LE.5
NO
FBI = 100.0*EVN/IVN
PRINT
FIVE BREATH INDEX (FBI)
22

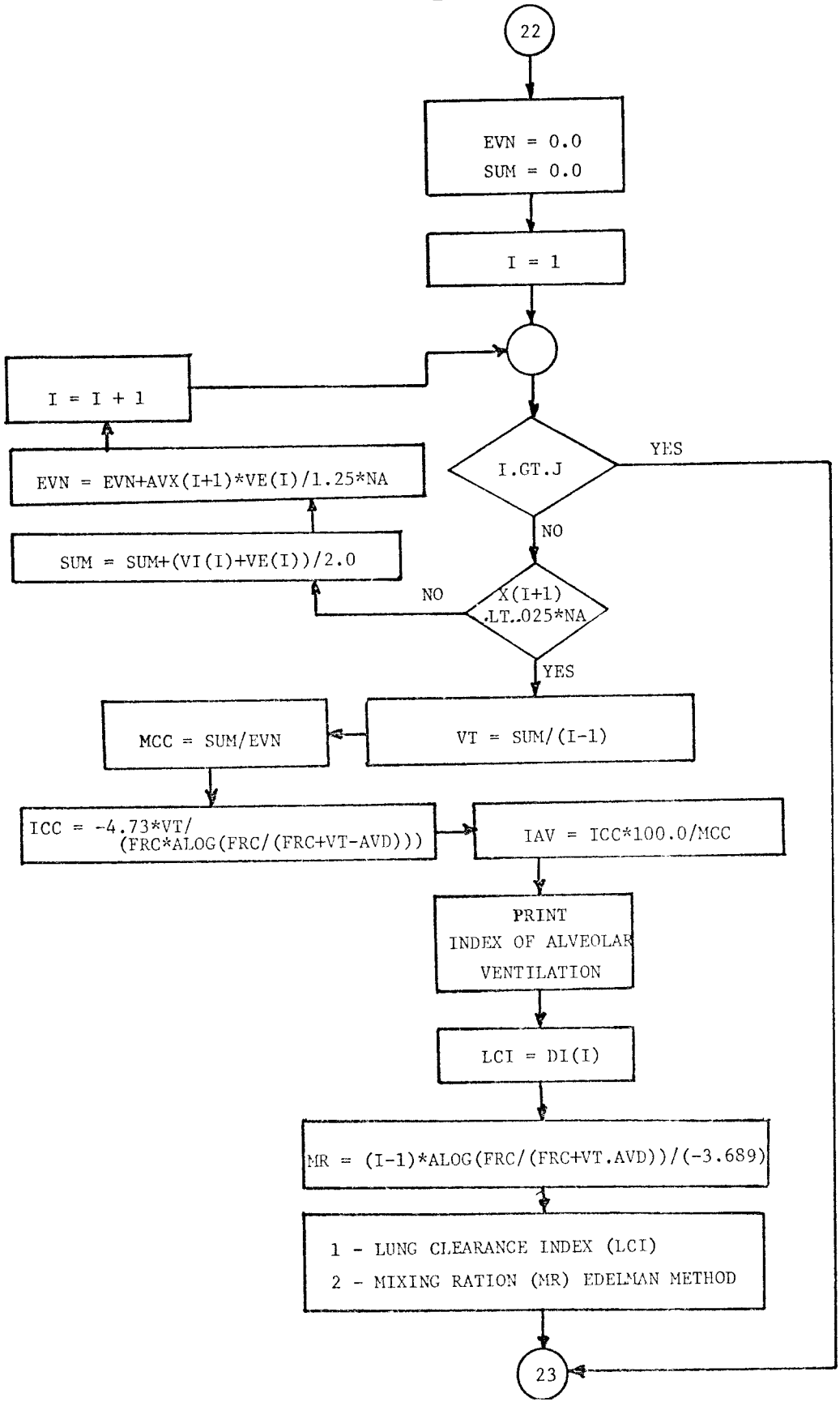
22
EVN = 0.0
SUM = 0.0
I = 1
I = I + 1
EVN = EVN+AVX(I+1)*VE(I)/1.25*NA
SUM = SUM+(VI(I)+VE(I))/2.0
I.GT.J
YES
NO
X(I+1) .LT..025*NA
NO
YES
MCC = SUM/EVN
VT = SUM/(I-1)
ICC = -4.73*VT/ (FRC*ALOG(FRC/(FRC+VT-AVD)))
IAV = ICC*100.0/MCC
PRINT INDEX OF ALVEOLAR VENTILATION
LCI = DI(I)
MR = (I-1)*ALOG(FRC/(FRC+VT.AVD))/(-3.689)
1 - LUNG CLEARANCE INDEX (LCI)
2 - MIXING RATION (MR) EDELMAN METHOD
23

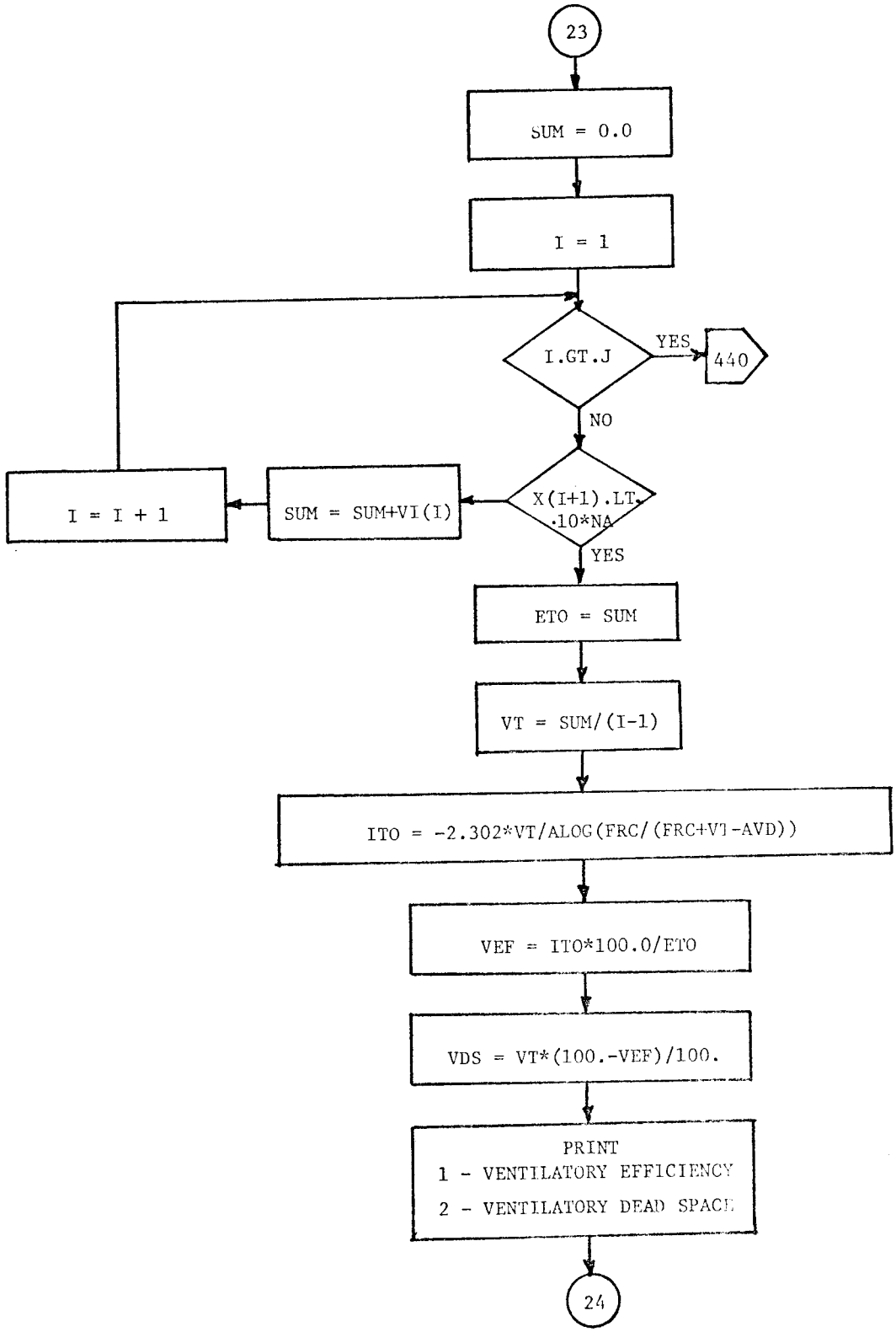
23
SUM = 0.0
I = 1
I.GT.J
YES
440
NO
X(I+1).LT.
.10*NA
SUM = SUM+VI(I)
I = I + 1
YES
ETO = SUM
VT = SUM/(I-1)
ITO = -2.302*VT/ALOG(FRC/(FRC+VT-AVD))
VEF = ITO*100.0/ETO
VDS = VT*(100.-VEF)/100.
PRINT
1 - VENTILATORY EFFICIENCY
2 - VENTILATORY DEAD SPACE
24

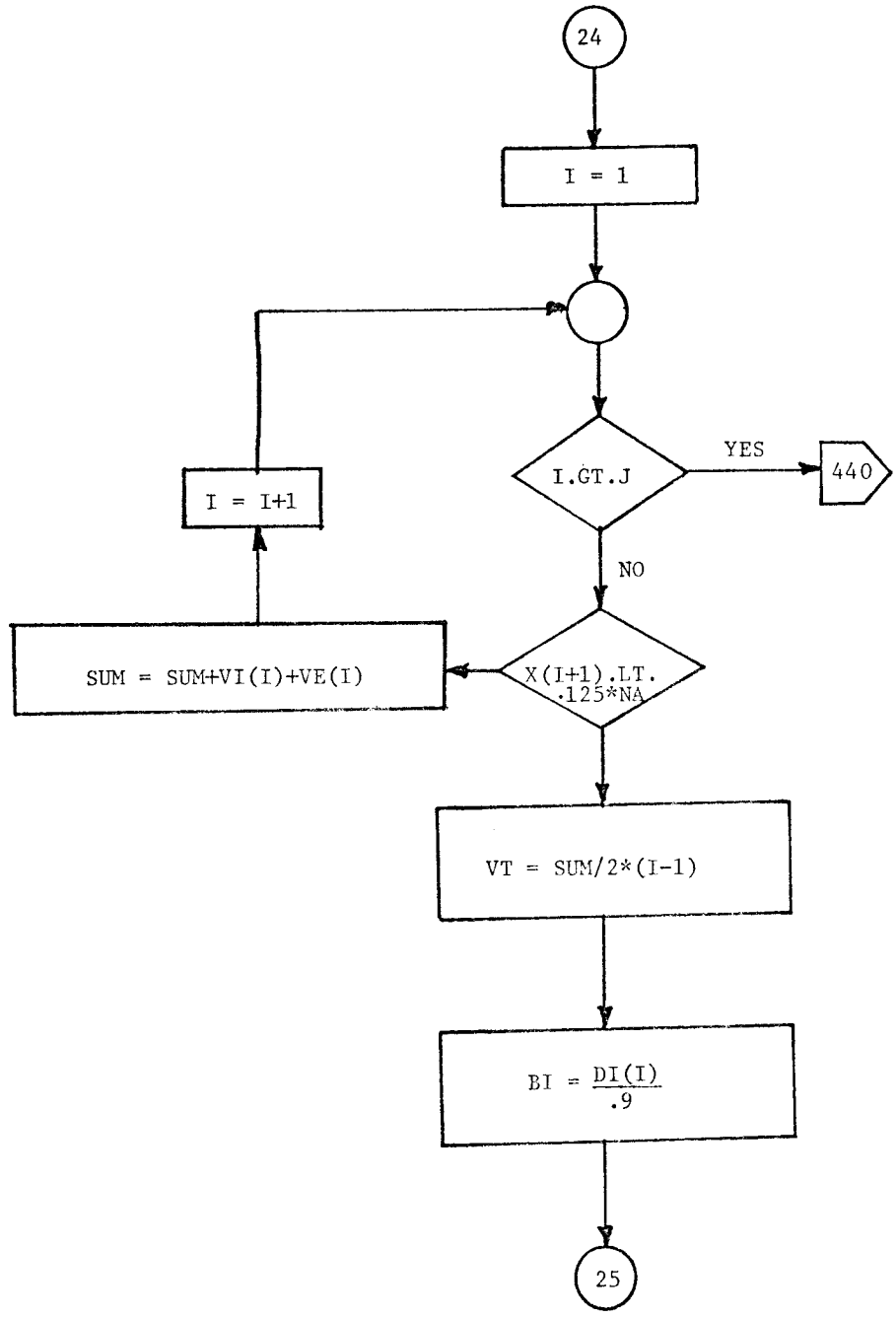
24
I = 1
I.GT.J
YES
440
NO
I = I+1
SUM = SUM+VI(I)+VE(I)
X(I+1).LT.
.125*NA
VT = SUM/2*(I-1)
BI = DI(I)/.9
25

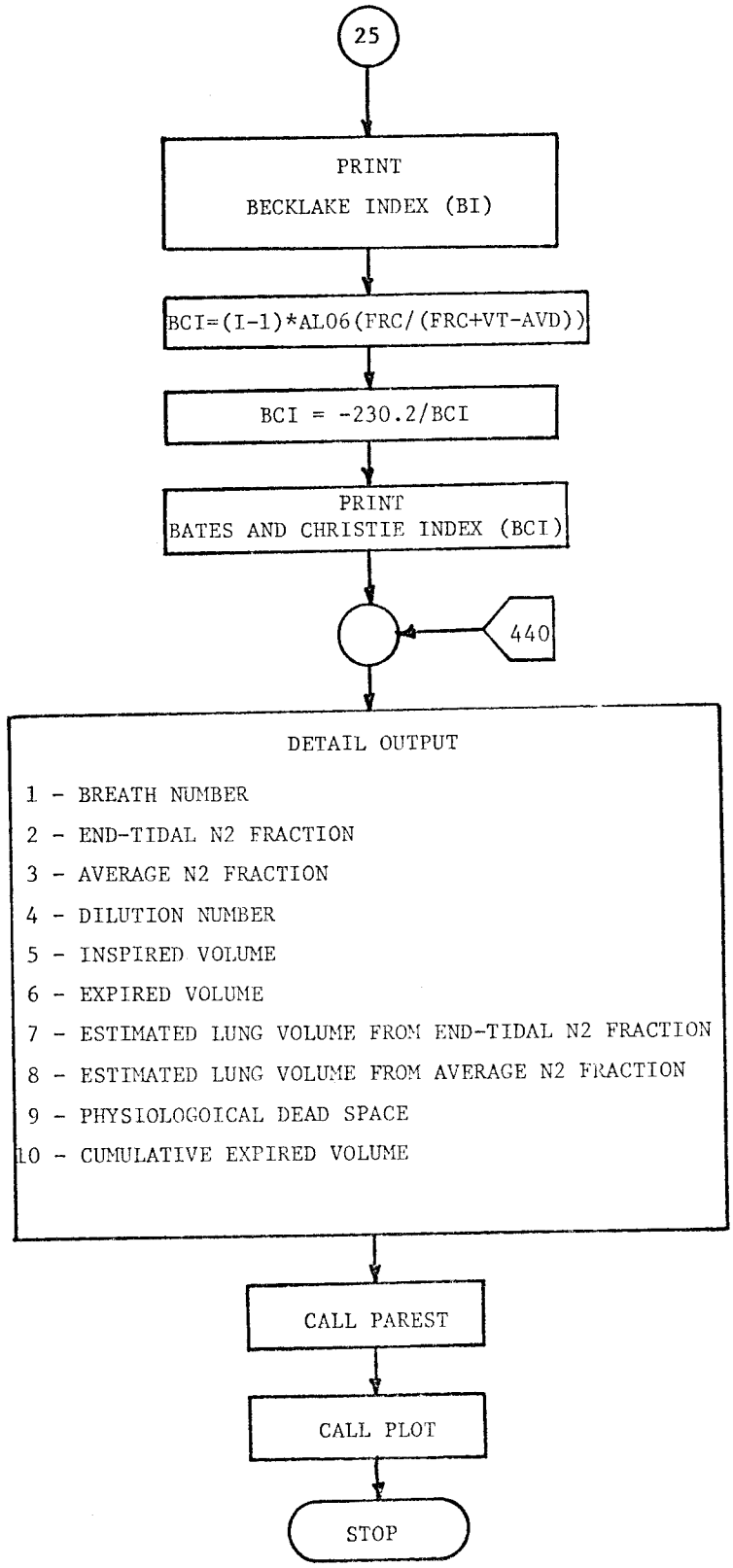
25
PRINT
BECKLAKE INDEX (BI)
BCI=(I-1)*AL06(FRC/(FRC+VT-AVD))
BCI = -230.2/BCI
PRINT
BATES AND CHRISTIE INDEX (BCI)
440
DETAIL OUTPUT
1 - BREATH NUMBER
2 - END-TIDAL N2 FRACTION
3 - AVERAGE N2 FRACTION
4 - DILUTION NUMBER
5 - INSPIRED VOLUME
6 - EXPIRED VOLUME
7 - ESTIMATED LUNG VOLUME FROM END-TIDAL N2 FRACTION
8 - ESTIMATED LUNG VOLUME FROM AVERAGE N2 FRACTION
9 - PHYSIOLOGOICAL DEAD SPACE
10 - CUMULATIVE EXPIRED VOLUME
CALL PAREST
CALL PLOT
STOP

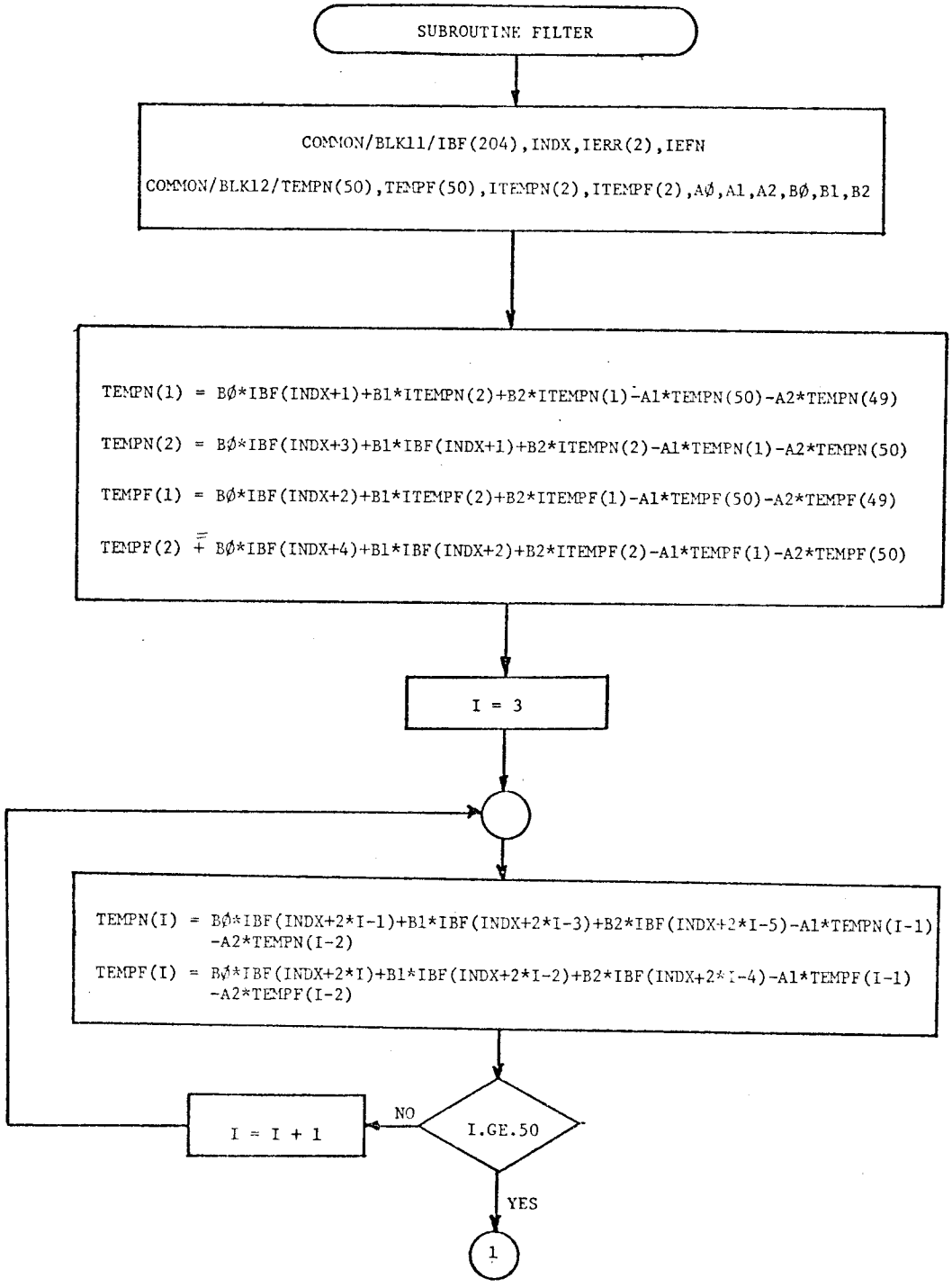
SUBROUTINE FILTER
COMMON/BLK11/IBF(204),INDX,IERR(2),IEFN
COMMON/BLK12/TEMPN(50),TEMPF(50),ITEMPN(2),ITEMPF(2),AØ,A1,A2,BØ,B1,B2
TEMPN(1) = BØ*IBF(INDX+1)+B1*ITEMPN(2)+B2*ITEMPN(1)-A1*TEMPN(50)-A2*TEMPN(49)
TEMPN(2) = BØ*IBF(INDX+3)+B1*IBF(INDX+1)+B2*ITEMPN(2)-A1*TEMPN(1)-A2*TEMPN(50)
TEMPF(1) = BØ*IBF(INDX+2)+B1*ITEMPF(2)+B2*ITEMPF(1)-A1*TEMPF(50)-A2*TEMPF(49)
TEMPF(2) = BØ*IBF(INDX+4)+B1*IBF(INDX+2)+B2*ITEMPF(2)-A1*TEMPF(1)-A2*TEMPF(50)
I = 3
TEMPN(I) = BØ*IBF(INDX+2*I-1)+B1*IBF(INDX+2*I-3)+B2*IBF(INDX+2*I-5)-A1*TEMPN(I-1)
-A2*TEMPN(I-2)
TEMPF(I) = BØ*IBF(INDX+2*I)+B1*IBF(INDX+2*I-2)+B2*IBF(INDX+2*I-4)-A1*TEMPF(I-1)
-A2*TEMPF(I-2)
I.GE.50
NO
I = I + 1
YES
1

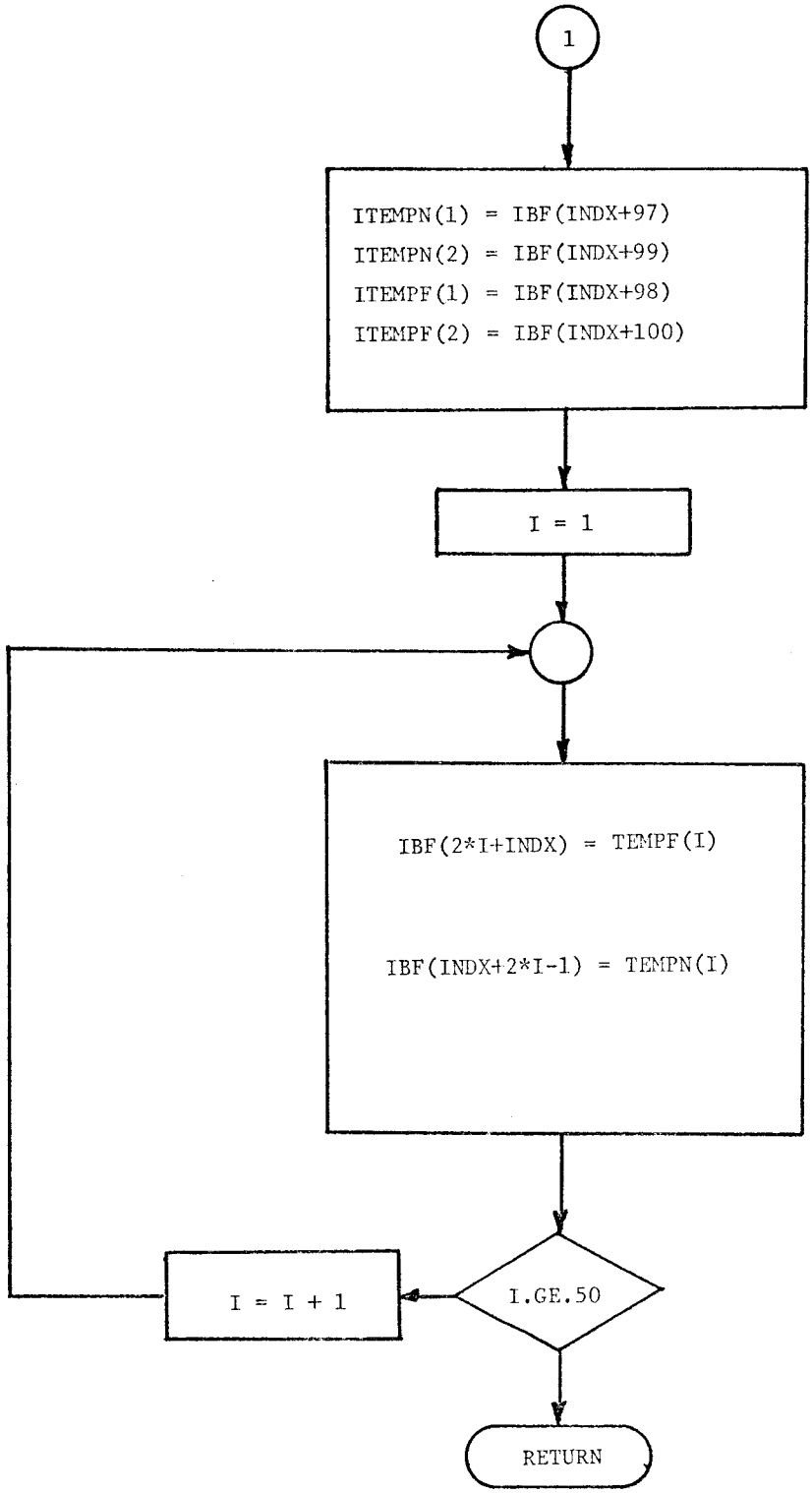
1
ITEMPN(1) = IBF(INDX+97)
ITEMPN(2) = IBF(INDX+99)
ITEMPF(1) = IBF(INDX+98)
ITEMPF(2) = IBF(INDX+100)
I = 1
IBF(2*I+INDX) = TEMPF(I)
IBF(INDX+2*I-1) = TEMPN(I)
I.GE.50
I = I + 1
RETURN

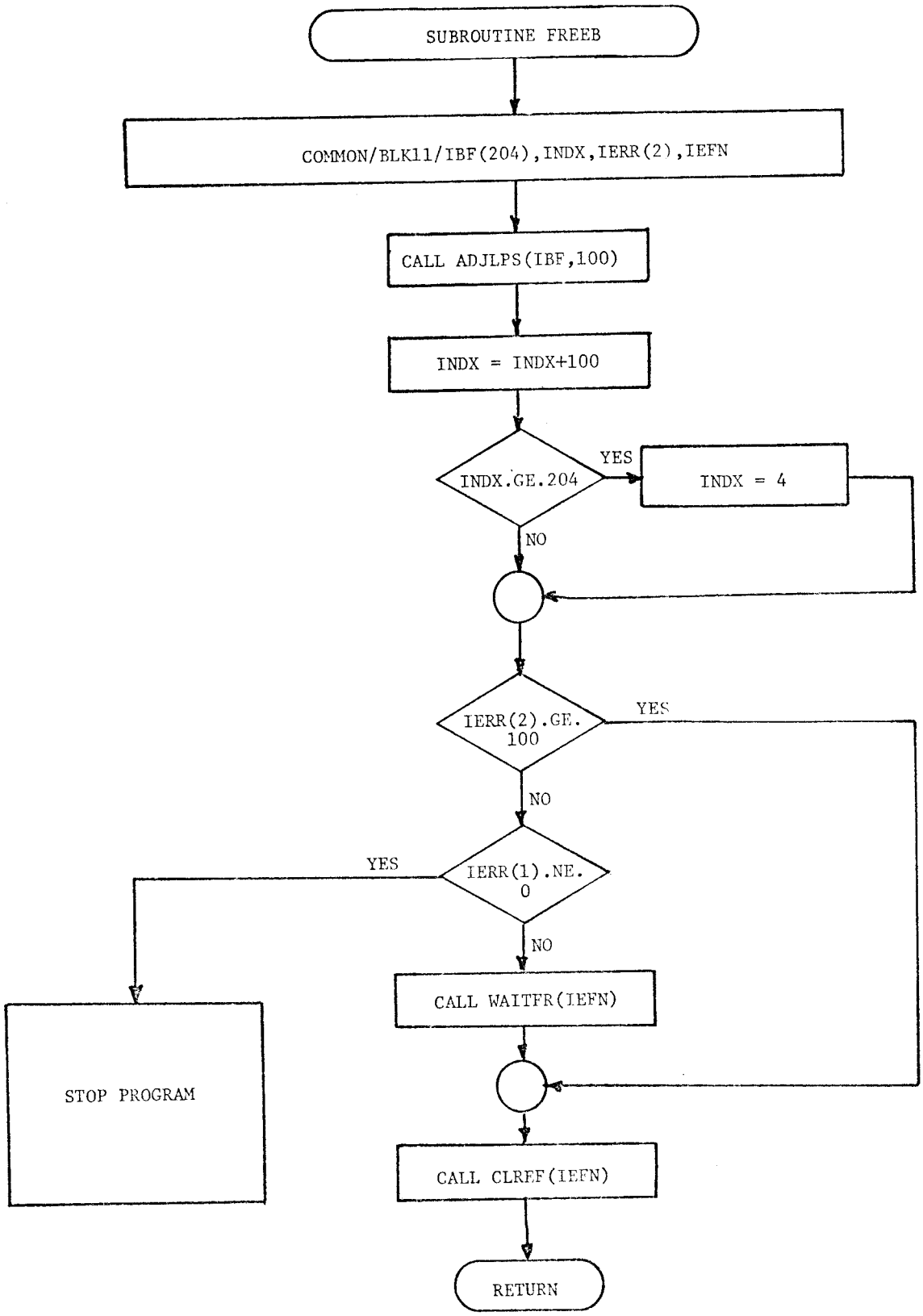
SUBROUTINE FREEB
COMMON/BLK11/IBF(204),INDX,IERR(2),IEFN
CALL ADJLPS(IBF,100)
INDX = INDX+100
INDX.GE.204
YES
INDX = 4
NO
IERR(2).GE. 100
YES
NO
IERR(1).NE. 0
YES
NO
STOP PROGRAM
CALL WAITFR(IEFN)
CALL CLREF(IEFN)
RETURN

## COMPUTATIONAL DESCRIPTION OF PARAMETER ESTIMATION

The parameter estimation program consists of a general function subprogram named PAREST. The MODEL subroutine determines the model's data points. The step size, $\Delta\underline{\theta}^i$, of parameters $f_2$ and $v_2$ are estimated by subroutine called GAUSN. Evaluation of $\Delta\underline{\theta}^i$ is done by PAREST subprogram. The subroutines FDER and VDER compute the partial derivatives of model equations. A flow sheet illustrating our computational algorithm is presented in Figure A-2.

## LIST OF SYMBOLS

| | |
|---|---|
| VI(K): | Inspired volume at K-th breath |
| X(K): | Measured end-tidal N2 fraction at K-th breath |
| AVX(K): | Measured average N2 fraction at K-th breath |
| CLV(K): | Lung volume change after K-th breath |
| FRC: | Functional residual capacity |
| AVD: | Dead space |
| J: | Number of breaths when end-tidal N2 fraction is 2% |
| NN: | Number of breaths when dilution number is less than or equal 10. |
| F2,F3: | Gas flow-splitting fraction [F2+F3=1] |
| V2,V3: | Initial alveolar volume fraction [V2+V3=1] |

LIST OF SYMBOLS-continued

XES1(K): Estimated end-tidal N2 fraction from the model at the end of K-th breath

Y2(K): Calculated N2 fraction in alveolar space (Compartment #2) at the end of K-th breath

Y3(K): Calculated N2 fraction in alveolar space (Compartment #3) at the end of K-th breath

YP2(k): Partial derivative of Y2(K) respect to F2 or V2

YP3(K): Partial derivative of Y3(K) respect to F2 or V2

XES2(K): Partial derivative of XESI(K) respect to F2

XES3(K): Partial derivative of XES1(K) respect to V2

VEI: Ventilation inhomogeneity index

ITER: Number of iteration

LSOF: Least square objective function

MODEL: A Fortran subroutine defines model equations and estimates XESI(K)

FDER: A Fortran subroutine defines derivatives of the model equations respect to F2

VDER: A Fortran subroutine defines derivatives

LIST OF SYMBOLS-continued

of the model equations respect to V2

GAUSN: A Fortran subroutine estimates step size for F2 (DELTA1) and V2 (DELTA2) Algorithem is based on Gauss Newton Method

VI2: Estimated alveolar volume fraction at the end of K-th breath

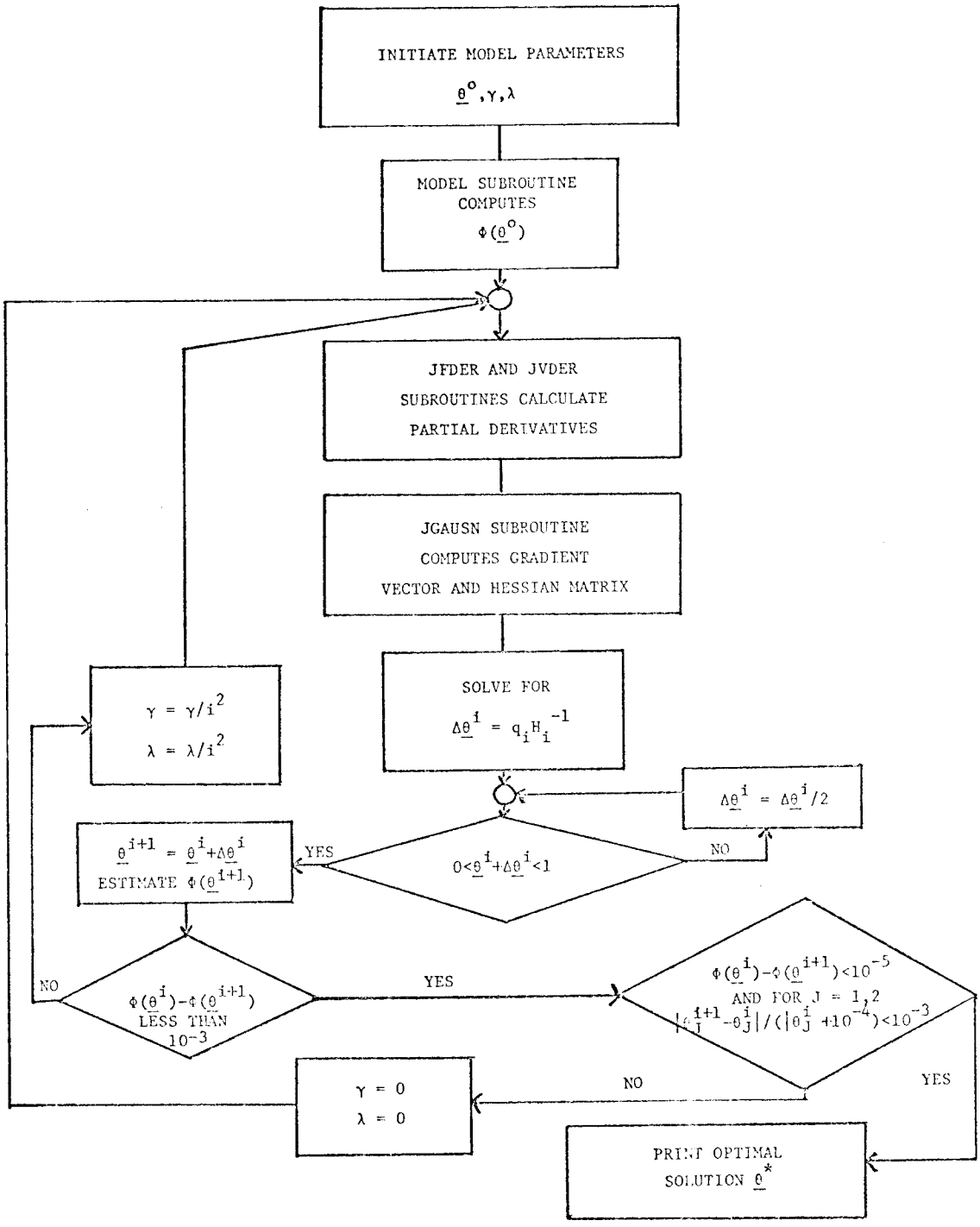


Figure A-2. Parameter estimation computational block diagram

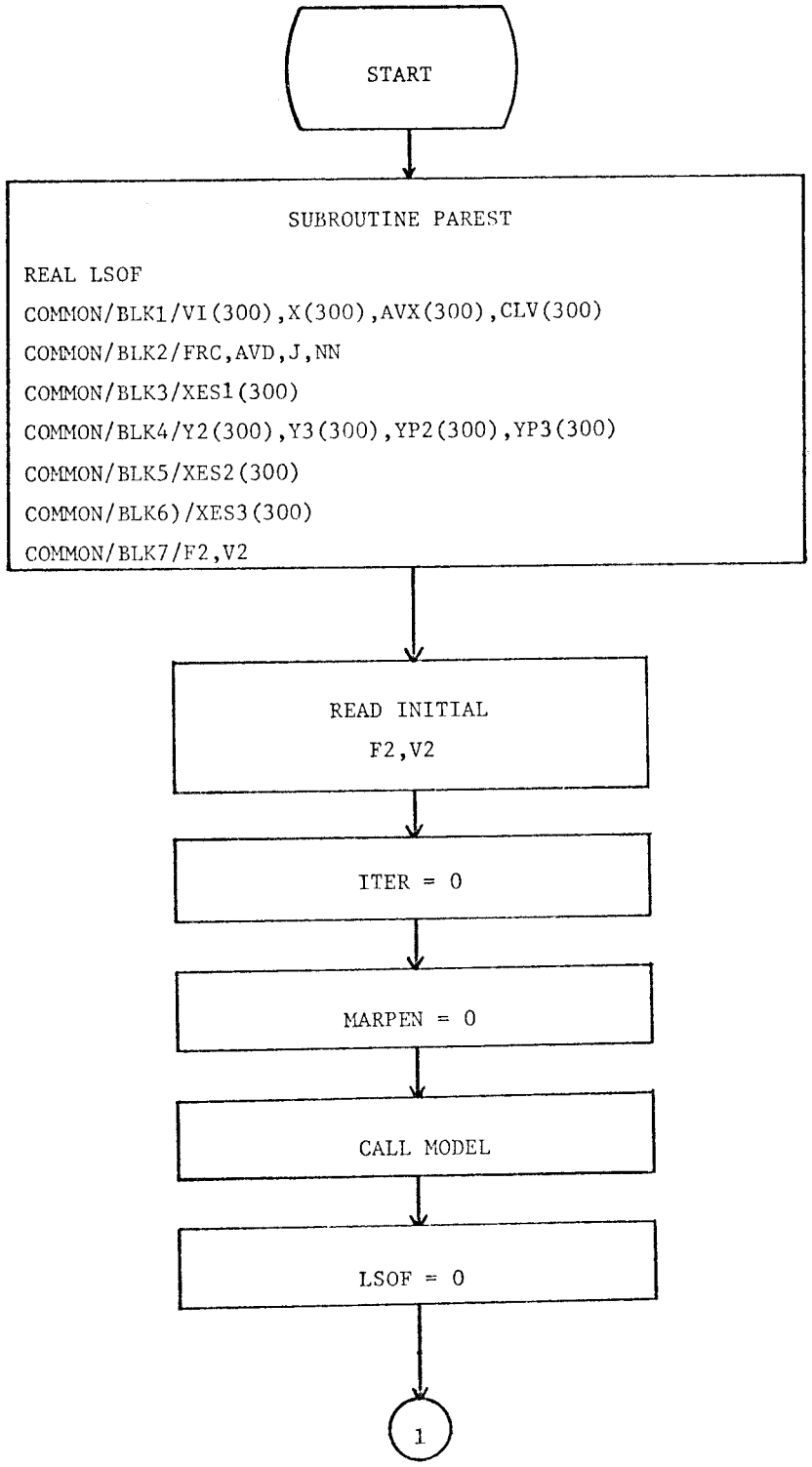
START
SUBROUTINE PAREST
REAL LSOF
COMMON/BLK1/VI(300),X(300),AVX(300),CLV(300)
COMMON/BLK2/FRC,AVD,J,NN
COMMON/BLK3/XES1(300)
COMMON/BLK4/Y2(300),Y3(300),YP2(300),YP3(300)
COMMON/BLK5/XES2(300)
COMMON/BLK6)/XES3(300)
COMMON/BLK7/F2,V2
READ INITIAL
F2,V2
ITER = 0
MARPEN = 0
CALL MODEL
LSOF = 0
1

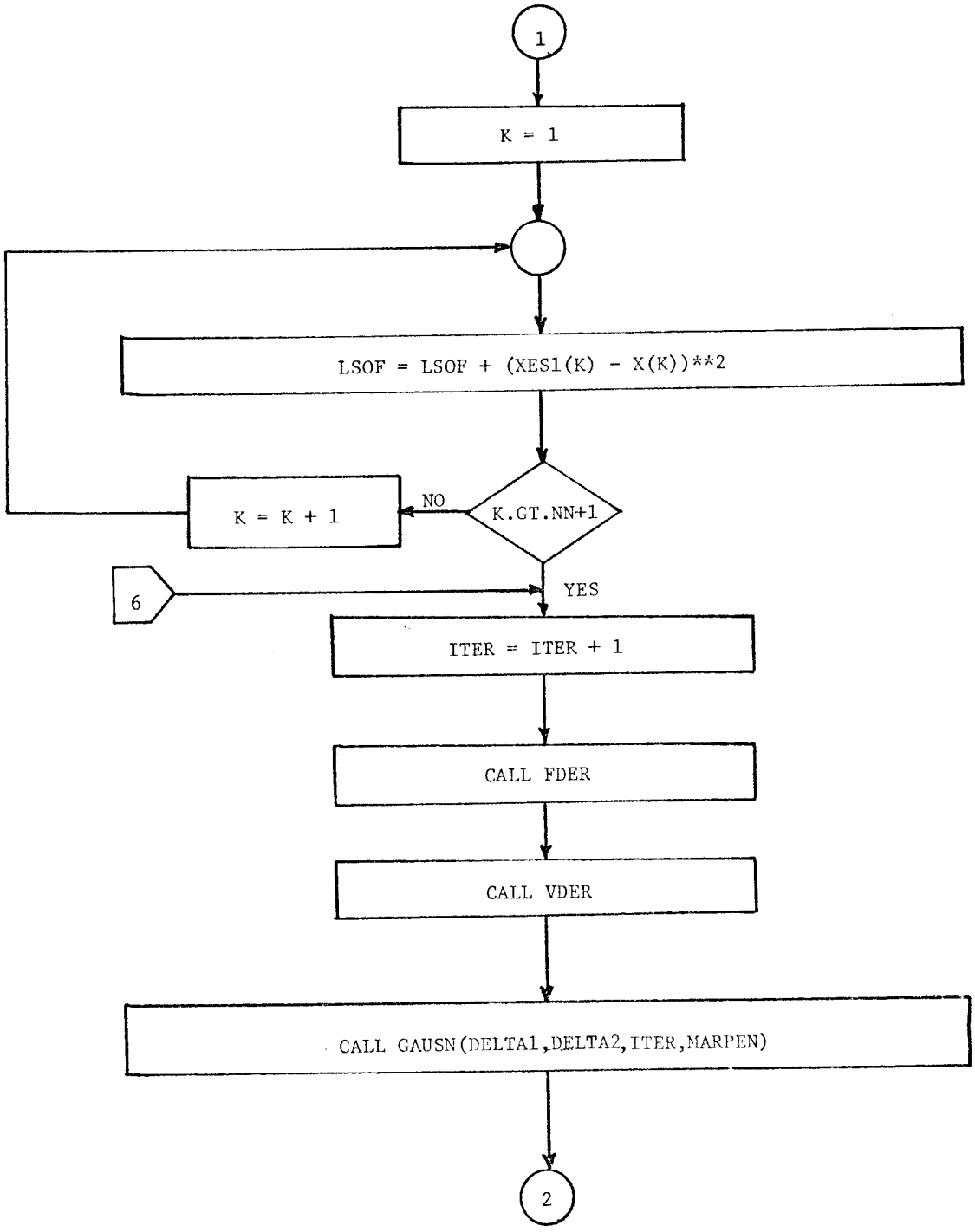
1
K = 1
LSOF = LSOF + (XES1(K) - X(K))**2
K.GT.NN+1
NO
K = K + 1
YES
6
ITER = ITER + 1
CALL FDER
CALL VDER
CALL GAUSN(DELTA1,DELTA2,ITER,MARPEN)
2

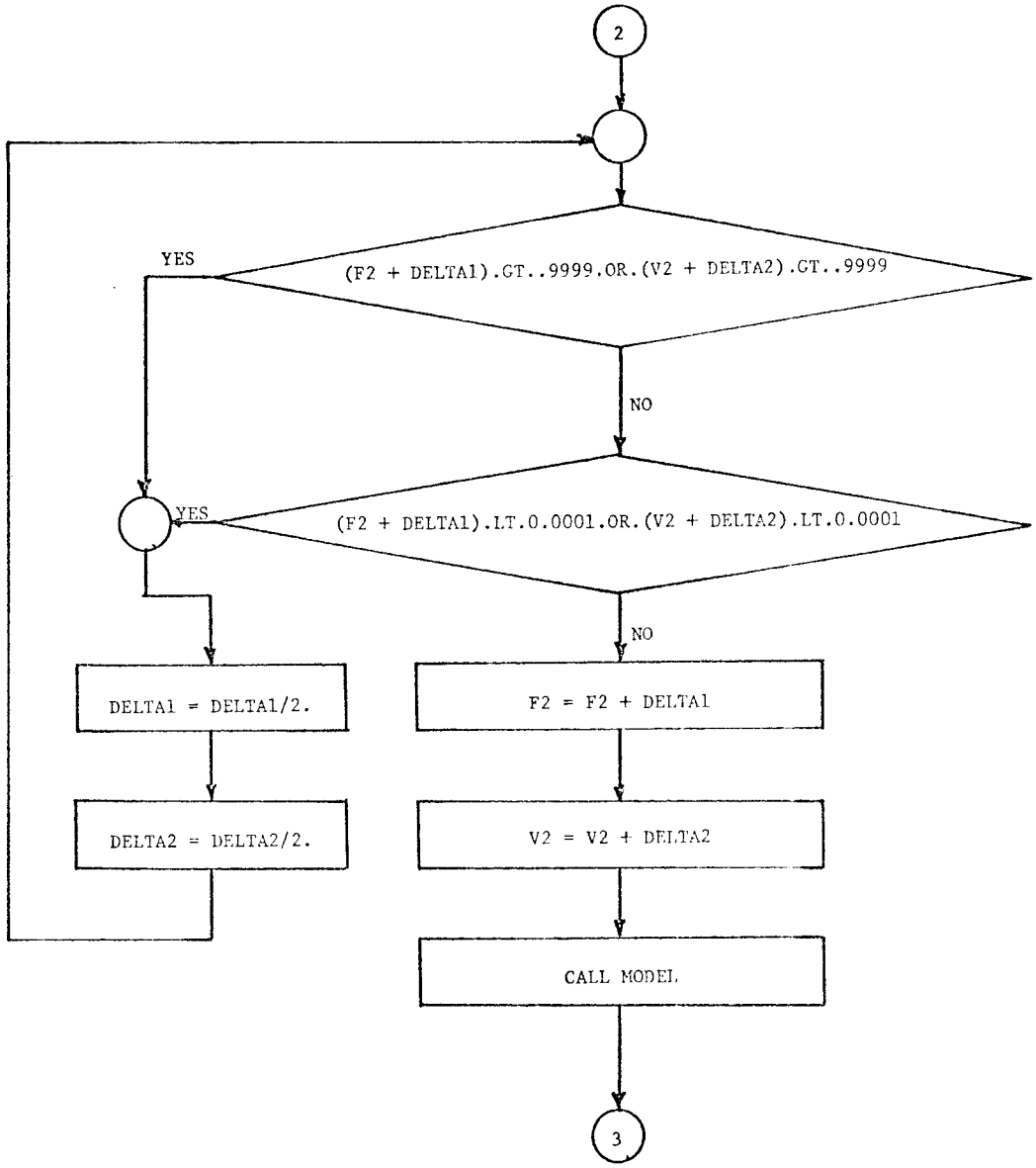
2
YES
(F2 + DELTA1).GT..9999.OR.(V2 + DELTA2).GT..9999
NO
YES
(F2 + DELTA1).LT.0.0001.OR.(V2 + DELTA2).LT.0.0001
NO
DELTA1 = DELTA1/2.
DELTA2 = DELTA2/2.
F2 = F2 + DELTA1
V2 = V2 + DELTA2
CALL MODEL
3

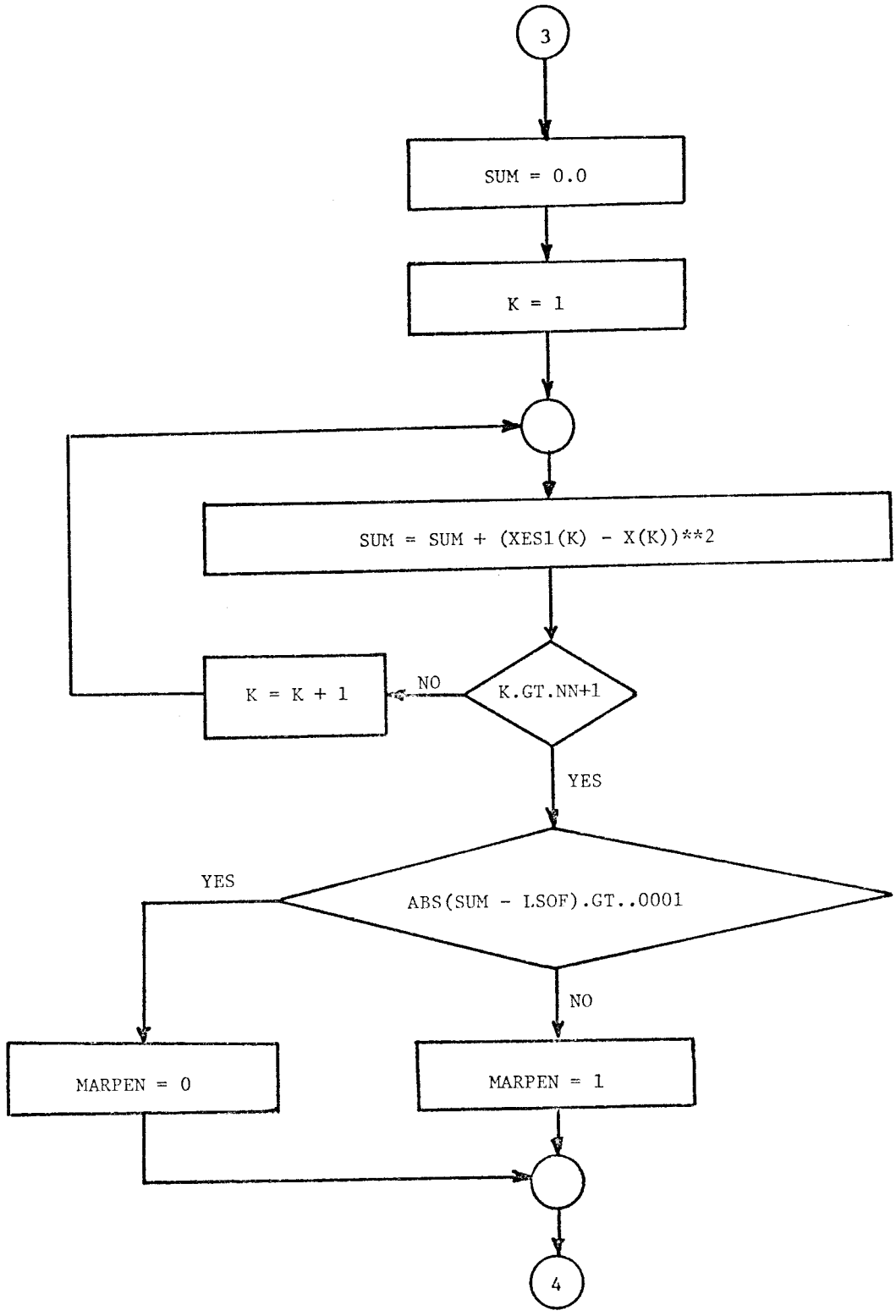
3
SUM = 0.0
K = 1
SUM = SUM + (XES1(K) - X(K))**2
K.GT.NN+1
NO
K = K + 1
YES
ABS(SUM - LSOF).GT..0001
YES
NO
MARPEN = 0
MARPEN = 1
4

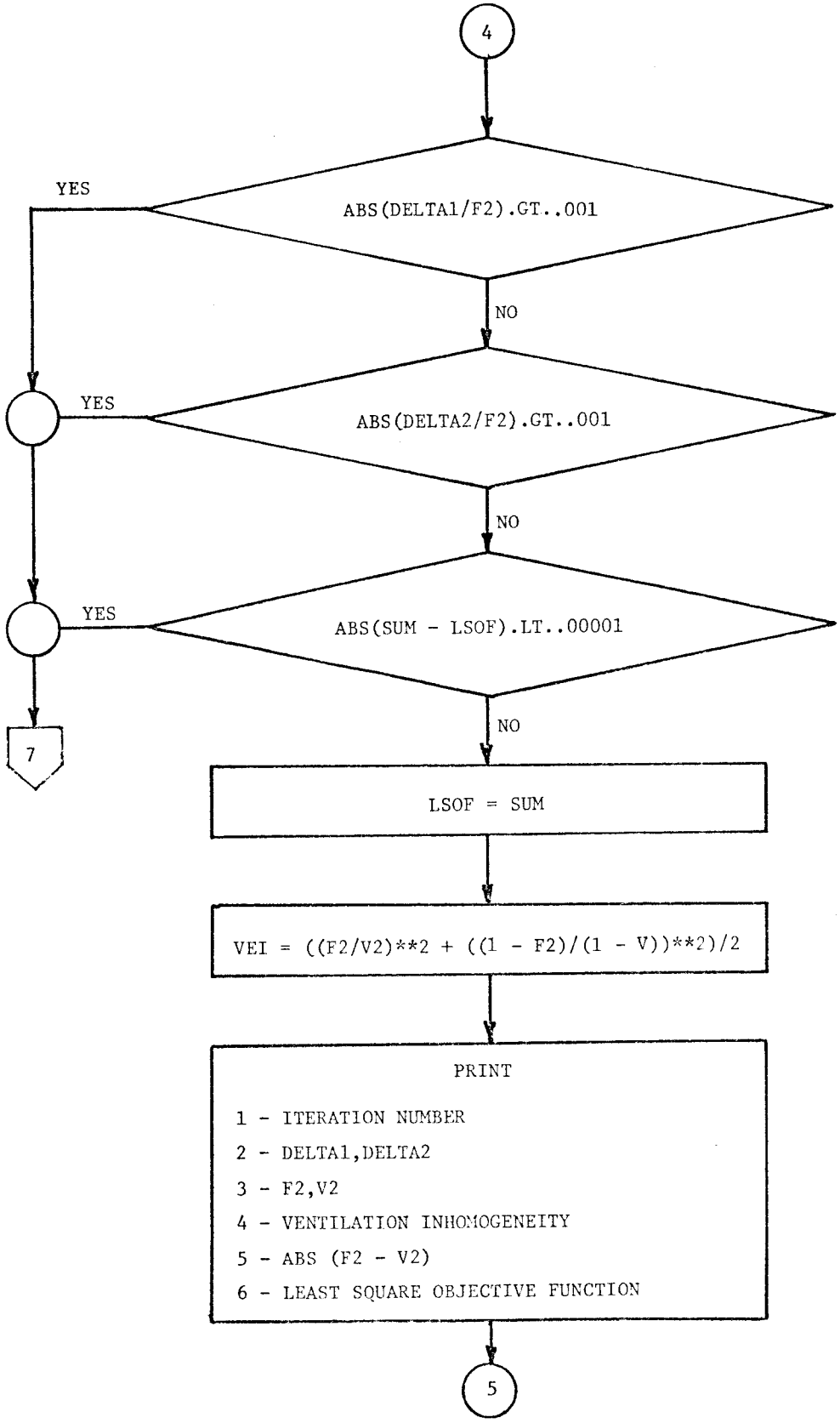
4
YES
ABS(DELTA1/F2).GT..001
NO
YES
ABS(DELTA2/F2).GT..001
NO
YES
ABS(SUM - LSOF).LT..00001
NO
7
LSOF = SUM
VEI = ((F2/V2)**2 + ((1 - F2)/(1 - V))**2)/2
PRINT
1 - ITERATION NUMBER
2 - DELTA1,DELTA2
3 - F2,V2
4 - VENTILATION INHOMOGENEITY
5 - ABS (F2 - V2)
6 - LEAST SQUARE OBJECTIVE FUNCTION
5

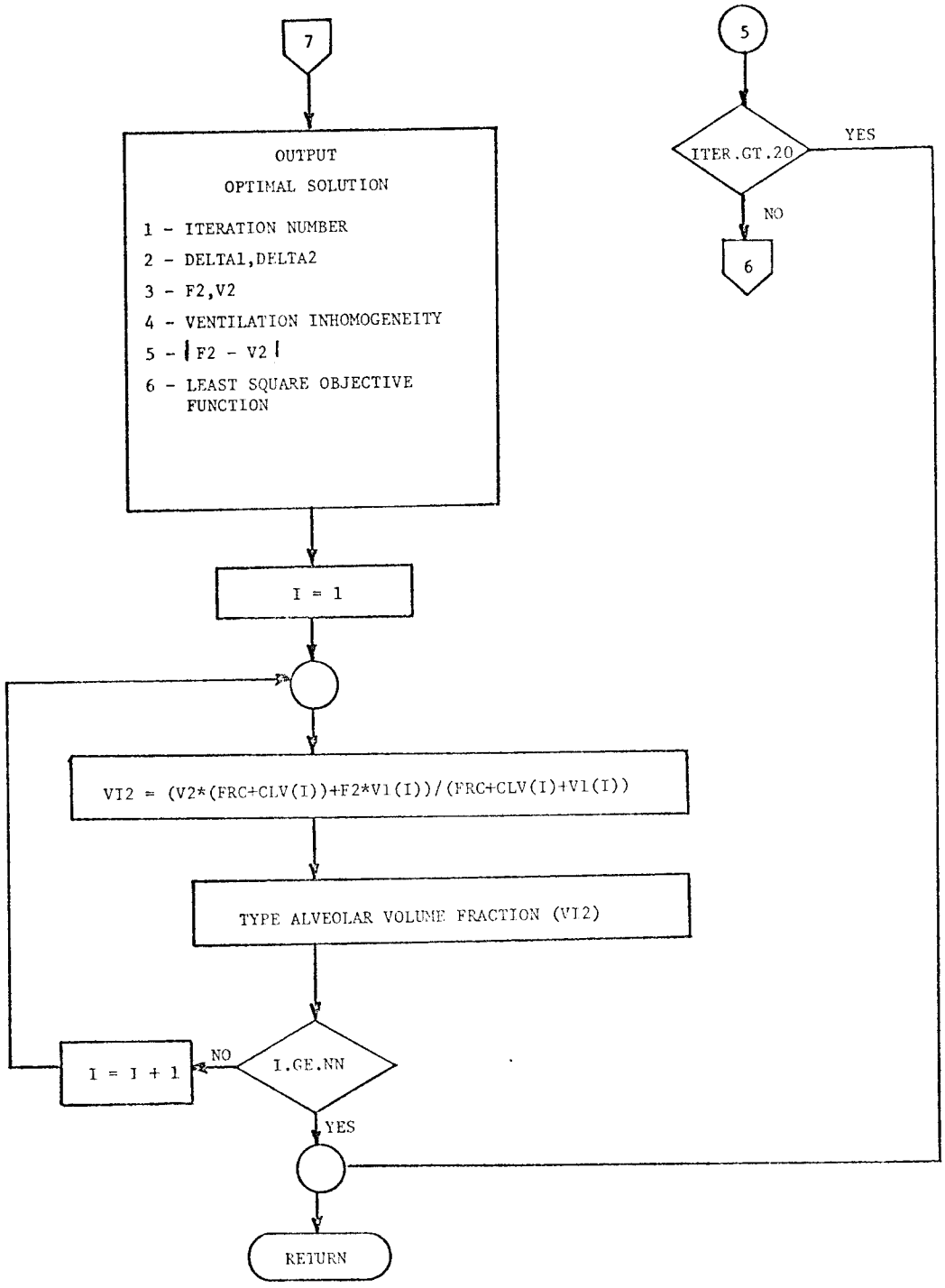
7
OUTPUT
OPTIMAL SOLUTION
1 - ITERATION NUMBER
2 - DELTA1,DELTA2
3 - F2,V2
4 - VENTILATION INHOMOGENEITY
5 - | F2 - V2 |
6 - LEAST SQUARE OBJECTIVE FUNCTION
I = 1
VI2 = (V2*(FRC+CLV(I))+F2*V1(I))/(FRC+CLV(I)+V1(I))
TYPE ALVEOLAR VOLUME FRACTION (VI2)
I.GE.NN
NO
I = I + 1
YES
RETURN
5
ITER.GT.20
YES
NO
6

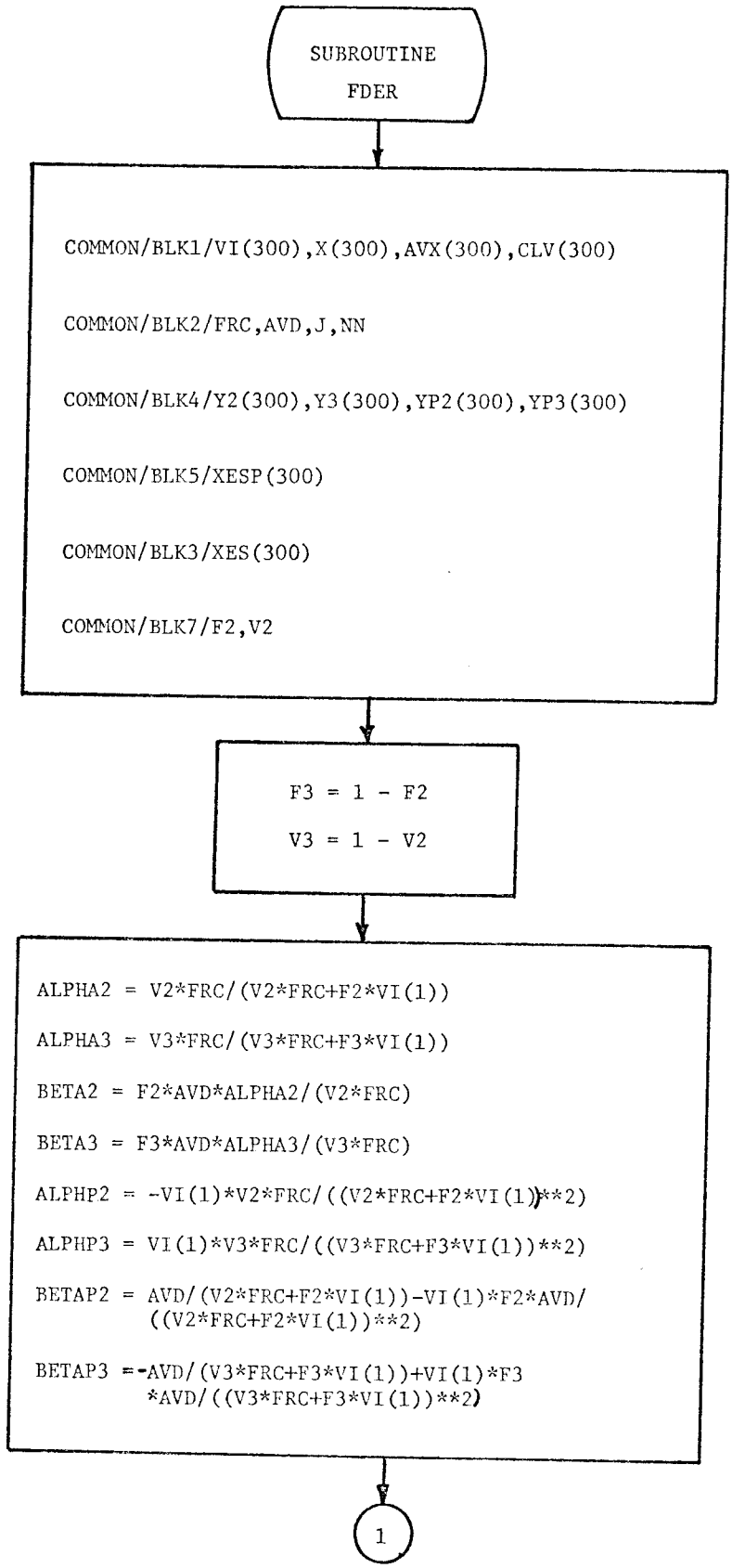
SUBROUTINE
FDER
COMMON/BLK1/VI(300),X(300),AVX(300),CLV(300)
COMMON/BLK2/FRC,AVD,J,NN
COMMON/BLK4/Y2(300),Y3(300),YP2(300),YP3(300)
COMMON/BLK5/XESP(300)
COMMON/BLK3/XES(300)
COMMON/BLK7/F2,V2
F3 = 1 - F2
V3 = 1 - V2
ALPHA2 = V2*FRC/(V2*FRC+F2*VI(1))
ALPHA3 = V3*FRC/(V3*FRC+F3*VI(1))
BETA2 = F2*AVD*ALPHA2/(V2*FRC)
BETA3 = F3*AVD*ALPHA3/(V3*FRC)
ALPHP2 = -VI(1)*V2*FRC/((V2*FRC+F2*VI(1))**2)
ALPHP3 = VI(1)*V3*FRC/((V3*FRC+F3*VI(1))**2)
BETAP2 = AVD/(V2*FRC+F2*VI(1))-VI(1)*F2*AVD/
((V2*FRC+F2*VI(1))**2)
BETAP3 =-AVD/(V3*FRC+F3*VI(1))+VI(1)*F3
*AVD/((V3*FRC+F3*VI(1))**2)
1

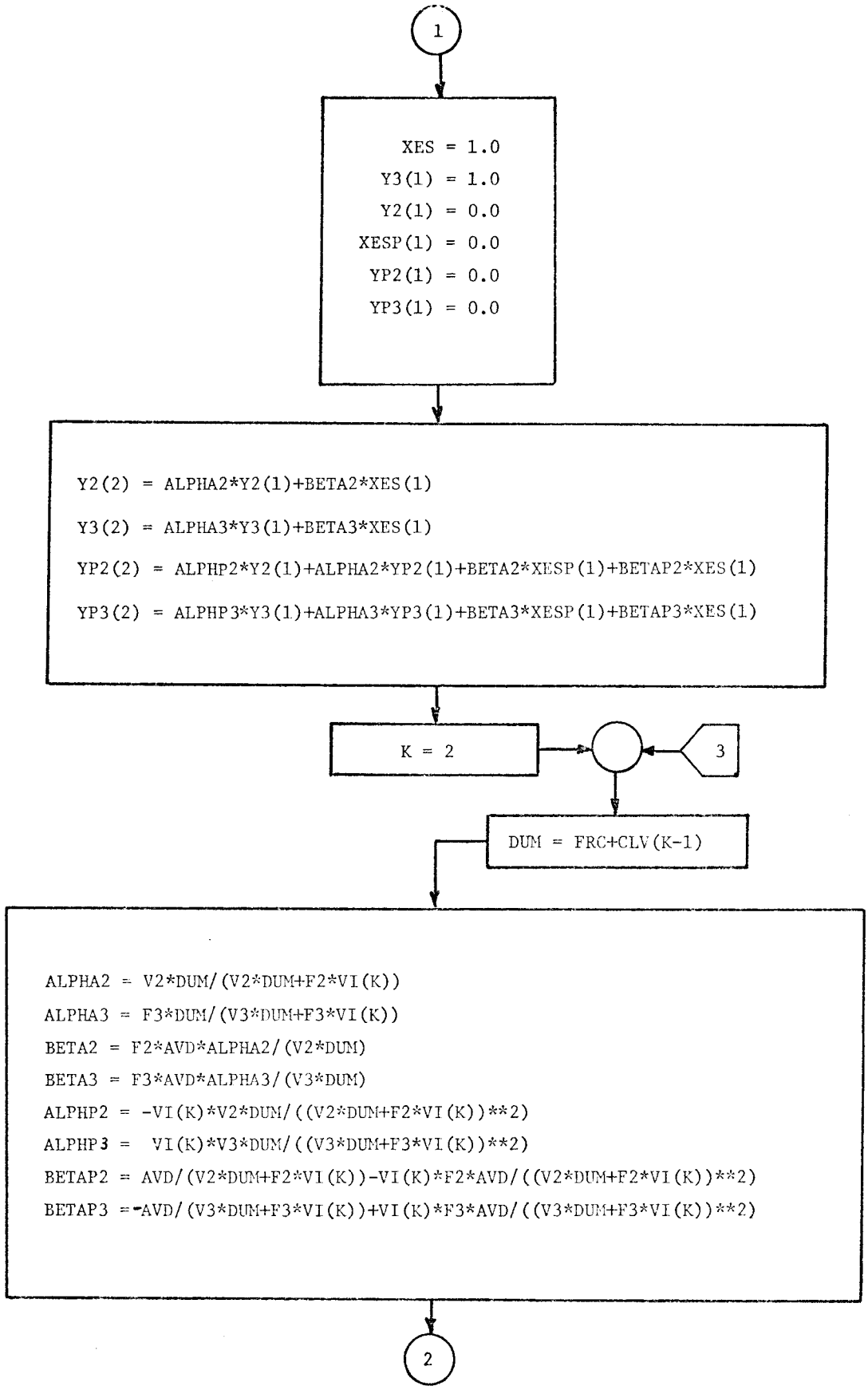
1
XES = 1.0
Y3(1) = 1.0
Y2(1) = 0.0
XESP(1) = 0.0
YP2(1) = 0.0
YP3(1) = 0.0
Y2(2) = ALPHA2*Y2(1)+BETA2*XES(1)
Y3(2) = ALPHA3*Y3(1)+BETA3*XES(1)
YP2(2) = ALPHP2*Y2(1)+ALPHA2*YP2(1)+BETA2*XESP(1)+BETAP2*XES(1)
YP3(2) = ALPHP3*Y3(1)+ALPHA3*YP3(1)+BETA3*XESP(1)+BETAP3*XES(1)
K = 2
3
DUM = FRC+CLV(K-1)
ALPHA2 = V2*DUM/(V2*DUM+F2*VI(K))
ALPHA3 = F3*DUM/(V3*DUM+F3*VI(K))
BETA2 = F2*AVD*ALPHA2/(V2*DUM)
BETA3 = F3*AVD*ALPHA3/(V3*DUM)
ALPHP2 = -VI(K)*V2*DUM/((V2*DUM+F2*VI(K))**2)
ALPHP3 = VI(K)*V3*DUM/((V3*DUM+F3*VI(K))**2)
BETAP2 = AVD/(V2*DUM+F2*VI(K))-VI(K)*F2*AVD/((V2*DUM+F2*VI(K))**2)
BETAP3 =-AVD/(V3*DUM+F3*VI(K))+VI(K)*F3*AVD/((V3*DUM+F3*VI(K))**2)
2

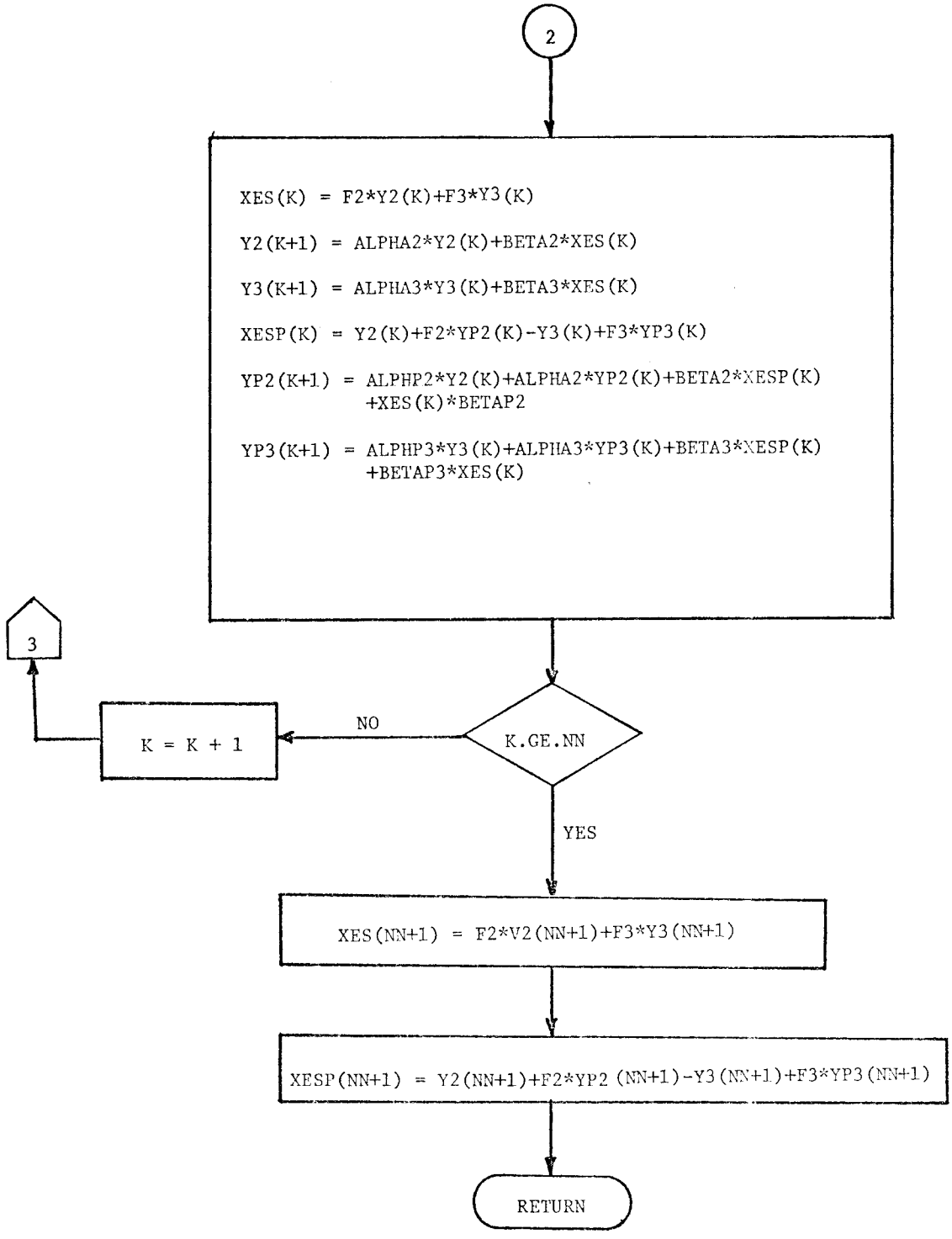
2
XES(K) = F2*Y2(K)+F3*Y3(K)
Y2(K+1) = ALPHA2*Y2(K)+BETA2*XES(K)
Y3(K+1) = ALPHA3*Y3(K)+BETA3*XES(K)
XESP(K) = Y2(K)+F2*YP2(K)-Y3(K)+F3*YP3(K)
YP2(K+1) = ALPHP2*Y2(K)+ALPHA2*YP2(K)+BETA2*XESP(K)
+XES(K)*BETAP2
YP3(K+1) = ALPHP3*Y3(K)+ALPHA3*YP3(K)+BETA3*XESP(K)
+BETAP3*XES(K)
3
K = K + 1
NO
K.GE.NN
YES
XES(NN+1) = F2*V2(NN+1)+F3*Y3(NN+1)
XESP(NN+1) = Y2(NN+1)+F2*YP2 (NN+1)-Y3(NN+1)+F3*YP3(NN+1)
RETURN

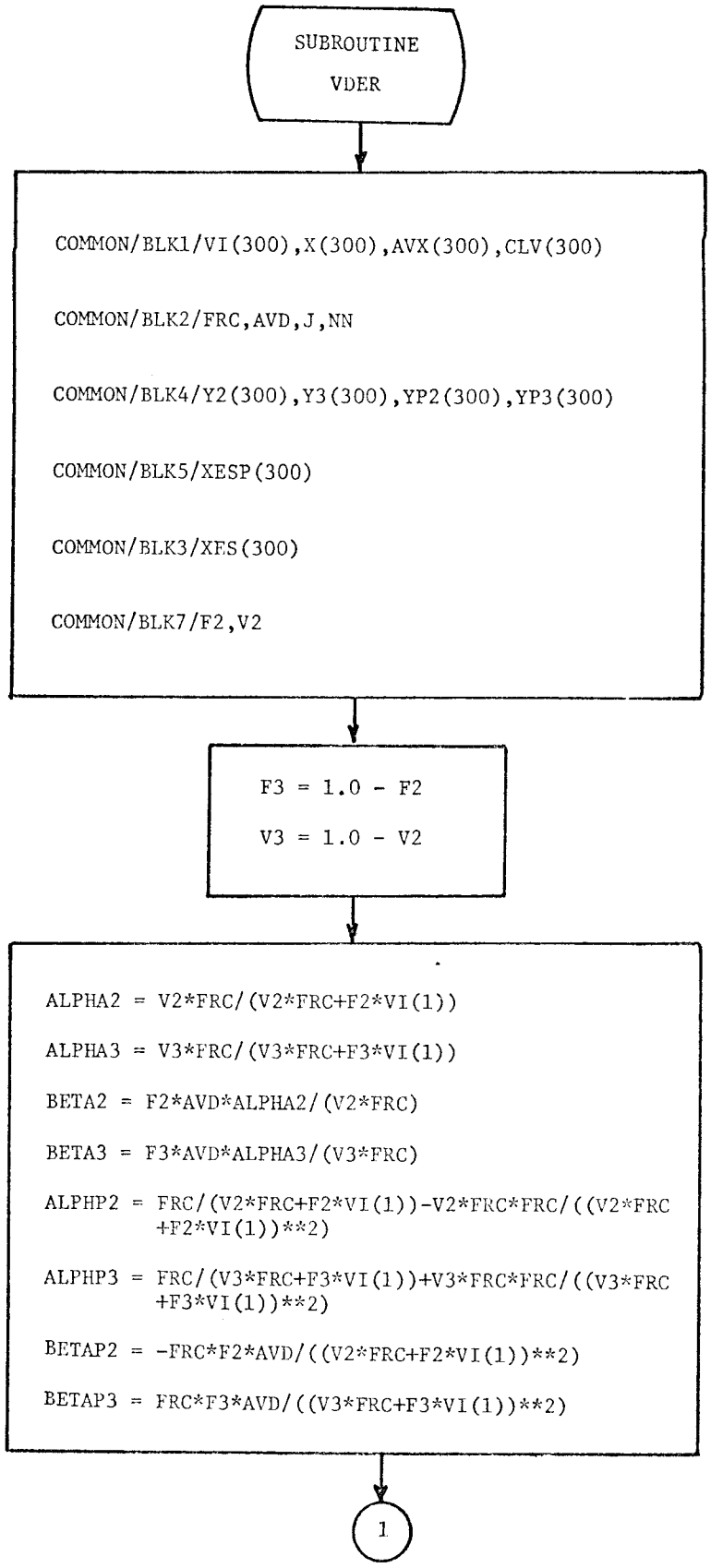
SUBROUTINE
VDER
COMMON/BLK1/VI(300),X(300),AVX(300),CLV(300)
COMMON/BLK2/FRC,AVD,J,NN
COMMON/BLK4/Y2(300),Y3(300),YP2(300),YP3(300)
COMMON/BLK5/XESP(300)
COMMON/BLK3/XFS(300)
COMMON/BLK7/F2,V2
F3 = 1.0 - F2
V3 = 1.0 - V2
ALPHA2 = V2*FRC/(V2*FRC+F2*VI(1))
ALPHA3 = V3*FRC/(V3*FRC+F3*VI(1))
BETA2 = F2*AVD*ALPHA2/(V2*FRC)
BETA3 = F3*AVD*ALPHA3/(V3*FRC)
ALPHP2 = FRC/(V2*FRC+F2*VI(1))-V2*FRC*FRC/((V2*FRC +F2*VI(1))**2)
ALPHP3 = FRC/(V3*FRC+F3*VI(1))+V3*FRC*FRC/((V3*FRC +F3*VI(1))**2)
BETAP2 = -FRC*F2*AVD/((V2*FRC+F2*VI(1))**2)
BETAP3 = FRC*F3*AVD/((V3*FRC+F3*VI(1))**2)
1

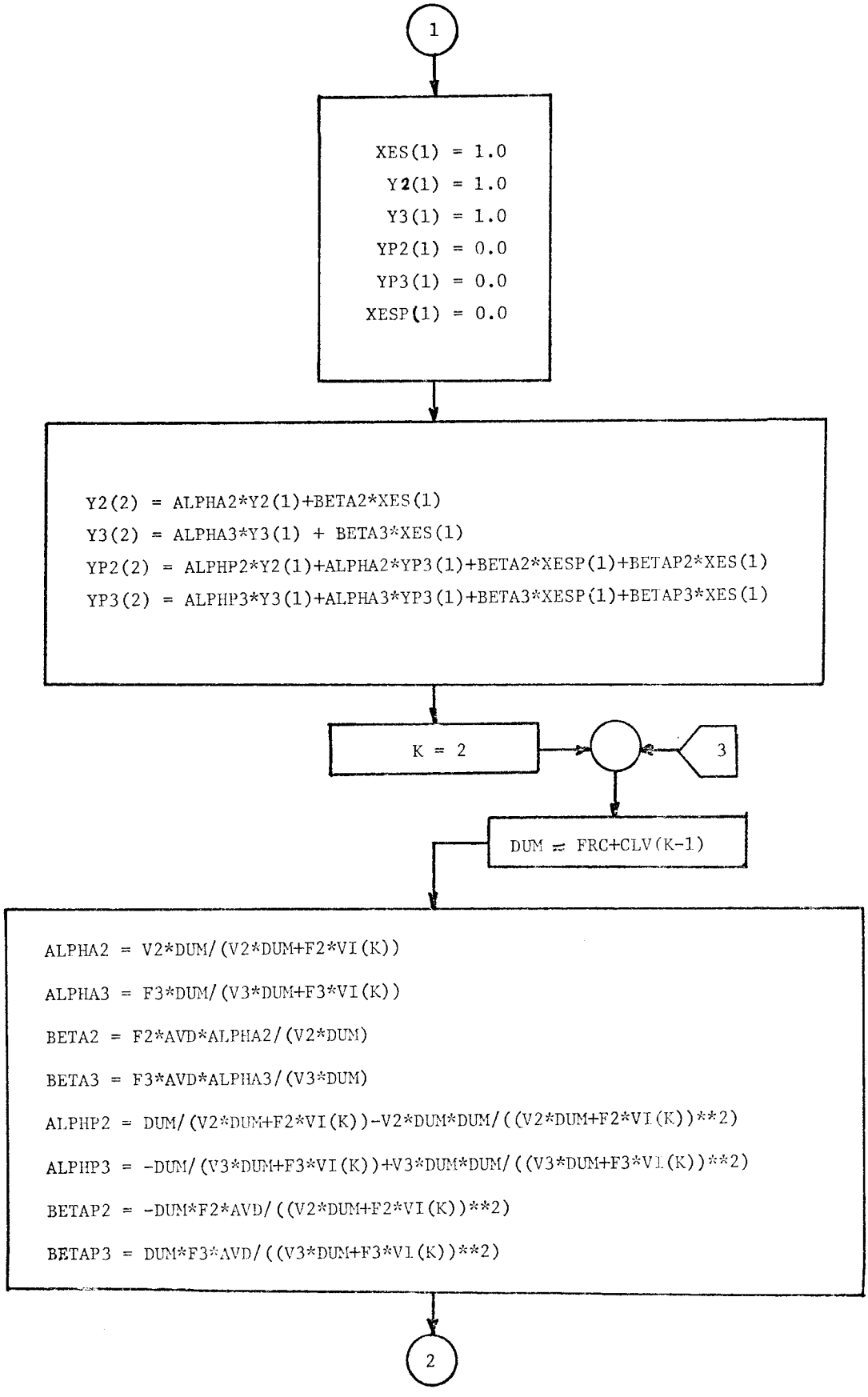
1
XES(1) = 1.0
Y2(1) = 1.0
Y3(1) = 1.0
YP2(1) = 0.0
YP3(1) = 0.0
XESP(1) = 0.0
Y2(2) = ALPHA2*Y2(1)+BETA2*XES(1)
Y3(2) = ALPHA3*Y3(1) + BETA3*XES(1)
YP2(2) = ALPHP2*Y2(1)+ALPHA2*YP3(1)+BETA2*XESP(1)+BETAP2*XES(1)
YP3(2) = ALPHP3*Y3(1)+ALPHA3*YP3(1)+BETA3*XESP(1)+BETAP3*XES(1)
K = 2
3
DUM = FRC+CLV(K-1)
ALPHA2 = V2*DUM/(V2*DUM+F2*VI(K))
ALPHA3 = F3*DUM/(V3*DUM+F3*VI(K))
BETA2 = F2*AVD*ALPHA2/(V2*DUM)
BETA3 = F3*AVD*ALPHA3/(V3*DUM)
ALPHP2 = DUM/(V2*DUM+F2*VI(K))-V2*DUM*DUM/((V2*DUM+F2*VI(K))**2)
ALPHP3 = -DUM/(V3*DUM+F3*VI(K))+V3*DUM*DUM/((V3*DUM+F3*VI(K))**2)
BETAP2 = -DUM*F2*AVD/((V2*DUM+F2*VI(K))**2)
BETAP3 = DUM*F3*AVD/((V3*DUM+F3*VI(K))**2)
2

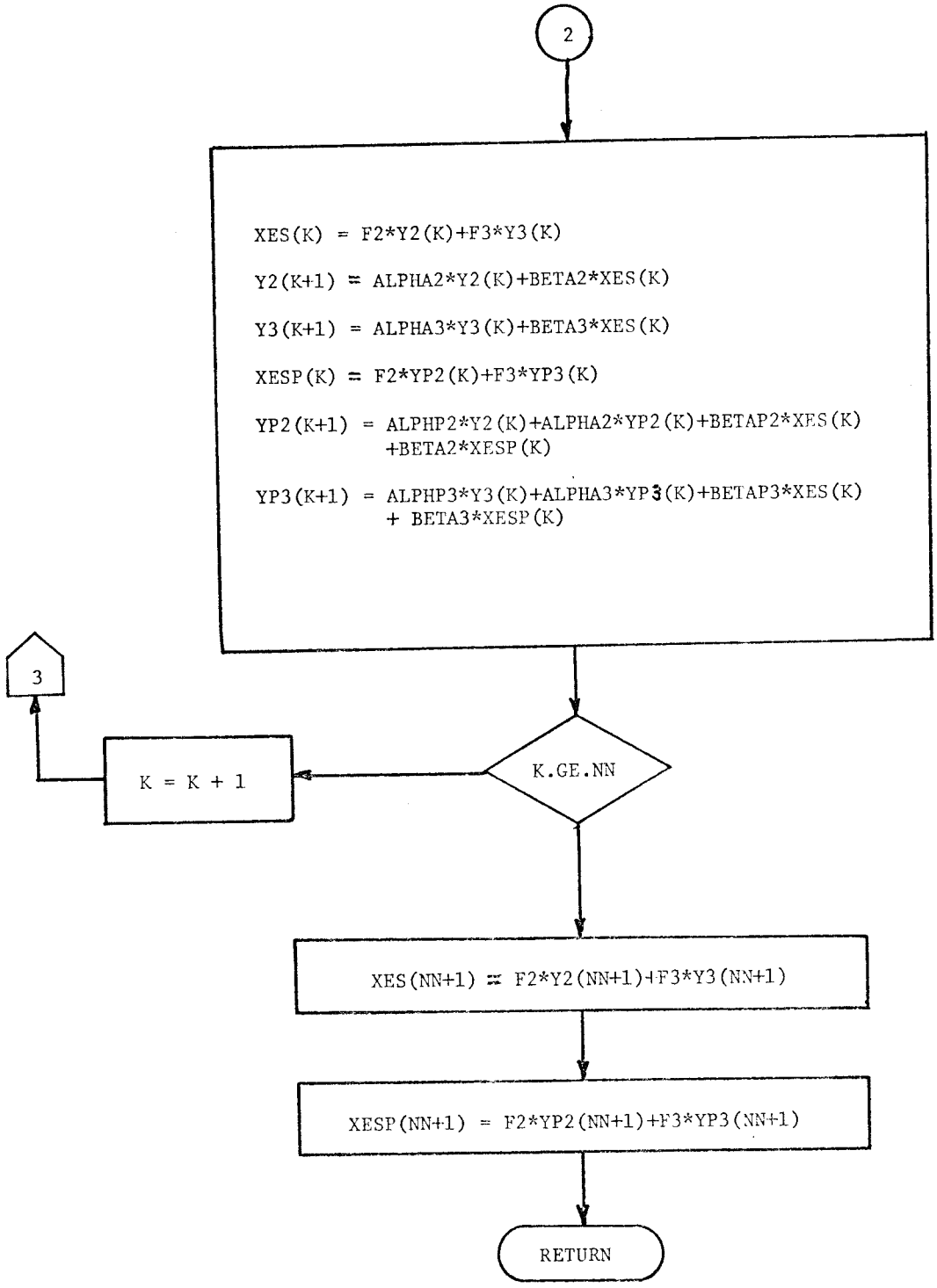
2
XES(K) = F2*Y2(K)+F3*Y3(K)
Y2(K+1) = ALPHA2*Y2(K)+BETA2*XES(K)
Y3(K+1) = ALPHA3*Y3(K)+BETA3*XES(K)
XESP(K) = F2*YP2(K)+F3*YP3(K)
YP2(K+1) = ALPHP2*Y2(K)+ALPHA2*YP2(K)+BETAP2*XES(K)
+BETA2*XESP(K)
YP3(K+1) = ALPHP3*Y3(K)+ALPHA3*YP3(K)+BETAP3*XES(K)
+ BETA3*XESP(K)
3
K = K + 1
K.GE.NN
XES(NN+1) = F2*Y2(NN+1)+F3*Y3(NN+1)
XESP(NN+1) = F2*YP2(NN+1)+F3*YP3(NN+1)
RETURN

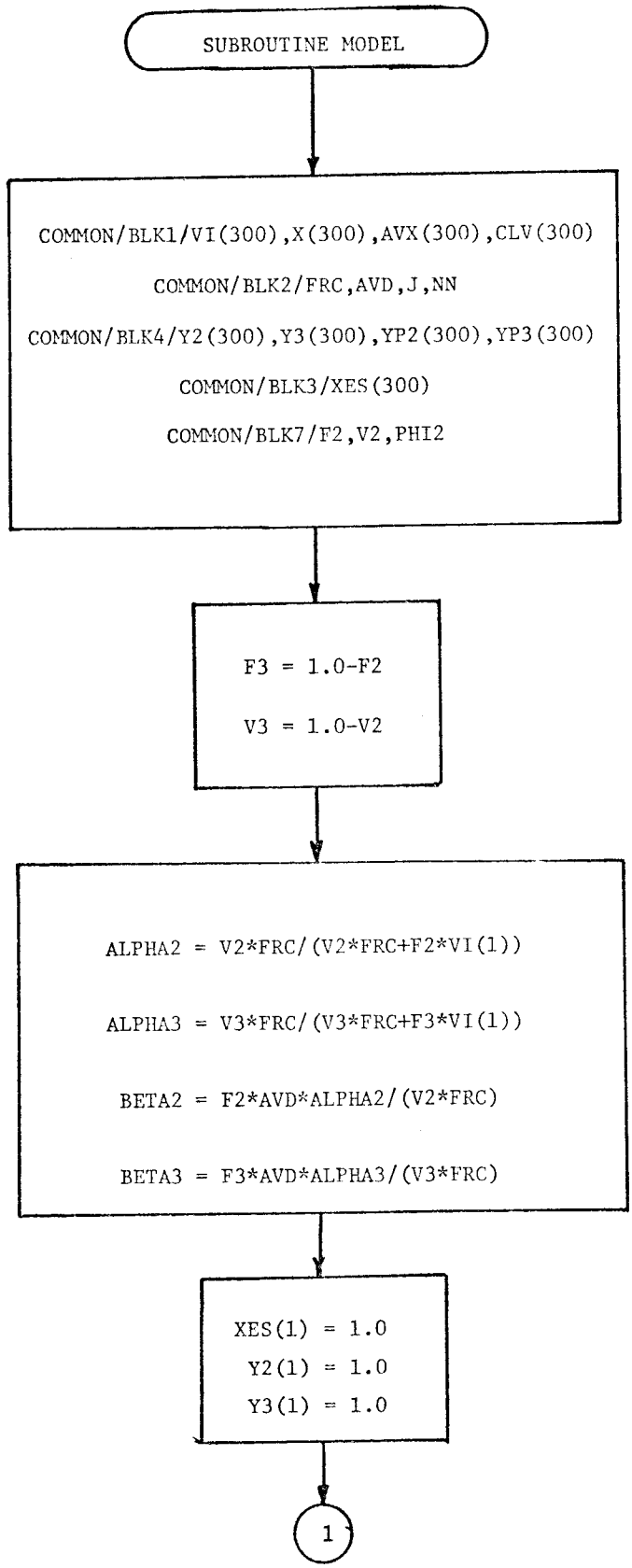
SUBROUTINE MODEL
COMMON/BLK1/VI(300),X(300),AVX(300),CLV(300)
COMMON/BLK2/FRC,AVD,J,NN
COMMON/BLK4/Y2(300),Y3(300),YP2(300),YP3(300)
COMMON/BLK3/XES(300)
COMMON/BLK7/F2,V2,PHI2
F3 = 1.0-F2
V3 = 1.0-V2
ALPHA2 = V2*FRC/(V2*FRC+F2*VI(1))
ALPHA3 = V3*FRC/(V3*FRC+F3*VI(1))
BETA2 = F2*AVD*ALPHA2/(V2*FRC)
BETA3 = F3*AVD*ALPHA3/(V3*FRC)
XES(1) = 1.0
Y2(1) = 1.0
Y3(1) = 1.0
1

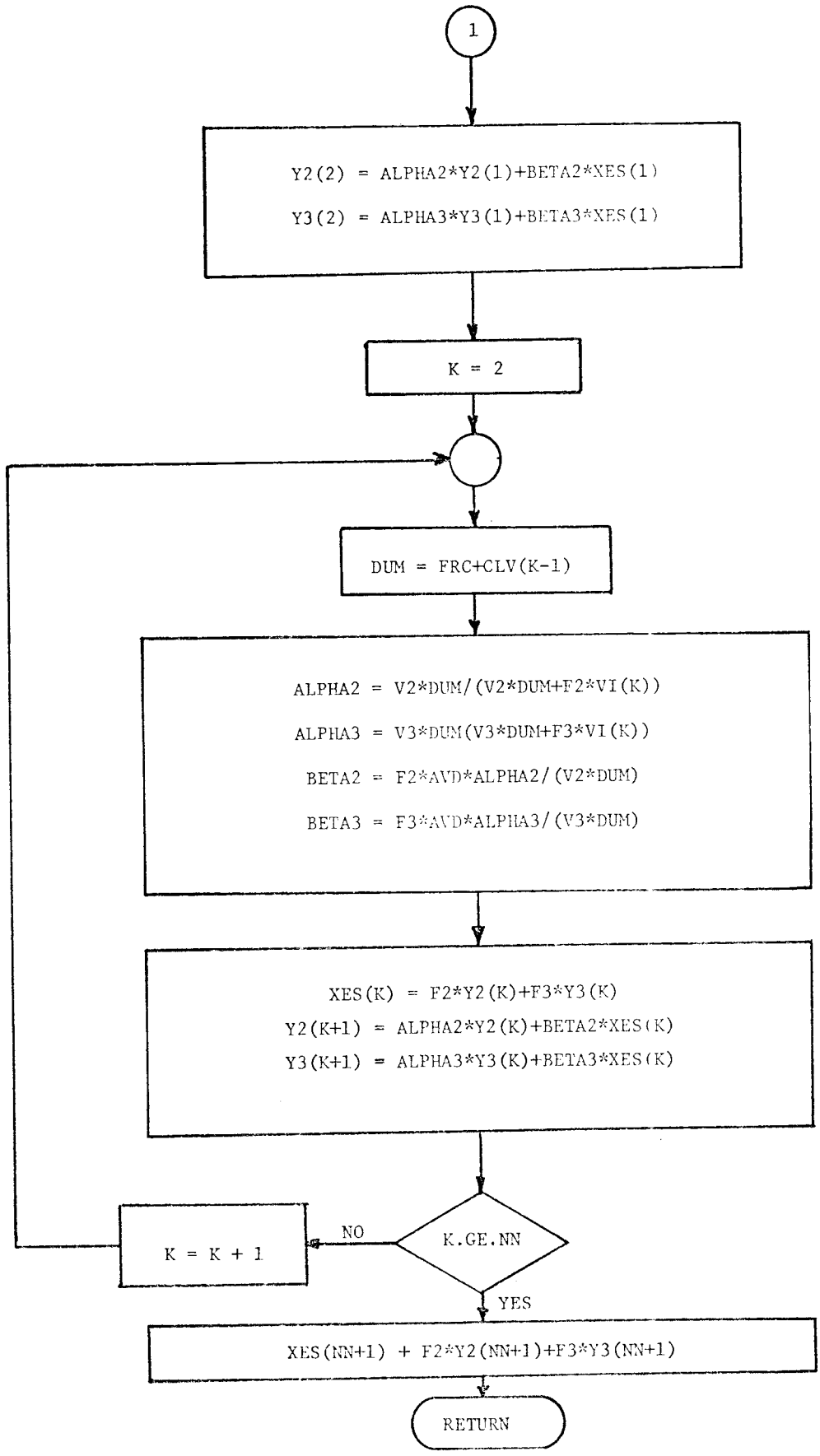
1
Y2(2) = ALPHA2*Y2(1)+BETA2*XES(1)
Y3(2) = ALPHA3*Y3(1)+BETA3*XES(1)
K = 2
DUM = FRC+CLV(K-1)
ALPHA2 = V2*DUM/(V2*DUM+F2*VI(K))
ALPHA3 = V3*DUM(V3*DUM+F3*VI(K))
BETA2 = F2*AVD*ALPHA2/(V2*DUM)
BETA3 = F3*AVD*ALPHA3/(V3*DUM)
XES(K) = F2*Y2(K)+F3*Y3(K)
Y2(K+1) = ALPHA2*Y2(K)+BETA2*XES(K)
Y3(K+1) = ALPHA3*Y3(K)+BETA3*XES(K)
K.GE.NN
NO
K = K + 1
YES
XES(NN+1) + F2*Y2(NN+1)+F3*Y3(NN+1)
RETURN

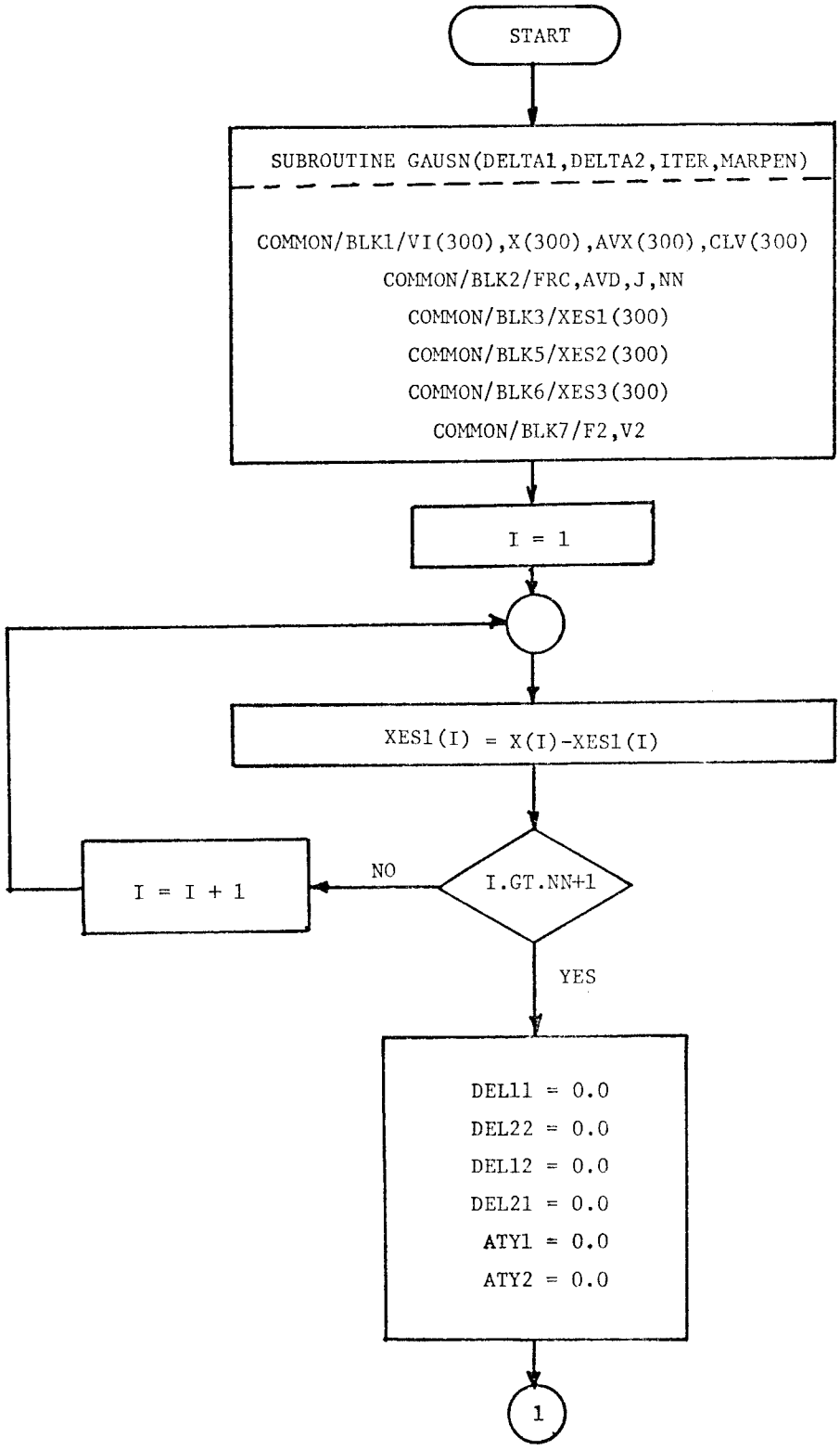
START
SUBROUTINE GAUSN(DELTA1,DELTA2,ITER,MARPEN)
COMMON/BLK1/VI(300),X(300),AVX(300),CLV(300)
COMMON/BLK2/FRC,AVD,J,NN
COMMON/BLK3/XES1(300)
COMMON/BLK5/XES2(300)
COMMON/BLK6/XES3(300)
COMMON/BLK7/F2,V2
I = 1
XES1(I) = X(I)-XES1(I)
I.GT.NN+1
NO
I = I + 1
YES
DEL11 = 0.0
DEL22 = 0.0
DEL12 = 0.0
DEL21 = 0.0
ATY1 = 0.0
ATY2 = 0.0
1

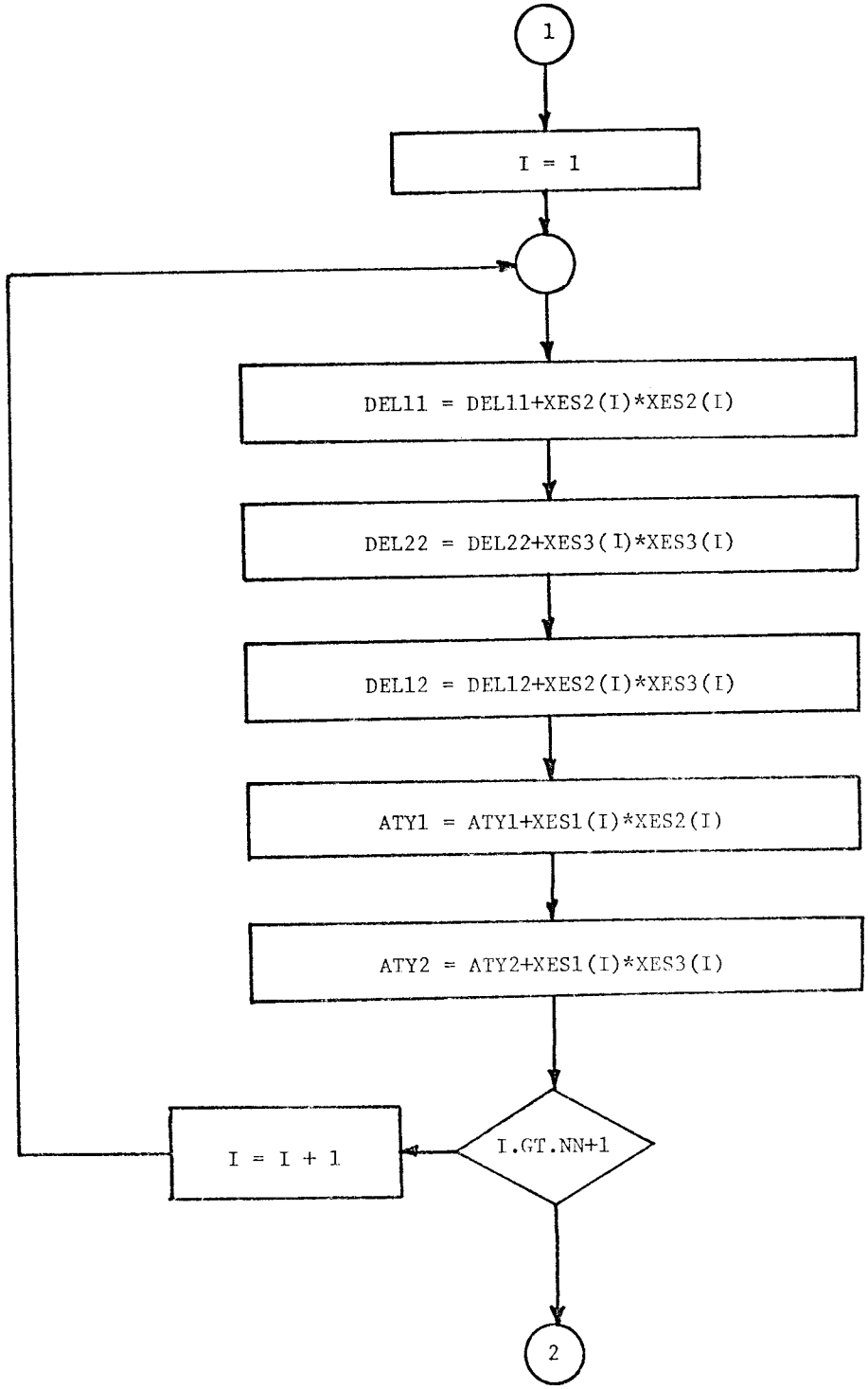
1
I = 1
DEL11 = DEL11+XES2(I)*XES2(I)
DEL22 = DEL22+XES3(I)*XES3(I)
DEL12 = DEL12+XES2(I)*XES3(I)
ATY1 = ATY1+XES1(I)*XES2(I)
ATY2 = ATY2+XES1(I)*XES3(I)
I.GT.NN+1
I = I + 1
2

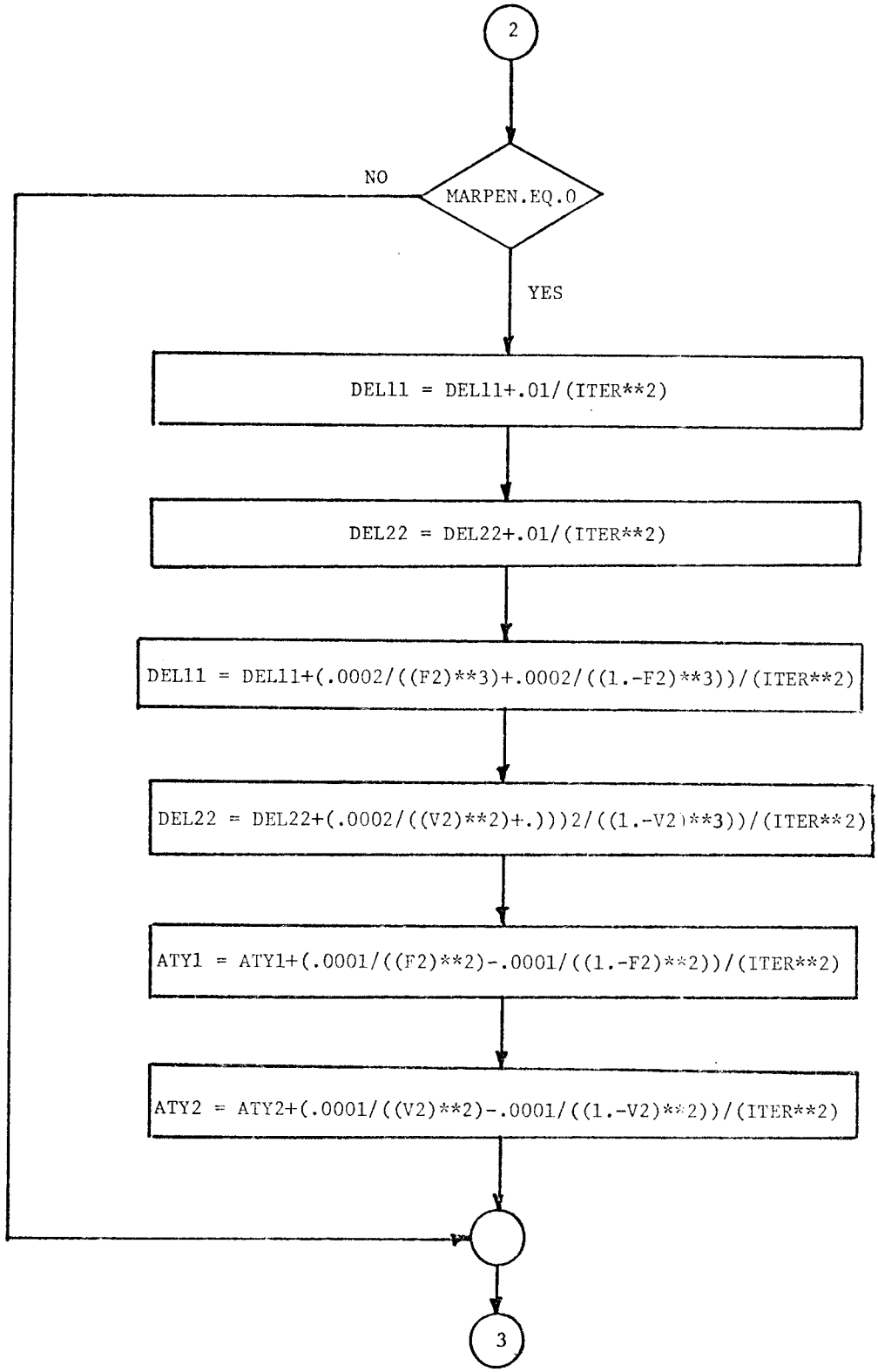
2
NO
MARPEN.EQ.0
YES
DEL11 = DEL11+.01/(ITER**2)
DEL22 = DEL22+.01/(ITER**2)
DEL11 = DEL11+(.0002/((F2)**3)+.0002/((1.-F2)**3))/(ITER**2)
DEL22 = DEL22+(.0002/((V2)**2)+.)))2/((1.-V2)**3))/(ITER**2)
ATY1 = ATY1+(.0001/((F2)**2)-.0001/((1.-F2)**2))/(ITER**2)
ATY2 = ATY2+(.0001/((V2)**2)-.0001/((1.-V2)**2))/(ITER**2)
3

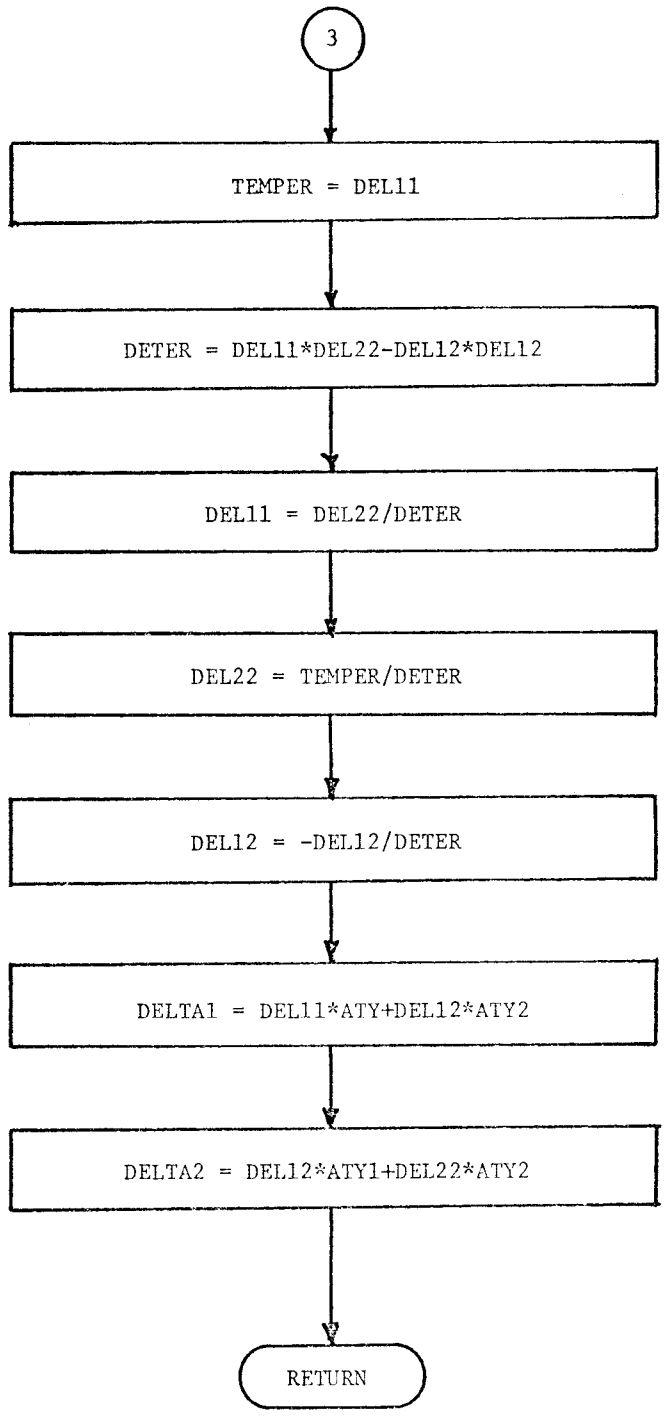
3
TEMPER = DEL11
DETER = DEL11*DEL22-DEL12*DEL12
DEL11 = DEL22/DETER
DEL22 = TEMPER/DETER
DEL12 = -DEL12/DETER
DELTA1 = DEL11*ATY+DEL12*ATY2
DELTA2 = DEL12*ATY1+DEL22*ATY2
RETURN

## Computational Description of Calibration Program

Calibration program estimates flow signal DC offset, nitrogen signal DC offset and volume calibration coefficient. These values are stored on disk under CALIB.DAT; 1 and VLCL.DAT;1. Flow and nitrogen signals are sampled at a rate 40 samples per second and digitally filtered with Butterworth second order low-pass filter, cutoff frequency of 20 Hz. The subroutine that taking care of filtering is called FILT. Program checks all estimated values based on their standard deviation. If the standard deviation of parameters falls outside expected range, it will ask the operator to do calibration over. Calibration program block diagram is shown in Fig. A-3.

### Input Signals

1- Nitrogen signal is channel 4, maximum input range is $\pm 5$ Volts.

2- Flow signal is channel 5, maximum input range is $\pm 5$ Volts

### Output Parameters

1- DC offset for nitrogen signal
2- DC offset for flow signal
3- Volume calibration coefficient
4- Standard deviation of $N_2$ signal DC offset
5- Standard deviation of flow signal DC offset
6- Estimated value of one liter inspired air with standard deviation
7- Estimated value of one liter expired air with standard deviation

8- Mean value of volume calibration coefficient

List of Symbols

IBUF: Buffer for zero input signals
IBF: Buffer for flow signal
VI: Inspire volume
VE: Expire volume
DF: Flow signal DC offset
DN: nitrogen signal DC offset
CC: Volume calibration coefficient
SR: Sampling rate
CF: Cutoff frequency
SDN: Standard deviation of $N_2$ signal DC offset
SDF: Standard deviation of flow signal DC offset
AVI: Average inspire volume
AVE: Average expire volume
FILT: filter subroutine
BUFREE: Fortran subroutine, which checks if another half buffer is ready
RTS: Sampling subroutine
A0, A1, A2, B0, B1, and B2 are filter parameters
ASSIGN: Assign logical unit number to file
ASLSLN: Assign logical unit number to LPS
READSW: Read switch subroutine
WAITFR: Wait for subroutine
CLREF: Clear Subroutine
CLOSE: Close file
INDX: Buffer index

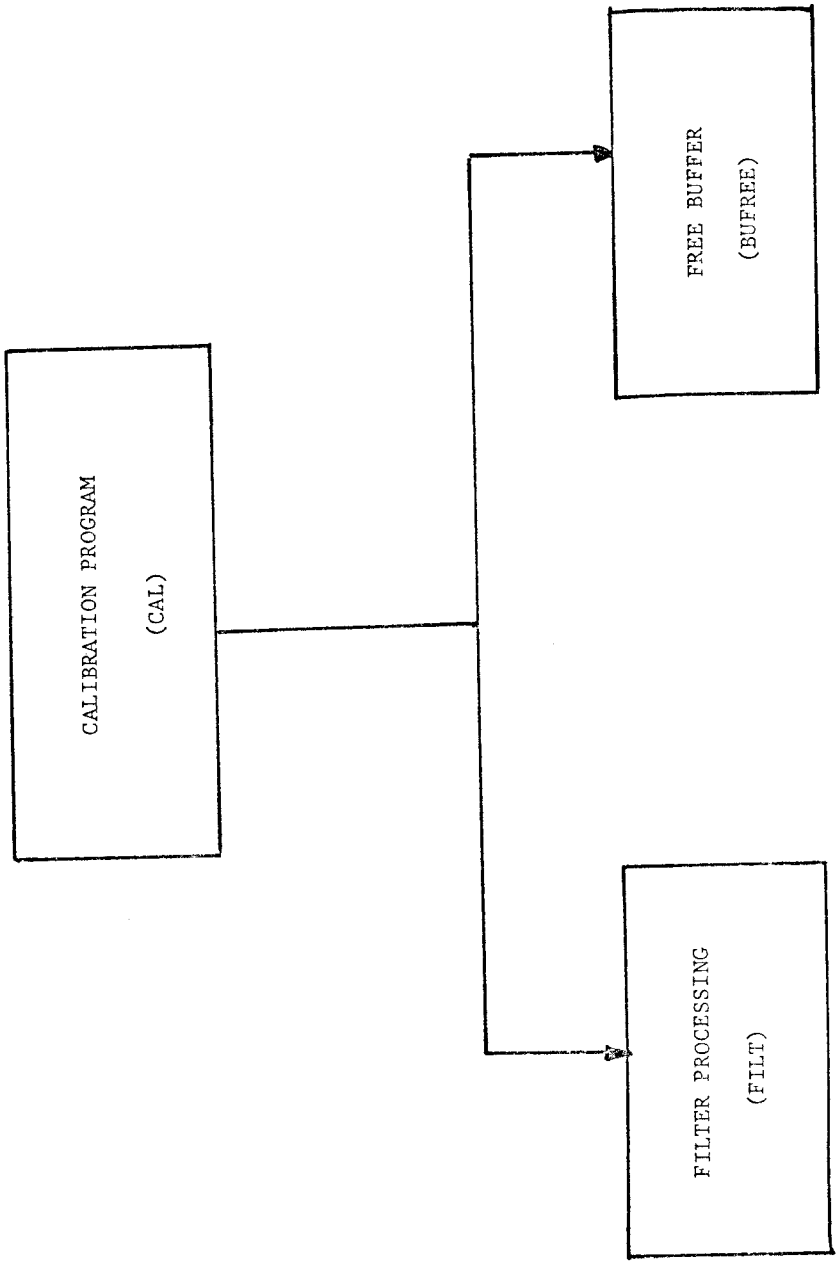


Figure A-3. Calibration program block diagram

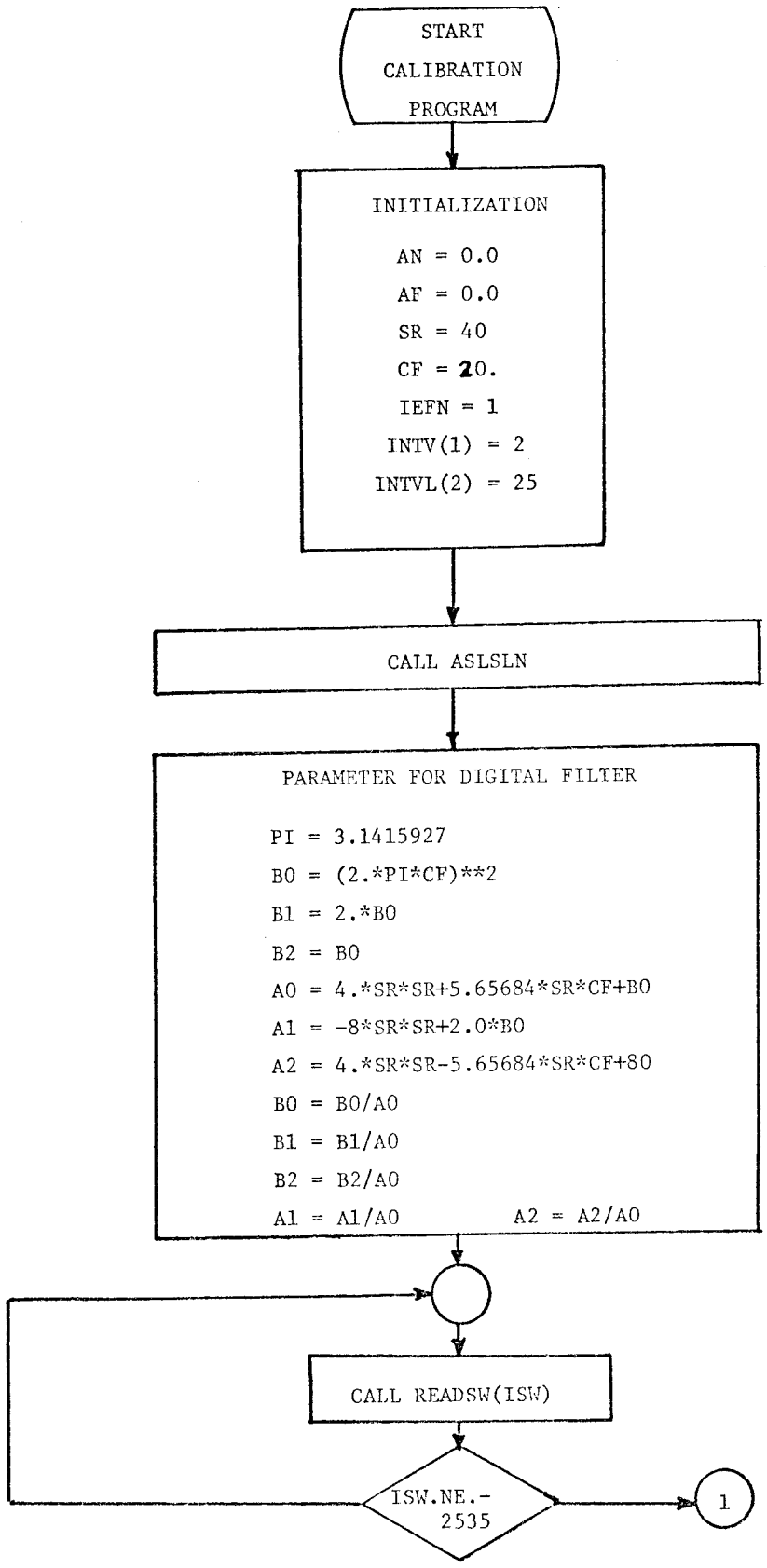
START
CALIBRATION
PROGRAM
INITIALIZATION
AN = 0.0
AF = 0.0
SR = 40
CF = 20.
IEFN = 1
INTV(1) = 2
INTVL(2) = 25
CALL ASLSLN
PARAMETER FOR DIGITAL FILTER
PI = 3.1415927
B0 = (2.*PI*CF)**2
B1 = 2.*B0
B2 = B0
A0 = 4.*SR*SR+5.65684*SR*CF+B0
A1 = -8*SR*SR+2.0*B0
A2 = 4.*SR*SR-5.65684*SR*CF+80
B0 = B0/A0
B1 = B1/A0
B2 = B2/A0
A1 = A1/A0 A2 = A2/A0
CALL READSW(ISW)
ISW.NE.-
2535
1

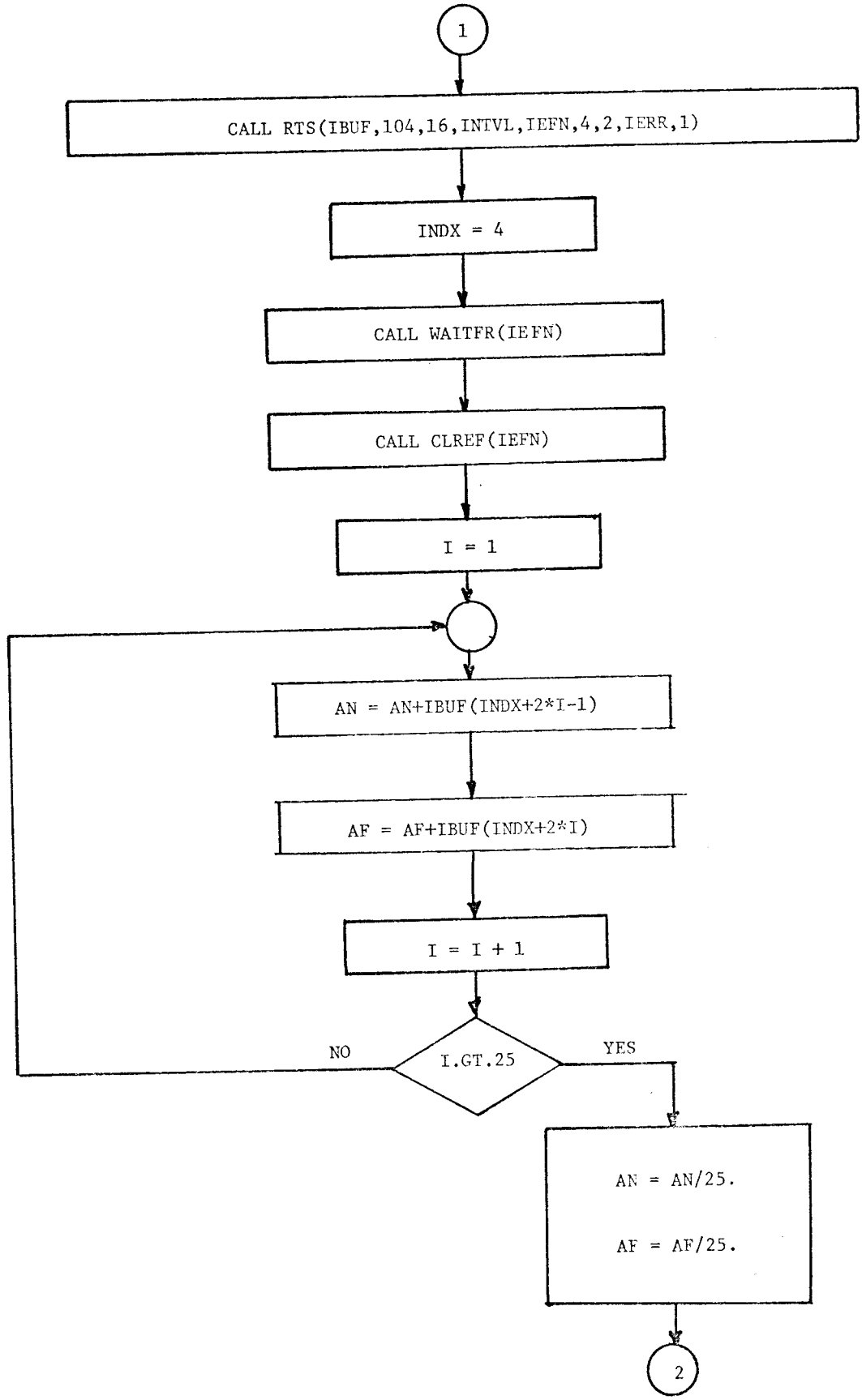
1
CALL RTS(IBUF,104,16,INTVL,IEFN,4,2,IERR,1)
INDX = 4
CALL WAITFR(IEFN)
CALL CLREF(IEFN)
I = 1
AN = AN+IBUF(INDX+2*I-1)
AF = AF+IBUF(INDX+2*I)
I = I + 1
I.GT.25
NO
YES
AN = AN/25.
AF = AF/25.
2

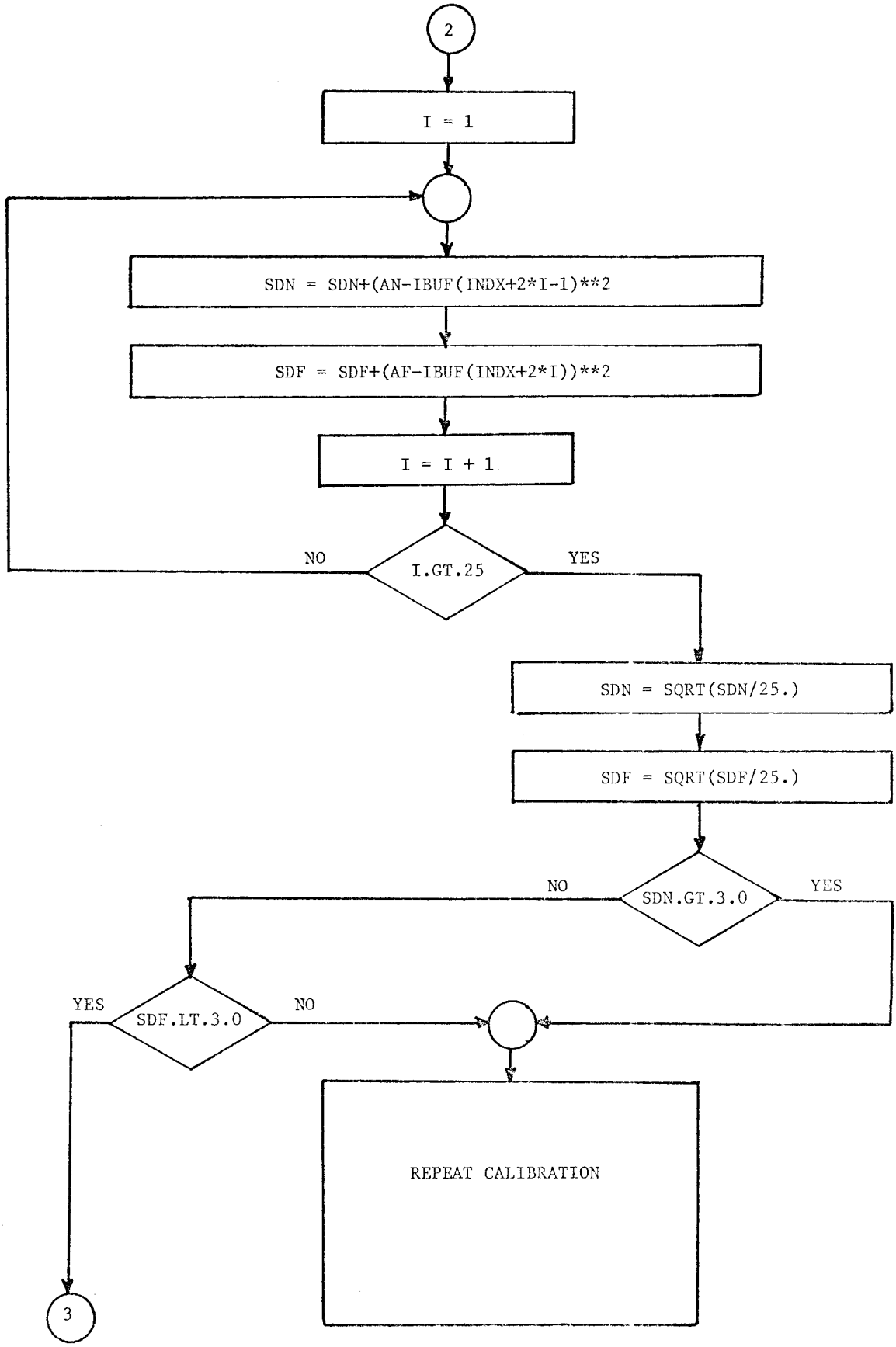
2
I = 1
SDN = SDN+(AN-IBUF(INDX+2*I-1)**2
SDF = SDF+(AF-IBUF(INDX+2*I))**2
I = I + 1
I.GT.25
NO
YES
SDN = SQRT(SDN/25.)
SDF = SQRT(SDF/25.)
SDN.GT.3.0
NO
YES
SDF.LT.3.0
YES
NO
REPEAT CALIBRATION
3

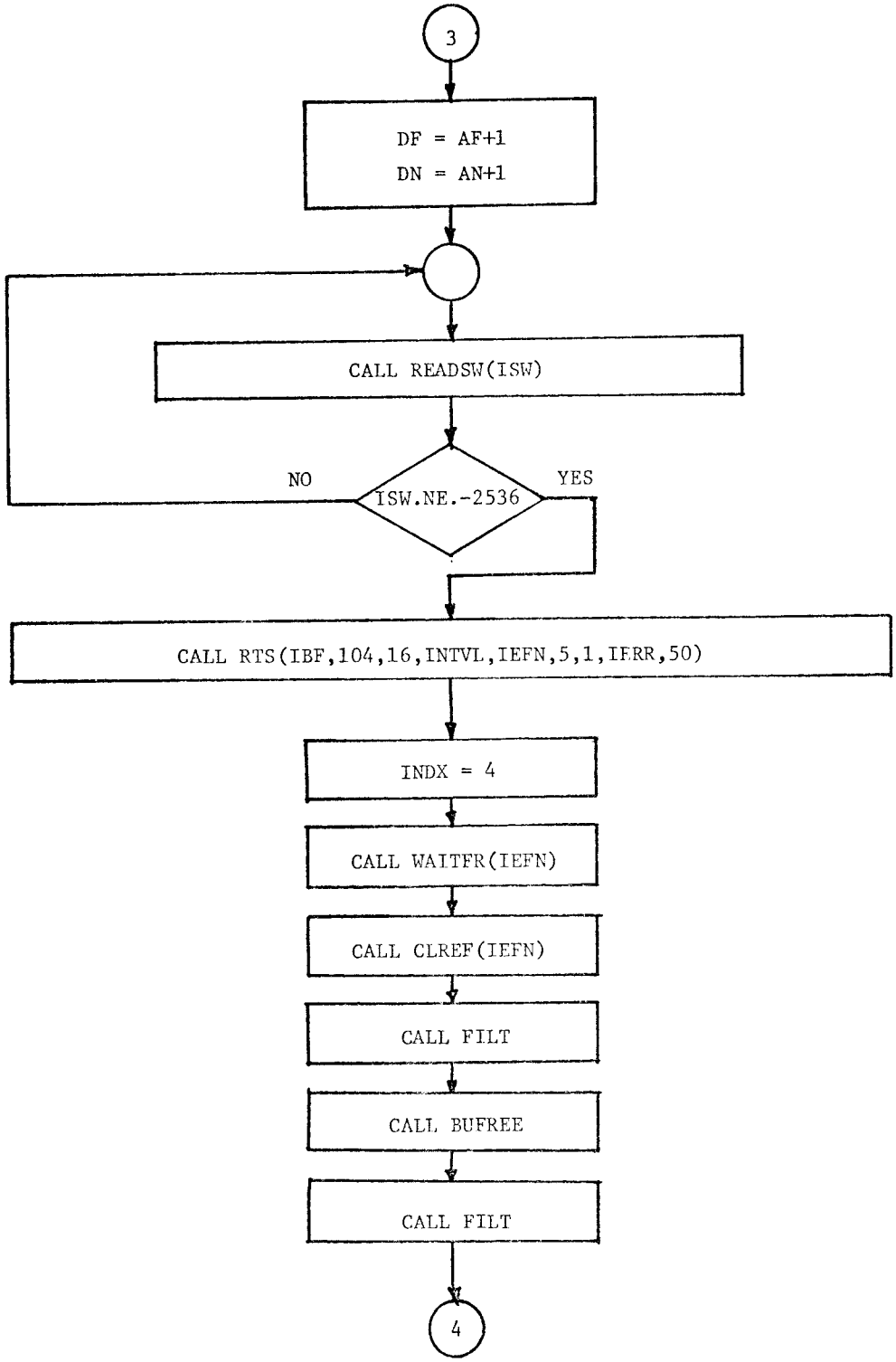
3
DF = AF+1
DN = AN+1
CALL READSW(ISW)
NO
ISW.NE.-2536
YES
CALL RTS(IBF,104,16,INTVL,IEFN,5,1,IERR,50)
INDX = 4
CALL WAITFR(IEFN)
CALL CLREF(IEFN)
CALL FILT
CALL BUFREE
CALL FILT
4

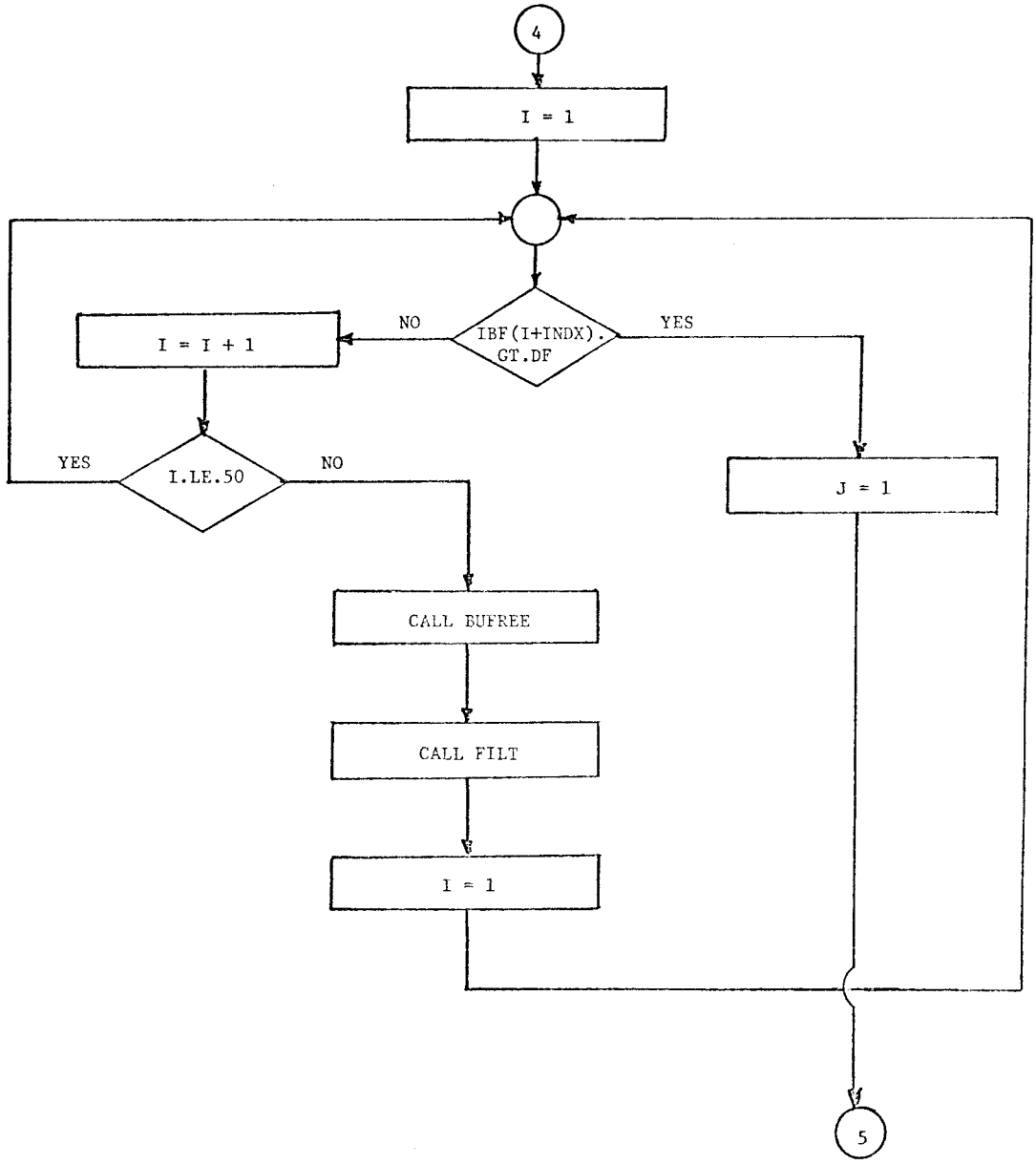
4
I = 1
IBF(I+INDX).
GT.DF
NO
YES
I = I + 1
YES
I.LE.50
NO
J = 1
CALL BUFREE
CALL FILT
I = 1
5

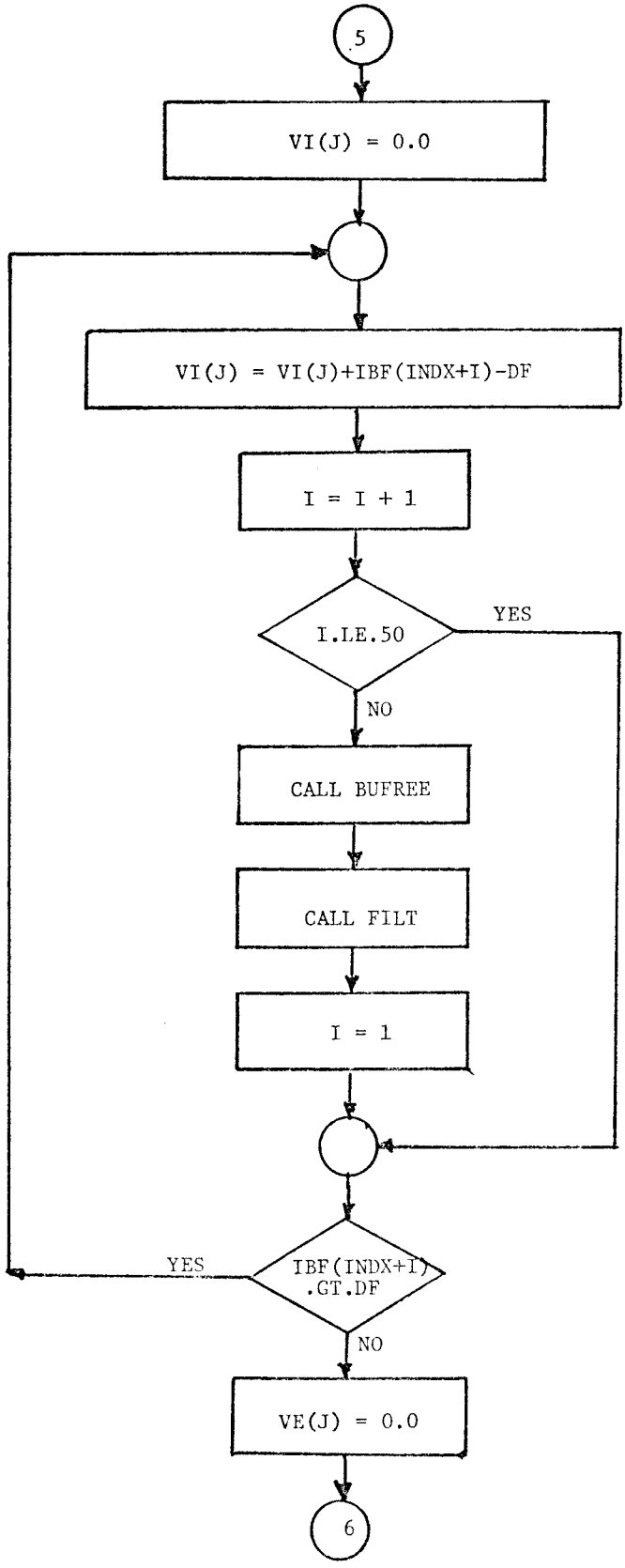
5
VI(J) = 0.0
VI(J) = VI(J)+IBF(INDX+I)-DF
I = I + 1
I.LE.50
YES
NO
CALL BUFREE
CALL FILT
I = 1
IBF(INDX+I)
.GT.DF
YES
NO
VE(J) = 0.0
6

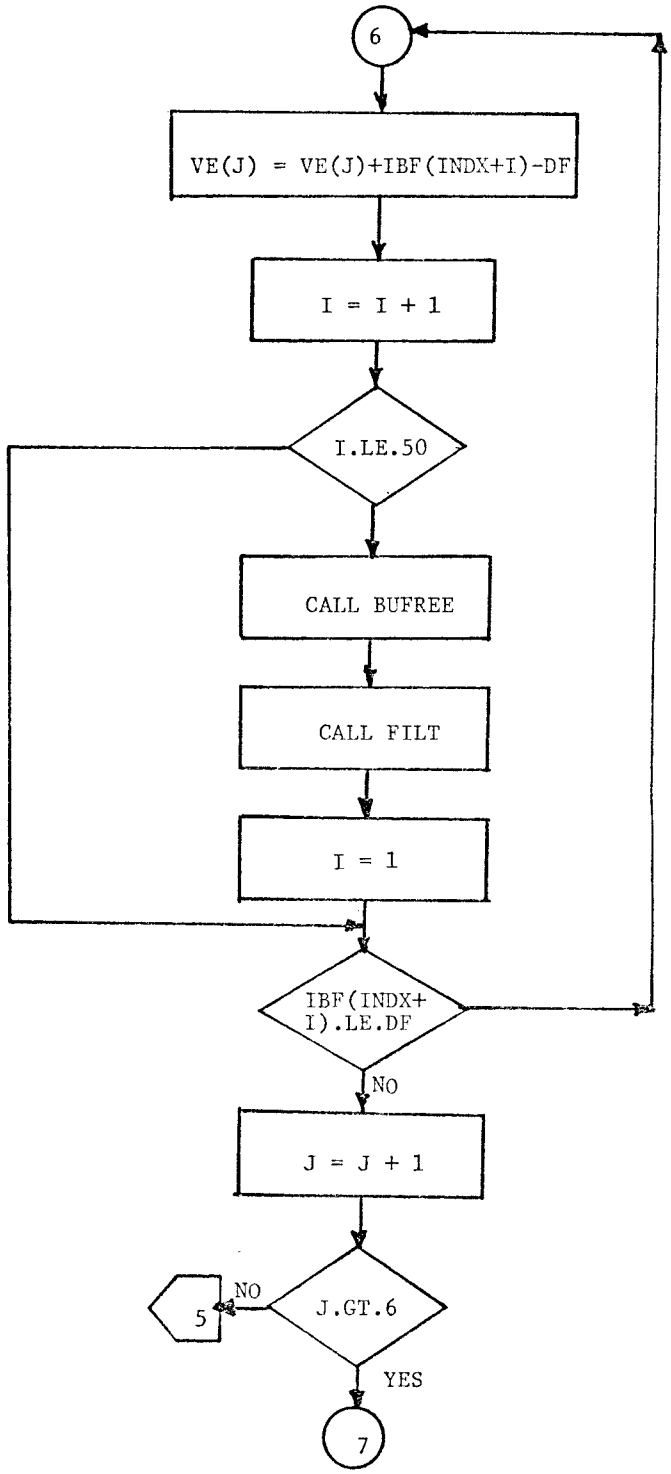
6
VE(J) = VE(J)+IBF(INDX+I)-DF
I = I + 1
I.LE.50
CALL BUFREE
CALL FILT
I = 1
IBF(INDX+
I).LE.DF
NO
J = J + 1
5
NO
J.GT.6
YES
7

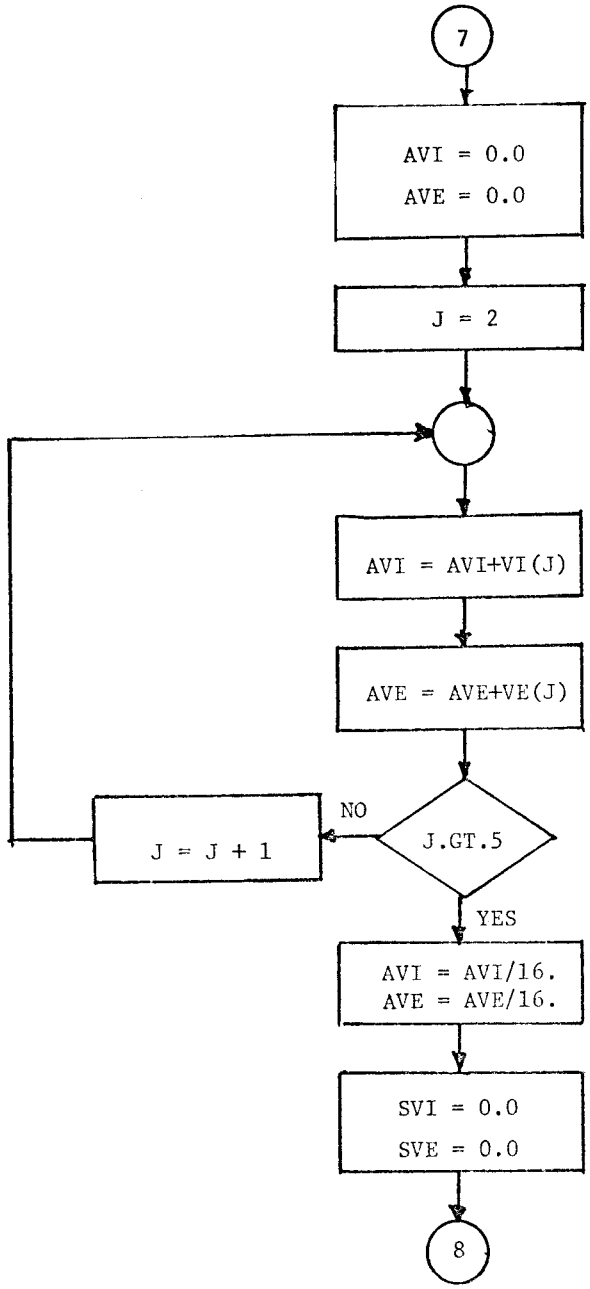
7
AVI = 0.0
AVE = 0.0
J = 2
AVI = AVI+VI(J)
AVE = AVE+VE(J)
J.GT.5
NO
J = J + 1
YES
AVI = AVI/16.
AVE = AVE/16.
SVI = 0.0
SVE = 0.0
8

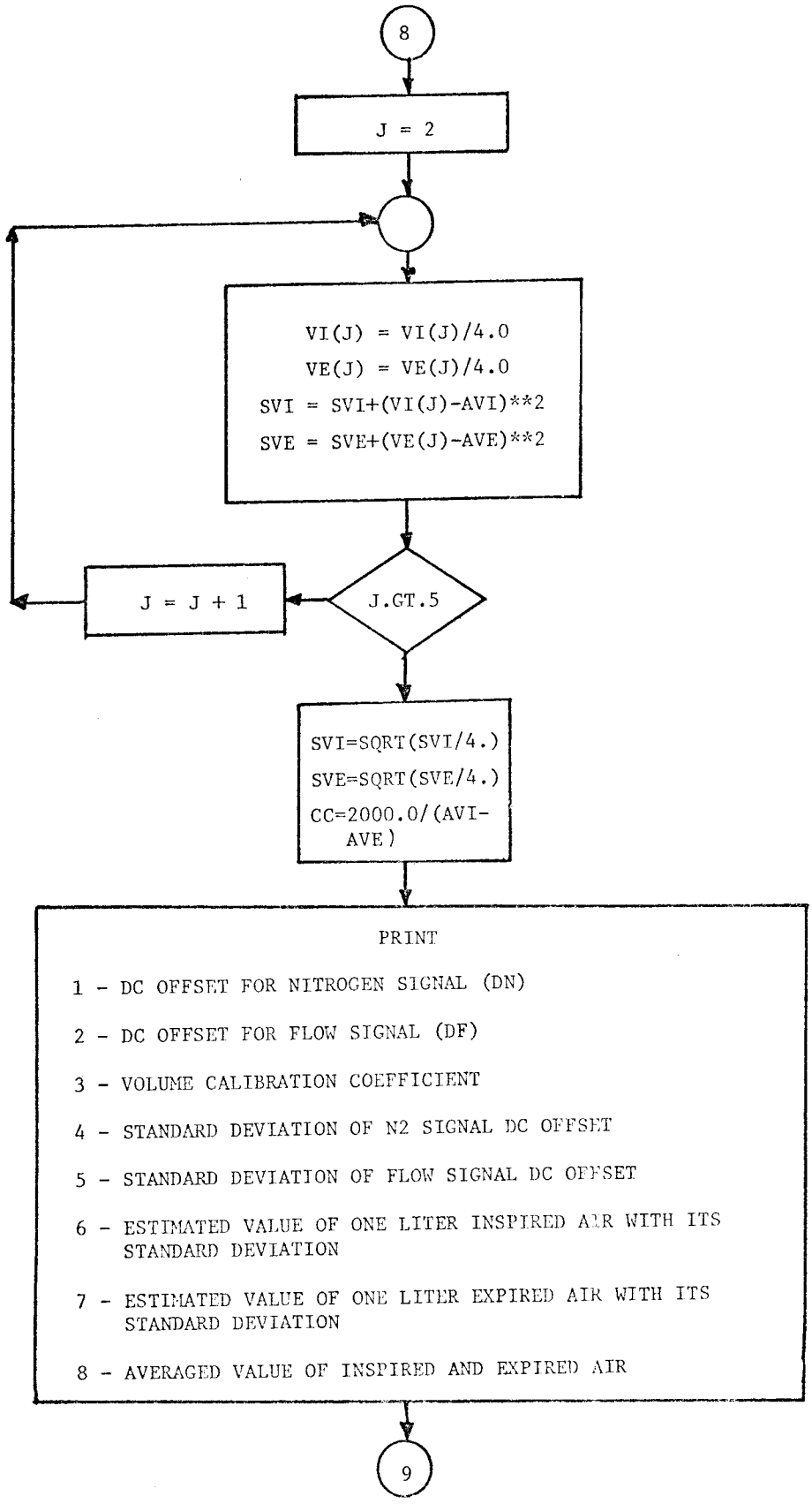
8
J = 2
VI(J) = VI(J)/4.0
VE(J) = VE(J)/4.0
SVI = SVI+(VI(J)-AVI)**2
SVE = SVE+(VE(J)-AVE)**2
J.GT.5
J = J + 1
SVI=SQRT(SVI/4.)
SVE=SQRT(SVE/4.)
CC=2000.0/(AVI-AVE)
PRINT
1 - DC OFFSET FOR NITROGEN SIGNAL (DN)
2 - DC OFFSET FOR FLOW SIGNAL (DF)
3 - VOLUME CALIBRATION COEFFICIENT
4 - STANDARD DEVIATION OF N2 SIGNAL DC OFFSET
5 - STANDARD DEVIATION OF FLOW SIGNAL DC OFFSET
6 - ESTIMATED VALUE OF ONE LITER INSPIRED AIR WITH ITS STANDARD DEVIATION
7 - ESTIMATED VALUE OF ONE LITER EXPIRED AIR WITH ITS STANDARD DEVIATION
8 - AVERAGED VALUE OF INSPIRED AND EXPIRED AIR
9

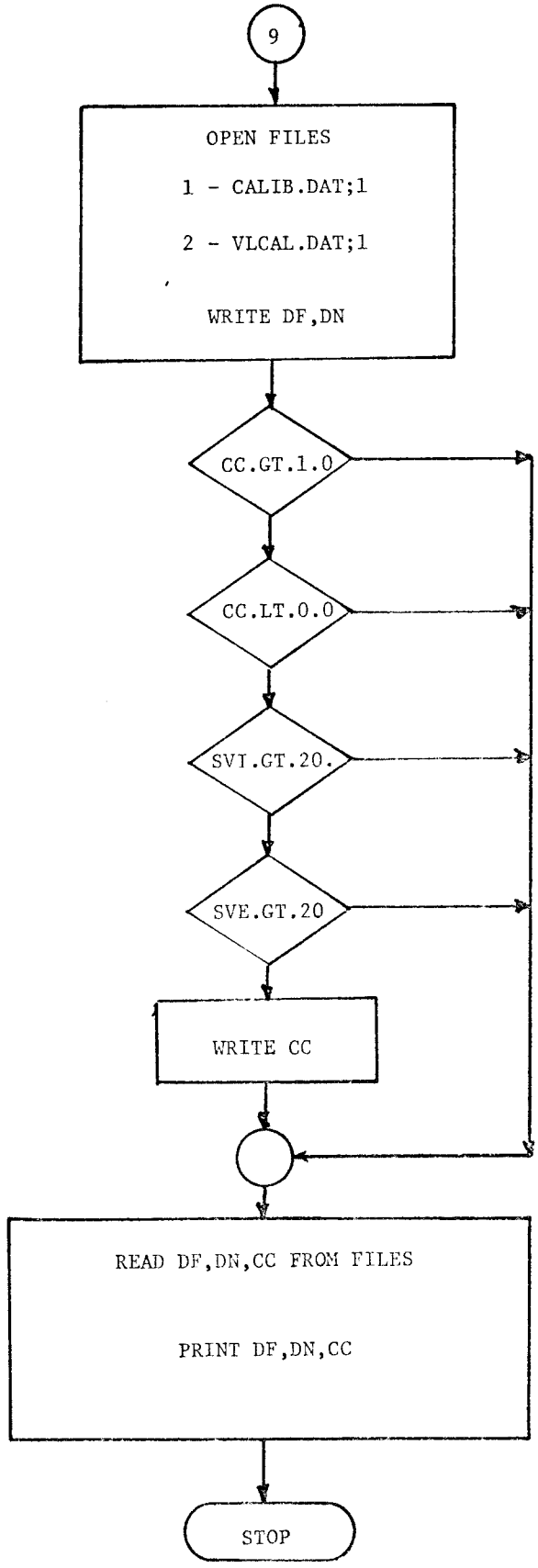
9
OPEN FILES
1 - CALIB.DAT;1
2 - VLCAL.DAT;1
WRITE DF,DN
CC.GT.1.0
CC.LT.0.0
SVI.GT.20.
SVE.GT.20
WRITE CC
READ DF,DN,CC FROM FILES
PRINT DF,DN,CC
STOP

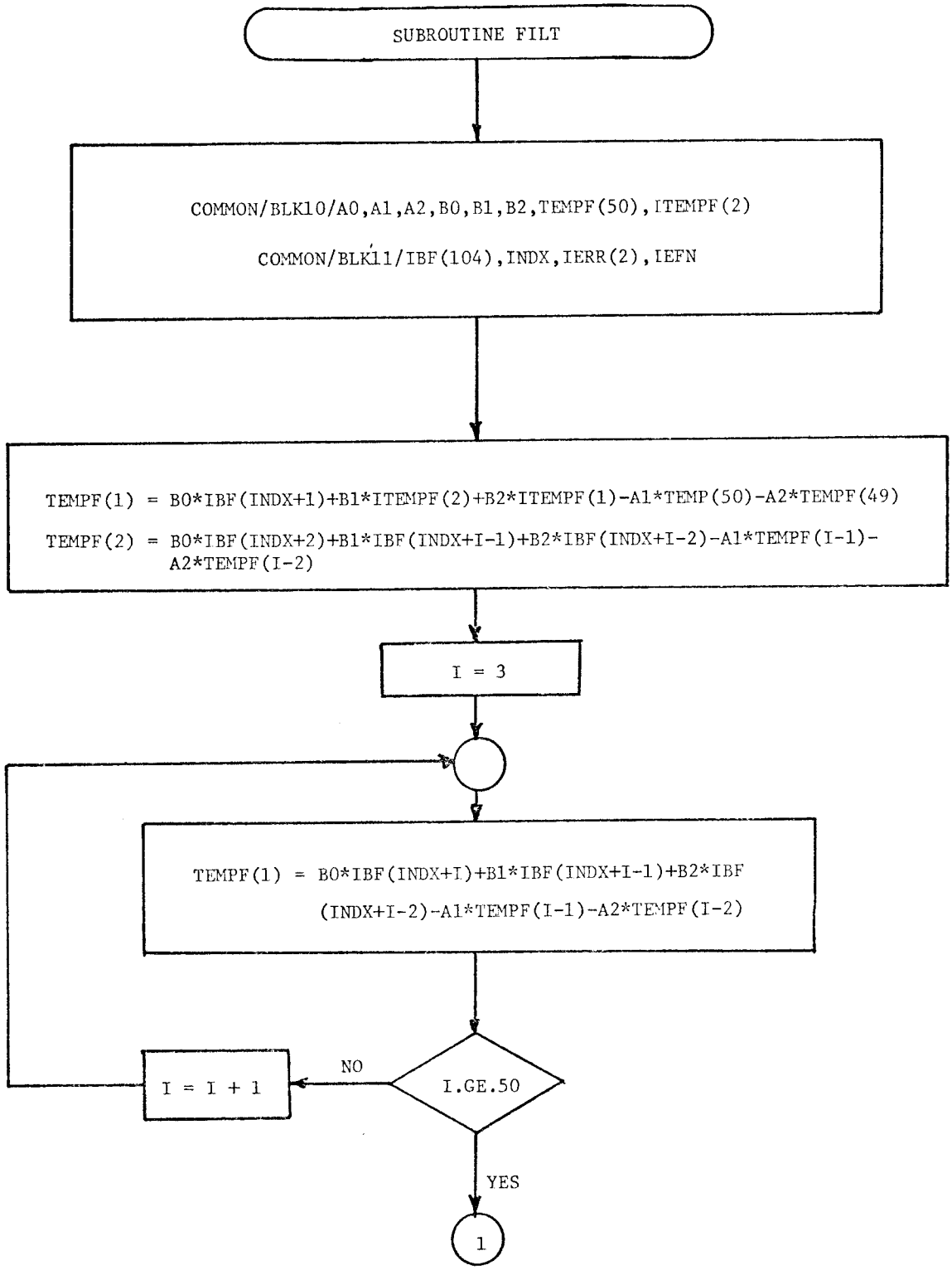
SUBROUTINE FILT
COMMON/BLK10/A0,A1,A2,B0,B1,B2,TEMPF(50),ITEMPF(2)
COMMON/BLK11/IBF(104),INDX,IERR(2),IEFN
TEMPF(1) = B0*IBF(INDX+1)+B1*ITEMPF(2)+B2*ITEMPF(1)-A1*TEMP(50)-A2*TEMPF(49)
TEMPF(2) = B0*IBF(INDX+2)+B1*IBF(INDX+I-1)+B2*IBF(INDX+I-2)-A1*TEMPF(I-1)-
A2*TEMPF(I-2)
I = 3
TEMPF(1) = B0*IBF(INDX+I)+B1*IBF(INDX+I-1)+B2*IBF
(INDX+I-2)-A1*TEMPF(I-1)-A2*TEMPF(I-2)
I.GE.50
NO
I = I + 1
YES
1

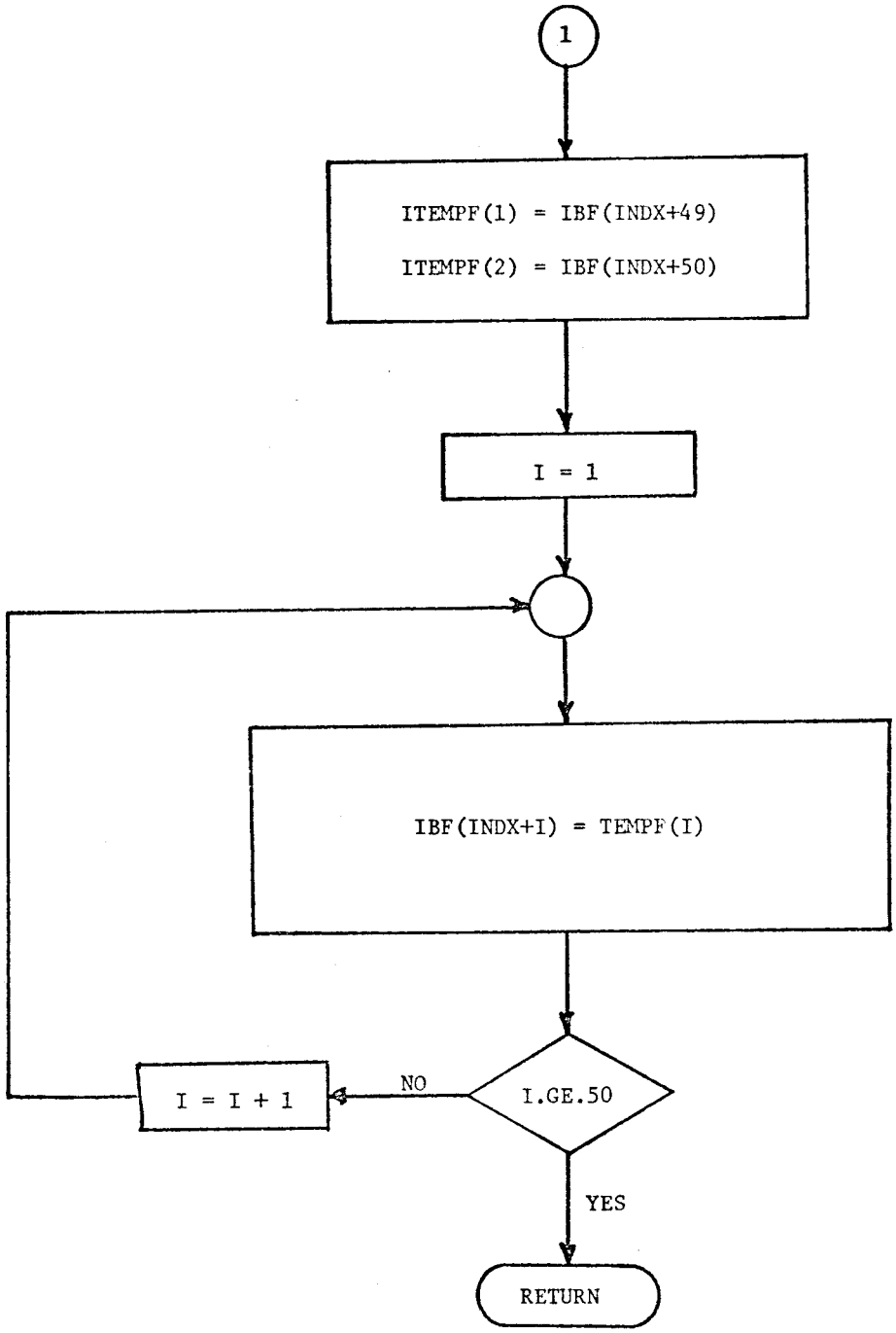
1
ITEMPF(1) = IBF(INDX+49)
ITEMPF(2) = IBF(INDX+50)
I = 1
IBF(INDX+I) = TEMPF(I)
I.GE.50
NO
I = I + 1
YES
RETURN

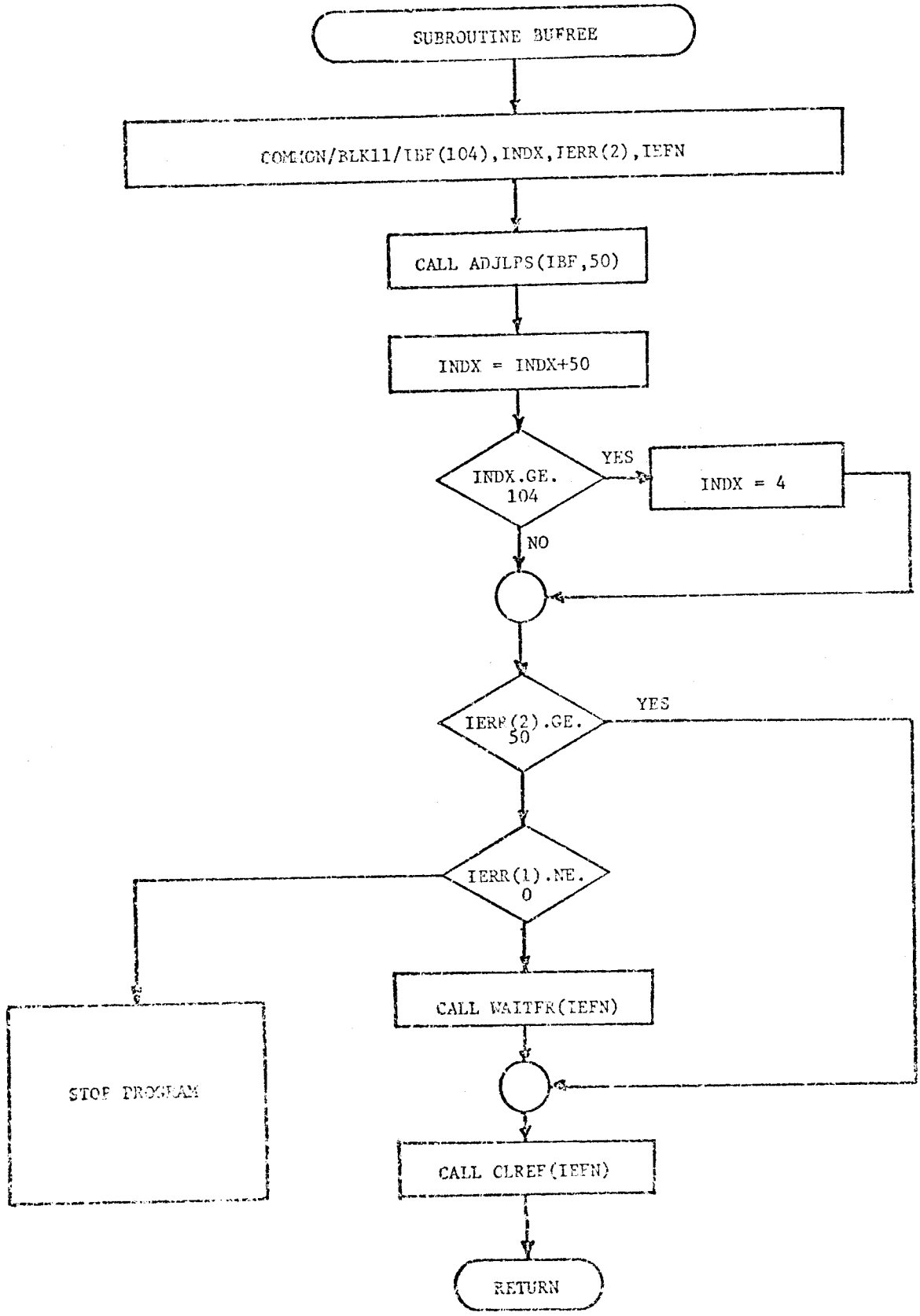
SUBROUTINE BUFREE
COMMON/BLK11/IBF(104),INDX,IERR(2),IEFN
CALL ADJLPS(IBF,50)
INDX = INDX+50
INDX.GE. 104
YES
INDX = 4
NO
IERR(2).GE. 50
YES
IERR(1).NE. 0
STOP PROGRAM
CALL WAITFR(IEFN)
CALL CLREF(IEFN)
RETURN